STRUCTURE AND CONFORMATIONAL SIGNALING IN THE ESCHERICHIA COLI ASPARTATE RECEPTOR TAR

A Dissertation

presented to

the Faculty of the Graduate School

at the University of Missouri-Columbia

In Partial Fulfillment

of the Requirements for the Degree

Doctor of Philosophy

---

by

NICHOLAS L. BARTELLI

Dr. Gerald Hazelbauer, Dissertation Supervisor

JULY 2014

The undersigned, appointed by the dean of the Graduate School, have examined the dissertation entitled

STRUCTURE AND CONFORMATIONAL SIGNALING IN THE ESCHERICHIA COLI ASPARTATE RECEPTOR TAR

presented by, Nicholas L. Bartelli

a candidate for the degree of doctor of philosophy

and hereby certify that, in their opinion, it is worthy of acceptance.

Professor Linda Randall

Professor Jason Cooley

Professor Michael Henzl

Professor Mark McIntosh

Professor Gerald Hazelbauer

ACKNOWLEDGMENTS

The successful completion of the work described in this dissertation required the efforts of numerous individuals. Thus I wish to acknowledge the following people for their contributions.

I thank Wing-Cheung Lai for producing the purified CheR methyltransferase used in chapter three and for producing large quantities of membrane scaffold protein used for making the Nanodiscs described in chapter four. Wing is also thanked for his efforts in cataloging (physically and by memory) *decades* worth of chemotaxis literature. I acknowledge Angela Lilly for the generation of about 60 plasmids bearing sequences for the expression of cysteine-substituted aspartate receptor (Tar) used in this work. I acknowledge Mingshan Li for providing frequent feedback regarding experimental design and for providing access to his previous results.

I thank Mary Belle Streit for the provision of countless snacks and helpful favors. Former lab member Divya Amin is due a special thanks for sharing her excellent cooking and recipes. I thank all other members of the Membrane Group (University of Missouri) for welcoming me into the lab and providing much needed support.

I acknowledge Lin Randall for providing initial training in EPR spectroscopy and providing an essential role in maintaining the EPR instrument (an otherwise thankless and frustrating task). I also thank her for providing frequent advice on experimental design and interpretation, as well as nurturing enthusiasm for my research efforts.

I thank Jerry Hazelbauer for his superior service as both a scientific advisor and departmental chair (perhaps another thankless task). It is likely that Jerry has done more on my behalf than I am aware; I am genuinely grateful.

Lin and Jerry have been generous, particularly in organizing and funding numerous memorable Membrane Group dinner engagements. I owe much of my success to both for accepting me into their laboratory and for nurturing my development as a research scientist. I consider both to be friends and colleagues.

I would also like to thank Peter Cornish for assistance and training on the single-molecule FRET instrument. Peiwu Qin, a former member of his lab, also generously provided time and effort to the successful, but ill-fated, completion of these experiments.

I acknowledge Songi Han and Chi-yuan Cheng (UCSB) for their essential efforts in our ongoing collaboration to resolve the nature of conformational signaling in the Tar cytoplasmic domain.

I would like to acknowledge Christian Altenbach (UCLA) for freely providing the software used to analyze EPR data. I also thank David Cafiso (University of Virginia) for reviewing the work described in chapter 3 of this dissertation.

Lastly I would like to acknowledge my Doctoral Program Committee members (Lin Randall, Jason Cooley, Michael Henzl, Mark McIntosh and Jerry Hazelbauer) for their time and critical review of this document.

TABLE OF CONTENTS

LIST OF FIGURES

LIST OF TABLES

Table **Page**

STRUCTURE AND CONFORMATIONAL SIGNALING IN THE ESCHERICHIA COLI ASPARTATE RECEPTOR TAR

Nicholas L. Bartelli

Dr. Gerald Hazelbauer, dissertation supervisor

ABSTRACT

Chemotaxis is the phenomenon of motile cells directing their movement in response to chemical signals from the environment; for bacteria this means moving toward favorable environments (attractant response) and away from unfavorable environments (repellent response). Sensing the environment is performed by a group of related chemoreceptors that communicate chemical sensory information from outside the cell, through the cellular membrane, and into the cytoplasm. This dissertation describes two studies employing site-directed spin labeling (SDSL) electron paramagnetic resonance (EPR) spectroscopy to probe important features of the *Escherichia coli* aspartate chemoreceptor (Tar). In the first, SDSL-EPR spectroscopy is used to resolve that the last 35 residues of Tar are intrinsically disordered and serving as a tether for interaction with the enzymes of adaptational modification. The second study describes efforts to use SDSL-EPR spectroscopy to resolve the nature of ligand-mediated and adaptational modification-mediated conformational signaling in the Tar cytoplasmic domain. The results indicate that adaptational modification modulates peptide backbone stability in a crucial region of the receptor but the consequence of ligand recognition is likely a distinct conformational phenomenon. In total the results described in this dissertation significantly enhance the collective understanding of bacterial chemoreceptor structure and signaling mechanism.

CHAPTER ONE

Fundamental features of chemotaxis in Escherichia coli

Chemotaxis in Escherichia coli

Chemotaxis is the phenomenon of motile cells directing their movement in response to chemical signals from the environment; for bacteria this means moving toward favorable environments (attractant response) and away from unfavorable environments (repellent response). In *Escherichia coli* there are two types of membrane-associated, multi-protein complexes central to this feature. One is the flagellum and motor responsible for propulsion. Another is the chemoreceptor signaling system responsible for communicating environmental stimuli into the interior of the cell.

Chemoreceptors are part of the large family of two-component signaling systems. Two-component signaling systems connect a sensory function to a histidine kinase that in turn signals through a soluble response regulator. Generally these systems modulate some feature of gene expression (Chang and Stewart, 1998; West and Stock, 2001; Stock *et al*., 2000). However the chemotaxis two-component system modulates the activity of the flagella motor and therefore connects chemo-sensation to motility. This background section will not discuss flagella or flagella motors but recent reviews are found in references Brown *et al*., 2011 and Zhao *et al*., 2014.

This section will describe the basic molecular components of the chemotaxis sensory system, the structural organization of those components and the cycle of sensory adaptation. A detailed description of chemoreceptor conformational signaling is found elsewhere in this dissertation (Chapter 4, introduction). A reader interested in the history of the field should consult Hazelbauer, 2012, an excellent review of early

developments in resolving the molecular features of bacterial chemotaxis. A reader seeking a more contemporary background regarding bacterial chemotaxis that expounds upon the fundamentals presented in this chapter should consult the references Hazelbauer *et al*., 2008 and Hazelbauer and Lai, 2010.

The components of Escherichia coli chemotaxis signaling

The chemotaxis signaling system is composed of relatively few components. Most components have resolved structures (only partial structures of chemoreceptors exist) and they are featured in figure 1-1.

At the core of chemotaxis signaling systems are the transmembrane receptors (chemoreceptors) that communicate environmental chemical signals from the periplasm, across the membrane, and into the cell. There are five chemoreceptors in *E. coli*, most of which have multiple ligands/inputs. Those receptors are Tar (*t*axis to *a*spartate and *r*epellents), Tsr (*t*axis to *s*erine and *r*epellents), Trg (*t*axis to *r*ibose and *g*alactose), Tap (*ta*xis to di*p*eptides) and Aer (taxis to oxygen) (Hazelbauer, *et al*., 2008). Some of these inputs are ligands recognized by the primary binding site located in the receptor periplasmic domain, others are first recognized by periplasmic binding proteins (for example, galactose-binding protein) that in turn interact with and modulate chemoreceptor conformation.

CheA is the histidine kinase associated with chemoreceptor signaling and it is CheA activity that is controlled by chemoreceptors. CheA is a homodimeric protein with five domains designated P1 through P5 (Fig. 1-1). The P1 domain contains the histidine to

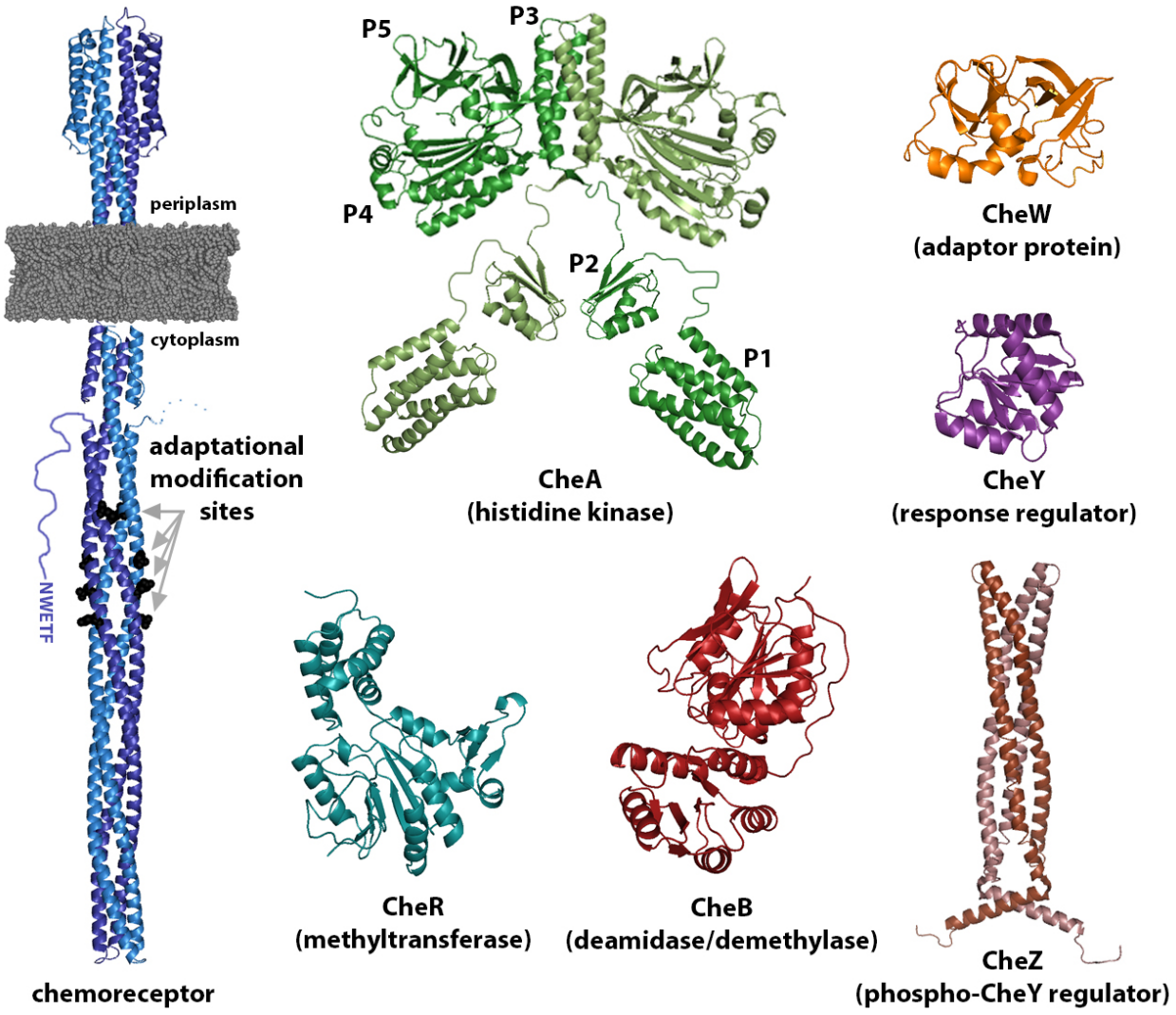

Figure 1-1: Components of the chemotaxis signaling system

The proteins of the *Escherichia coli* chemotaxis signaling system are shown above as ribbon diagram structures. The structures are not to scale. At left is a model of a chemoreceptor dimer in the cytoplasmic membrane. The sites of adaptational modification are indicated by black CPK residues. One of the disordered carboxyl terminal tails is shown (Tar and Tsr only) and terminates in the NWETF sequence that interacts with CheR and CheB. Besides receptors, the core unit of signaling includes a CheA dimer (green) and CheW (orange). CheY (violet) is the diffusible response regulator that when phosphorylated, associates with FliM (not shown) of the flagellar motor. A CheZ dimer (brown) associates with signaling complexes and regulates CheY phosphatase activity. The enzymes of adaptational modification are shown at bottom with CheR in teal and CheB in red.

be phosphorylated (Baker *et al*., 2005). The P2 domain binds the response regulator CheY (Baker *et al*., 2005). The P1 and P2 domains are on relatively long flexible tethers (Zhou *et al*., 1996). The remaining domains, P3-5 form the core of the enzyme with P3 acting as the dimerization domain, P4 as the ATP-binding catalytic domain and P5 as a regulatory domain (Baker *et al*., 2005). Phospho-transfer occurs through a trans-phosphorylation event, the P4 domain phosphorylates the P1 domain of the other subunit in the CheA dimer (Swanson *et al*., 1993), and the phosphate is then transferred to CheY. The intrinsic kinase activity of CheA is relatively low and is increased about 1000-fold upon assembling with receptors in the ternary signaling complex (Borkovich and Simon, 1990; Li and Hazelbauer, 2011). Thus CheA activity is allosterically activated by receptor association, but the molecular mechanisms of receptor-mediated CheA activation and control remain unresolved.

CheW is another protein that interacts with both the receptor and CheA in the ternary signaling complex (Figs. 1-2, 1-3). CheW has structural and sequence homology with CheA domain P5 (Bilwes *et al*., 1999) and is believed to have arisen as a gene duplication of that domain. CheW and CheA domain P5 associate with the same site on chemoreceptor trimers-of-dimers (Fig. 1-3). Relatively little is known about CheW function but it is known to potentiate CheA activation and association with receptors (Levit *et al*., 1999), to play a structural role in the ternary complex (Borkovich and Simon, 1990; Li *et al*., 2013), and to play a role in modulating CheA activity (Natale *et al*., 2013).

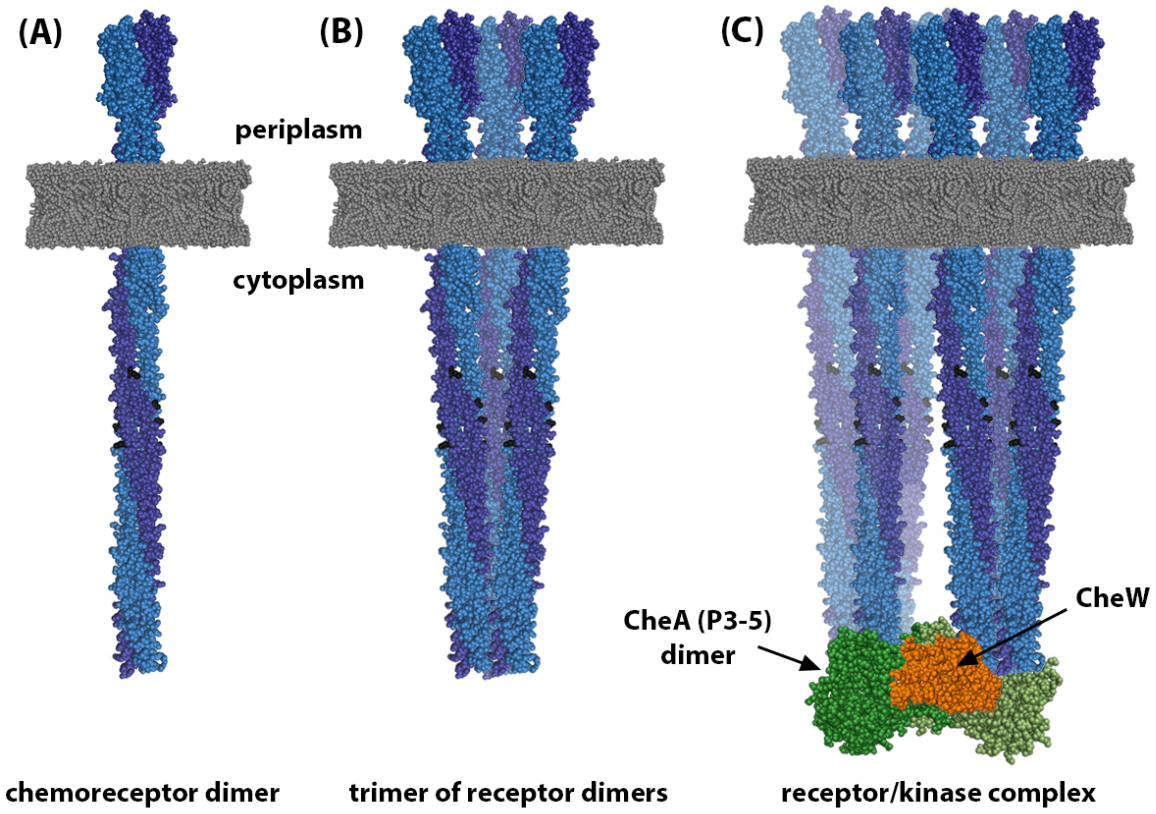

Figure 1-2: Chemoreceptor organization

(A) A chemoreceptor homodimer in the cytoplasmic membrane. (B) Chemoreceptor dimers interact at their cytoplasmic tips to form trimers of receptor dimers. (C) Two trimers of receptor dimers coordinate with the CheA kinase dimer (green) and two copies of CheW (orange) to form the minimum unit of kinase activation and control. Only CheA domains P3-5 are shown. The second CheW is obscured from view. Note that the figure is representative and not meant to communicate precise features of intermolecular association.

CheY is the diffusible response regulator of the chemotaxis signaling system and is phosphorylated by CheA. Phosphorylated CheY binds to FliM of the flagellar motor (Bren and Eisenbach, 1998; Dyer and Dahlquist, 2006). It is this binding that controls the rotational bias of the motor by changing the default counter-clockwise rotation to clockwise (Scharf *et al*., 1998).

CheZ is a protein that promotes dephosphorylation of CheY, thus helping to regulate cellular levels of phospho-CheY. Much of the cellular CheZ is associated with signaling complexes by binding to an alternative CheA that bears an N-terminal truncation (Cantwell *et al*., 2003). Other features of CheZ activity are reviewed in Baker *et al*., 2005.

CheB and CheR are the enzymes of adaptational modification. These enzymes and their crucial activity are described in a later section of this chapter.

Organization of the chemotaxis signaling complex

Chemoreceptors in bacteria are highly conserved at the receptor cytoplasmic tip region that interacts with the histidine kinase CheA, this allows the same kinase to be shared amongst the various types of receptors (Alexander and Zhulin, 2007). Cryo-electron microscopy, X-ray crystallography, and biochemical analyses have revealed that chemoreceptors are homodimers that form an extended, alpha-helical structure of approximately 300 Å from the periplasmic ligand binding site to the cytoplasmic tip (Fig. 1-1) (Milligan and Koshland, 1998; Kim *et al*., 1999; Falke and Kim, 2000; Weis *et al*.,

2003). Receptor dimers assemble into trimers-of-dimers via interactions at their cytoplasmic tip (Ames *et al*., 2002, Kim *et al*., 1999).

A combination of biochemical methods, X-ray crystallography and cryo-EM tomography have revealed important details about the organization of the ternary signaling complex composed of receptors, CheA and CheW. An important development was the resolution that the minimum unit of kinase-activation and control is two receptor trimers-of-dimers, in a ternary complex with a dimer of CheA and two CheW (Li and Hazelbauer, 2011). Briegel and others have elucidated the hexagonal arrangement of signaling complexes in extended arrays composed of up to thousands of receptors (Briegel *et al*., 2014; Briegel *et al*., 2012; Liu *et al*., 2012; Briegel *et al*., 2009). This hexagonal packing arrangement was observed across diverse bacterial species (Briegel *et al*., 2009). As depicted in figure 1-3 a dimer of CheA is bound between two receptor trimers-of-dimers with a CheW binding to each trimer-of-dimers. This basic organization provides the template to form extended arrays (Fig. 1-3). Crystallographic resolution by (Li *et al*., 2013) helped to resolve the fine details of these interactions and the proposed contacts are further supported by other biophysical and biochemical evidence (Piasta *et al*., 2013; Wang *et al*., 2012; Vu *et al*., 2012; Li *et al*., 2013; Liu *et al*., 2012). The chemotaxis signaling system exhibits high gain (Sourjik and Berg, 2002), it is believed that the molecular details of signaling array structure (Fig. 1-3) enable this feature but the mechanism remains unresolved.

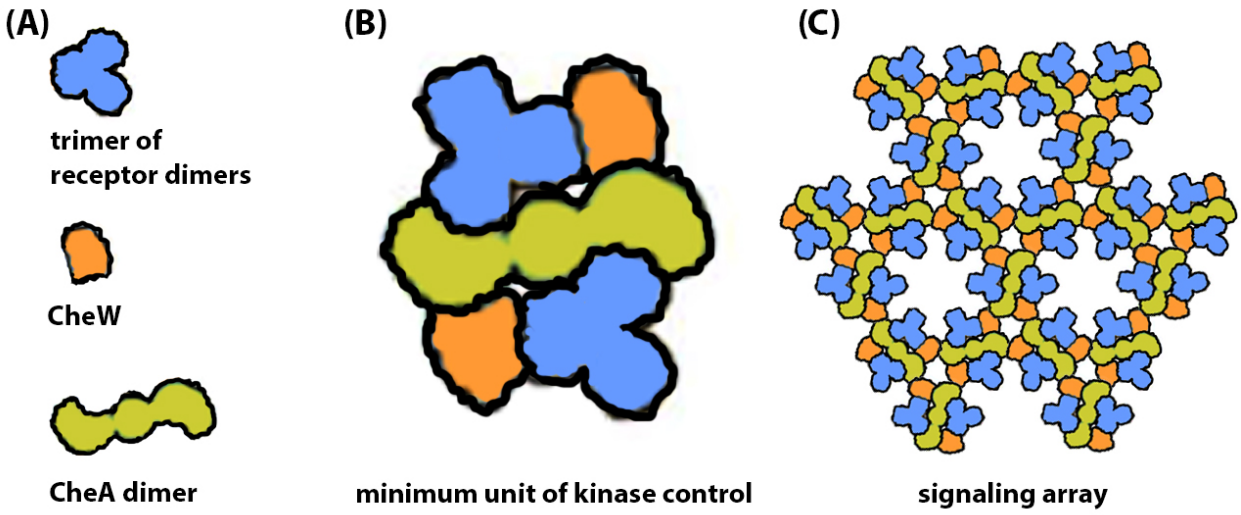

Figure 1-3: Organization of chemoreceptor signaling complexes and arrays

The above cartoon summarizes the current model of chemoreceptor signaling complex organization and array assembly. The model assumes a top-down view of the receptor cytoplasmic tips. (A) The components of the complex, a receptor trimer-of-dimers in blue, CheW in orange and a CheA dimer in green. (B) The minimum unit of kinase activation and control with a dimer of CheA bound between two receptor trimers-of-dimers and a CheW binding to each trimer-of-dimers. (C) Signaling complexes organize into extended arrays with a hexagonal packing arrangement. The number of signaling units in these arrays is variable.

Sensory adaptation is a crucial component of chemotaxis

Bacterial chemoreceptors are often referred to as MCPs, standing for *m*ethyl-accepting *c*hemotaxis *p*roteins. The cycle of methylation and demethylation is referred to as adaptational modification and these post-translational modifications are an essential feature of bacterial chemotaxis. Modification modulates the sensitivity and response range of the signaling response (Amin and Hazelbauer, 2010; Bornhorst and Falke, 2001), and when the enzymes (or sites) of adaptation are eliminated cells are deficient in chemotaxis behavior (Weis and Koshland, 1988; Hazelbauer *et al*., 1989; Weis *et al*., 1990).

Each receptor bears 4 or 5 sites of adaptational modification in their cytoplasmic domain. Tar, the subject of this dissertation, has four sites per subunit. These sites are genetically encoded as QEQE (in the single letter code) as they occur in the amino acid sequence. The glutamines are deamidated by CheB to generate glutamates (Kehry, *et al*., 1983) and glutamates are methylated to generate methyl-glutamates (Kort, *et al*., 1975). Glutamines have been demonstrated to be functionally equivalent to methyl-glutamates (Dunten and Koshland, 1991; Borkovich *et al*., 1992; Lai *et al*., 2006) and in this dissertation receptors bearing four glutamines (4Q) at the sites of modification are used as an analogue of a fully methylated receptor. Bornhorst and Falke explored 16 potential combinations of glutamines (Q) and glutamates (E) at the sites of modification and demonstrated that the fully modified receptor (4Q) has relatively high intrinsic kinase activating potential and low operational efficiency of ligand coupling; the fully

unmodified receptor (4E) has very low kinase activating potential and relatively high operational efficiency of ligand coupling (Bornhorst and Falke, 2001). Intermediate levels of modification produced responses between the two extremes and certain modification sites produced more significant effects (Bornhorst and Falke, 2001).

In essence, adaptation restores the system to the pre-stimulus state and is a crucial feature of broad-range, gradient-sensitive chemotaxis as methylated (adapted or 4Q) receptors require increasingly high concentrations of attractant ligand to inhibit CheA kinase activity. The consequences of adaptational modification on receptor structure are described in chapter four of this dissertation.

Both CheR and CheB interact with the five carboxyl-terminal amino acids of Tar and Tsr; those residues are NWETF in the single letter code and this site has been designated the pentapeptide. For CheR the pentapeptide acts as a high-affinity binding site (Wu *et al*., 1996) and for CheB the pentapeptide acts as an allosteric activator (Barnakov *et al*., 2002). Not all receptors bear a pentapeptide (only Tar and Tsr, not Trg, Tap or Aer) to interact with the enzymes of modification (Feng *et* al., 1999; Barnakov *et al*., 1998). The work described in this dissertation (chapter three) indicates that there are about 30 residues preceding the pentapeptide that are structurally disordered (Bartelli and Hazelbauer, 2011). The disordered flexible linker bearing the pentapeptide allows for a modification enzyme attached to a pentapeptide-bearing receptor to reach and modify nearby receptors without the site (Bartelli and Hazelbauer, 2011; Li and Hazelbauer, 2006; Muppirala *et al*., 2009), and the proposed packing density of receptors in

complexes (Briegel *et al*., 2014; Briegel *et al*., 2012; Briegel *et al*., 2009; Liu *et al*., 2012) supports models of tether-mediated assistance in adaptational modification chemistries (Li and Hazelbauer, 2005; Muppirala *et al*., 2009).

In total the bacterial chemotaxis signaling system is quite complex despite being composed of relatively few components. The super structure of the signaling array and the feature of adaptation impart a function on the chemosensory array beyond mere receptor. Instead the system acts as a highly-organized macro-molecular *sensory node* for the bacterium with a broad range of sensitivity. This dissertation describes two features of the chemoreceptor Tar, expanding the collective understanding of bacterial chemotaxis. Chapter three describes the structure of the Tar carboxyl-terminal region. Chapter four describes features of Tar conformational signaling in isolated receptor dimers.

CHAPTER TWO

SDSL-EPR spectroscopy at helices and disordered protein regions

Introduction

Electron paramagnetic resonance (EPR) spectroscopy combined with site-directed spin-labeling (SDSL) has proven to be a powerful tool to explore protein structure and conformational dynamics. The work in this dissertation relies heavily upon EPR spectroscopy as a probe of features of the aspartate receptor (Tar) from *Escherichia coli*. A description of the physical basis of EPR spectroscopy is unnecessary to understand the results presented here and is beyond the scope of this dissertation. A reader more interested in the physical basis of EPR spectroscopy should consult Weil, *et al.*, 1994 or Fajer, 2000. This section will, however, review the major conclusions drawn from SDSL-EPR studies of proteins with an emphasis on results derived from the two types of spin-labeled sites encountered in this dissertation, solvent-exposed alpha-helices and structurally disordered sites.

Fundamental features of continuous-wave nitroxide SDSL-EPR spectroscopy

Site-directed spin labeling requires that a cysteine be substituted at a site of interest via mutagenesis. The SDSL reaction involves reacting a nitroxide methanethiosulfonate (MTSL) spin label with the cysteine sulfhydryl to generate a new paramagnetic side chain at the site of interest called R1. The nitroxide moiety has a stable unpaired electron with a magnetic moment that in the magnetic field of an EPR spectrometer can be oriented with the magnetic field in a minimum energy state or against the field in a maximum energy state. This results in an energy difference that can be exploited by the absorption of microwave frequency radiation resulting in transitions to the higher energy state. These transitions disturb the spin orientation

equilibrium and it is the process and nature of the relaxation pathway that is the determinant of subtle continuous-wave EPR spectral features. Those and more basic features are described in the following paragraphs.

As a means to increase signal sensitivity the EPR instrument applies a modulation of 1-3 Gauss at 100 kHz and what is detected are absorption amplitude changes with the same frequency as the applied modulation. The data reported is the amplitude change over the width of modulation, thus EPR spectra appear as first-derivative absorption spectra. The three components of a nitroxide EPR spectrum are the result of hyperfine splitting as a consequence of the radical electron spin interacting with the local magnetic field of the ^{14}N nuclei (spin = 1) of the nitroxide moiety.

The specific nature of an EPR lineshape is sensitively coupled to the magnitude, anisotropy, and rate (correlation time) of spin-label motion. Continuous-wave EPR spectroscopy is sensitive to spin-label motions with correlation times 0.1 to 100 ns, this is the timescale of side-chain and peptide backbone fluctuations (Hubbell *et al*., 2013). For rapidly rotating, loosely ordered labels at disordered protein regions, the acquired spectra have sharp peaks narrowly distributed along the x-axis. As labels become increasingly restricted in motion as a function of backbone secondary structure or steric restriction by tertiary contact, the spectral features are broadened along the x-axis. An example of the types of spectra associated with certain protein structural features is given in figure 2-1. The precise features of these lineshapes are extremely sensitive to

perturbation and thus provide a means to probe site-specific changes induced by external effectors, for example: ligand binding, osmolality, or temperature.

SDSL-EPR as a probe of solvent-exposed alpha-helices and disordered protein regions

Much effort has been made correlating structural phenomenon with continuous-wave EPR lineshapes acquired using MTSL, the most studied nitroxide spin-label. A triple approach of empirical (and quantitative) lineshape analyses, crystallography of spin-labeled proteins, and quantitative modeling of spin-label rotamer fluctuations has allowed for a strong correlation between EPR nitroxide lineshapes and protein structural phenomenon for certain types of protein sites. Readers interested in reviews broadly exploring the application of SDSL-EPR as applied to protein research should consult the following references: Columbus and Hubbell, 2002; Hubbell *et al*., 2000; Fanucci and Cafiso, 2006; Hubbell *et al*., 2013; Klug and Feix, 2008.

The principal finding from extensive studies on spin-labeled, solvent-exposed, alpha-helical and disordered sites uninvolved in tertiary contacts is that variations in spectral features between these sites are largely the result of variations in peptide-backbone dynamics (Columbus and Hubbell 2004; Mchaourab *et al*., 1996; Fleissner *et al*., 2009). For alpha-helical sites and loops the presence of an orienting, intra-residue bond between the delta-sulfur in the MTSL (R1) side-chain and the alpha-carbon hydrogen results in a limited rotamer population where most of the internal motion is occurring about the two bonds preceding the nitroxide-bearing ring (Fleissner *et al*., 2009; Langen *et al.*, 2000). This feature orients the nitroxide-bearing ring in a manner

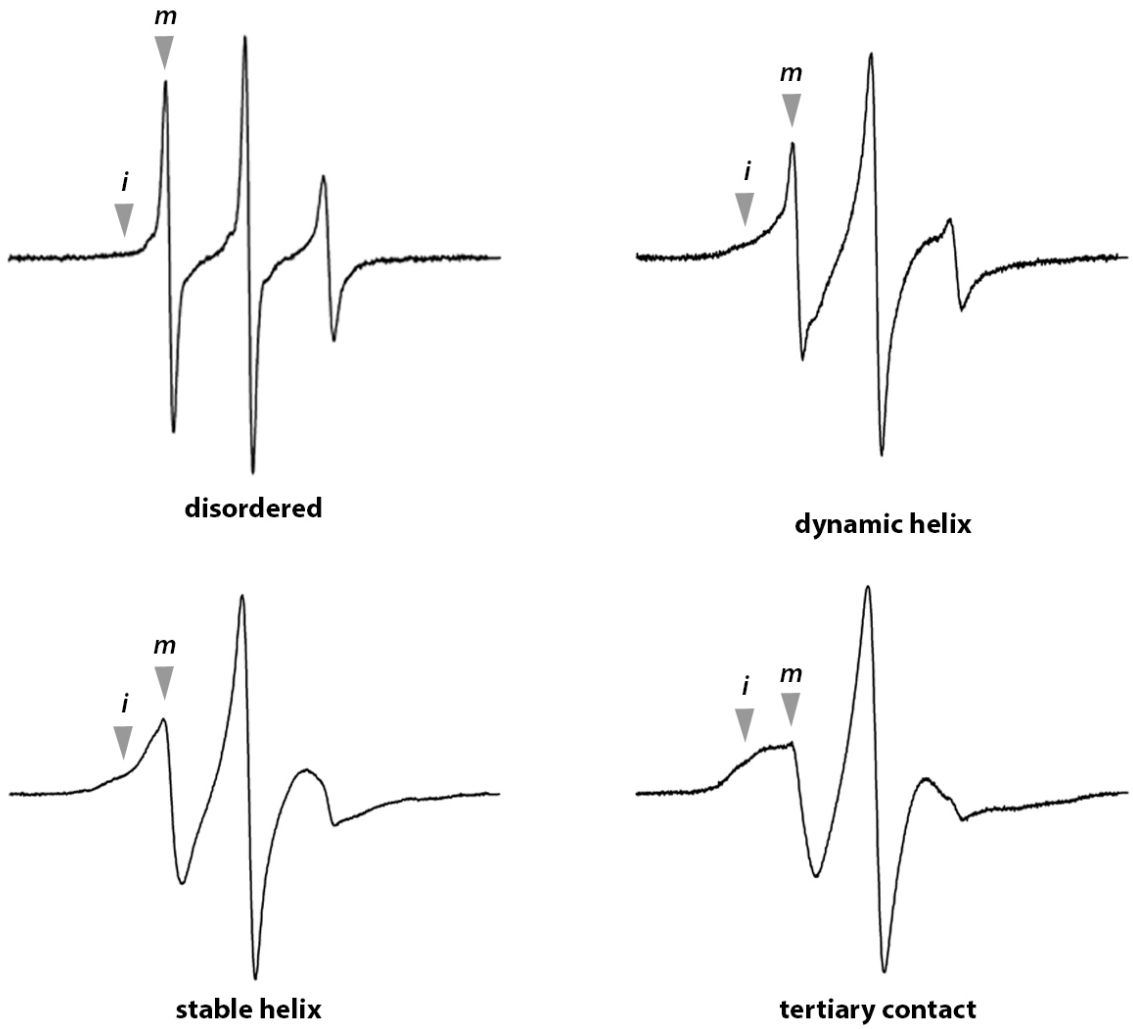

Figure 2-1: **Example continuous wave nitroxide EPR spectra for four structural conditions**

Arrows and notation (*m* or *i*) indicate spectral components arising from relatively mobile (*m*) and relatively immobile (*i*) states of the spin label.

that limits steric contact between the spin-label and neighboring side chains at a solvent-exposed alpha-helical site (Mchaourab *et al*., 1996; Fleissner *et al*., 2009). Thus, a label at these types of sites is insensitive to the local sequence and should produce the same lineshape, independent of the specific protein labeled or position in the alpha-helix. However, some variation does occur and studies of the transcription factor GCN4 revealed that spectral variation correlates with peptide backbone fluctuation (Columbus and Hubbell, 2004). In that work the authors used EPR to demonstrate a gradient of backbone mobility that correlated strongly with NMR-derived order parameters describing backbone stability (Columbus and Hubbell, 2004; Saudek *et al*., 1991). Thus, continuous wave EPR spectroscopy at non-interacting, solvent-exposed alpha-helical sites is a probe of site-specific peptide backbone dynamics.

In the same study the authors note that the EPR spectra derived from the GCN4 DNA-binding region are consistent with a relatively disordered region that they describe as an ensemble of structures with helical tendencies. They observe a dampening of backbone dynamics when the GCN4 DNA substrate was added, inducing a stabilization of helicity in those regions (Columbus and Hubbell, 2004). Thus, continuous wave EPR spectroscopy has also proven an effective probe of regions with dynamic secondary structure.

As a natural consequence of continuous-wave EPR sensitivity to peptide backbone stability, numerous studies have employed manipulation via stabilizing osmolytes to explore protein features by inducing disordered-to-ordered structural transitions. For

example work by Cafiso, *et al.* exploring the dynamic amino-terminus of BtuB showed that EPR was sensitive to backbone dynamics via direct modulation with osmolyte (Kim *et al*., 2006; Flores Jiménez, 2009) and as a consequence of ligand binding (Kim *et al*., 2007). In a somewhat distinct approach recent work described the use of osmolyte to distinguish whether spectra with multiple-components (heterogeneous label populations) are the result of protein backbone conformational heterogeneity or spin-label rotameric heterogeneity (López *et al*., 2009).

This dissertation describes the elucidation of a structurally disordered segment in the Tar carboxyl-terminal region. Intrinsically disordered protein regions are increasingly recognized for their importance in diverse protein functions and are enriched in signaling-related proteins (Dunker *et al*., 2008). EPR spectroscopy has proven a productive tool to investigate features of these sites and numerous examples exist in the literature.

A study exploring the disordered carboxyl-terminal domain of the measles virus nucleoprotein showed that introduction of its binding partner or the addition of a stabilizing osmolyte induced disorder-to-helix transitions as detected by EPR (Morin *et al*., 2006; Belle *et al*., 2008). Also, the spectra derived from a study of the multidrug ABC transporter BmrA revealed a domain in conformational exchange between extended (more disordered) and stably structured (Do Cao *et al*., 2009). Another study exploring the conformation of proteinase inhibitor IA_3 used EPR to demonstrate osmolyte-induced folding of what is otherwise an unstructured peptide (Pirman *et al*., 2011). In a study

particularly related to this dissertation (chapter three), an exploration of the bovine rhodopsin carboxyl-terminal tail showed that the region was unstructured and could be modulated by the binding of an antibody recognizing the region (Langen *et al.*, 1999).

Simple quantitative analyses of nitroxide EPR spectra

As a means of comparing continuous wave EPR spectra quantitatively, two metrics were employed in the studies described in this dissertation (Fig. 2-2). The first, called scaled mobility (M_s) is a measure of mobility of a nitroxide spin label at a position of interest normalized to a relatively mobile and a relatively immobile protein-coupled nitroxide. Specifically, $M_s = (\delta_{exp}^{-1} - \delta_i^{-1}) / (\delta_m^{-1} - \delta_i^{-1})$, where δ_i and δ_m are the central line-widths of a relatively immobile (broadened) and a relatively mobile (sharp) nitroxide spectra, respectively, and δ_{exp} is the central linewidth of the position under investigation (Columbus and Hubbell, 2002; Hubbell *et al*., 2000). In this dissertation, the utilized values of the constants (δ_m^{-1}, δ_i^{-1}) were previously used in characterization of a relatively unstructured protein segment (Columbus and Hubbell, 2004): $\delta_m = 2.1$ and $\delta_i = 8.4$, corresponding, respectively, to values for a spin label near the end of the disordered carboxyl-terminal sequence of rhodopsin (Langen *et al*., 1999) and the average value of an immobilized, buried residue in a protein undergoing slow rotational diffusion.

A second, metric of spin-label mobility, the quotient of the amplitude of the low-field spectral feature divided by the amplitude of the central feature ($h_{(+1)}/h_{(0)}$), has also been employed in this dissertation. This method of quantitation provides a convenient

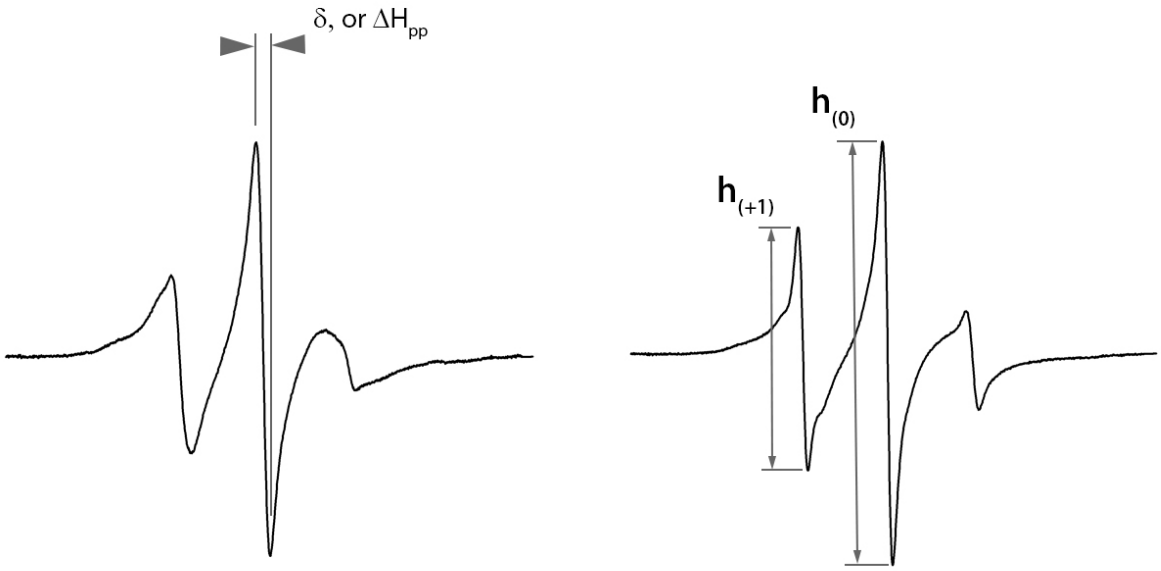

Figure 2-2: **Quantitative comparison of nitroxide EPR spectra**

(Left): the arrows show the measure of the central linewidth (δ or ΔH_{pp}), with units of Gauss. This parameter is used to quantify scaled mobility (M_s). $M_s = (\delta_{exp}^{-1} - \delta_i^{-1}) / (\delta_m^{-1} - \delta_i^{-1})$, where δ_i and δ_m are the central line-widths of a relatively immobile and a relatively mobile nitroxide spectra, respectively, and δ_{exp} is the central linewidth of the position under investigation. For this work the central linewidth values used were δ_m = 2.1 and δ_i = 8.4, corresponding, respectively, to values for a spin label near the end of the disordered carboxyl-terminal sequence of rhodopsin (Langen *et al*., 1999) and the average value of an immobilized, buried residue in a protein undergoing slow rotational diffusion. (Right): the mobility parameter $h_{(+1)}/h_{(0)}$, the quotient of the amplitudes of the low-field and central spectral lines. The parameter is useful for characterization of spectra characteristic of relatively high label mobility (Morin *et al*., 2006).

way to approximate spin-label mobility and has been applied by other research groups to assess similar spectra (Morin *et al*., 2006; Belle *et al*., 2008; Pirman *et al*., 2011). This method of quantitation is imperfect when applied to spectra with conspicuous multiple components arising from heterogeneous label populations, or significant immobilization due to tertiary contact. However ($h_{(+1)}/h_{(0)}$) is a sensitive parameter to assess spin-label mobility for the motional regime characteristic of labels on stable, solvent-exposed alpha-helices and labels on disordered protein regions, thus covering the range of labeled sites expected in this work (Morin *et al*., 2006; Belle *et al*., 2008; Pirman *et al*., 2011). Expected ($h_{(+1)}/h_{(0)}$) values start at around 0.35 for spin-labels at stable solvent-exposed alpha-helical sites (Cooper *et al*., 2008; López *et al*., 2012) and go up to 0.8 or more for labels at disordered sites (Morin *et al*., 2006; Belle *et al*., 2008; Pirman *et al*., 2011; Bartelli and Hazelbauer, 2011; Langen *et al*., 1999).

EPR spectroscopy as a probe of aspartate receptor structure and conformational features

Although still a field in development, the total efforts of EPR spectroscopists have made continuous-wave EPR spectroscopy an accessible technique to probe protein structural features and conformational dynamics. A fortunate coincidence is that the most thoroughly studied of spin-labeled protein sites are solvent-exposed alpha-helices, disordered regions, and loops (Hubbell *et al*., 2013). Thus, a large body of work allows for the direct comparison of EPR results described in this dissertation to the results of others. This dissertation describes two projects where EPR spectroscopy is employed to

resolve features of the *Escherichia coli* aspartate receptor Tar; the first is an exploration of a structurally disordered segment at the carboxyl-terminus (chapter three), the second describes signaling-related conformational features in the alpha-helical cytoplasmic domain (chapter four).

CHAPTER THREE

Direct evidence that the carboxyl-terminal sequence of a bacterial chemoreceptor is an unstructured linker and enzyme tether

ABSTRACT

Sensory adaptation in bacterial chemotaxis involves reversible methylation of specific glutamate residues on chemoreceptors. The reactions are catalyzed by a dedicated methyltransferase and dedicated methylesterase. In *Escherichia coli* and related organisms control of these enzymes includes an evolutionarily recent addition of interaction with a pentapeptide activator located at the carboxyl terminus of the receptor polypeptide chain. Effective enzyme activation requires not only the pentapeptide but also a segment of the receptor polypeptide chain between that sequence and the coiled-coil body of the chemoreceptor. This segment has features consistent with a role as a flexible and presumably unstructured linker and enzyme tether, but there has been no direct information about its structure. We used site-directed spin labeling and EPR spectroscopy to characterize structural features of the carboxyl-terminal 40 residues of *E. coli* chemoreceptor Tar. Beginning ~ 35 residues from the carboxyl terminus and continuing to the end of the protein, spectra of spin-labeled Tar embedded in native membranes or in reconstituted proteoliposomes, exhibited mobilities characteristic of unstructured, disordered segments. Binding of methyltransferase substantially reduced mobility for positions in or near the pentapeptide but mobility for the linker sequence remained high, being only modestly reduced in a gradient of decreasing effects for 10-15 residues, a pattern consistent with the linker providing a flexible arm that would allow enzyme diffusion within defined limits. Thus, our data identify that the carboxyl-terminal linker between the receptor

body and the pentapeptide is an unstructured, disordered segment that can serve as a flexible arm and enzyme tether.

INTRODUCTION

Sensory adaptation is central to the mechanism of bacterial chemotaxis (Hazelbauer *et al*., 2008; Hazelbauer and Lai, 2010). Adaptation is mediated by reversible covalent modification of chemoreceptors, methylation of specific glutamyl residues by methyltransferase CheR, and demethylation/deamidation of those methylesters by methylesterase/deamidase CheB. For *Escherichia coli* and its close relative, *Salmonella enterica*, efficient modification by these enzymes and thus effective chemotaxis requires an activity-enhancing pentapeptide, asparagine-tryptophan-glutamate-threonine or serine-phenylalanine (NWETF or NWESF in the single-letter code), at the receptor carboxyl terminus (Fig. 3-1(B)) (Engström and Hazelbauer, 1980; Yamamoto *et al*., 1990; Wu, *et al*., 1996; Feng *et al*., 1997; Le Moual *et al*., 1997; Barnakov *et al*., 1998; Okumura, *et al*., 1998; Weerasuriya *et al*., 1998; Barnakov *et al*., 1999; Feng *et al*., 1999; Lai, *et al*. 2006; Li and Hazelbauer 2006). This pentapeptide binds the two adaptation enzymes (Wu, *et al*., 1996; Djordjevic and Stock, 1997; Barnakov *et al*., 1999; Barnakov *et al.*, 2001*)*, and in doing so enhances rates of modification for the sequence-bearing receptor as well as for neighboring receptors in the same membrane via adaptational assistance (Le Moual *et al*., 1997; Li *et al*., 1997; Li and Hazelbauer, 2005). Related pentapeptide sequences are found in receptors of other proteobacteria (Alexander and Zhulin, 2007; Perez and Stock, 2007; Wuichet and Zhulin, 2010) and are likely to perform a similar role in enhancing adaptational modification.

The pentapeptide is thought to enhance modification by acting as a high-affinity binding site for the methyltransferase (Wu *et al*., 1996) and as an allosteric activator for the methylesterase (Barnakov *et al*., 2002). High-affinity binding to CheR would restrict diffusion of the enzyme, increasing its effective concentration and consequently the rate of modification (Windisch *et al.*, 2006). Allosteric activation of CheB by the pentapeptide would be expected to involve a ternary complex of pentapeptide, enzyme and the side chain to be modified. Both mechanisms of enhancement imply that the modification enzyme binds the activating pentapeptide at the same time it binds its substrate residue. This simultaneous binding of distant sites on a chemoreceptor is thought to be possible because a linker of 30 - 35 residues between the helical coiled-coil body of the receptor (Kim *et al*., 1999) and the carboxyl-terminal NWETF (Fig. 3-1(A)) could serve as a flexible arm. Flexibility would allow pentapeptide-tethered CheR to reach modification sites on the receptor to which it is bound as well as sites on neighboring receptors (Windisch *et al.*, 2006; Muppirala *et al.*, 2009). It would also allow the pentapeptide to reach CheB docked at a modification site (Barnakov *et al*., 2002). Consistent with this notion, the ability of a carboxyl-terminal NWETF to enhance the action of either enzyme or to enable effective chemotaxis is dependent on the length of the linker (Li and Hazelbauer, 2006). Many linker sequences contain several prolines and are enriched in polar residues, features commonly found in disordered protein segments (Oldfield *et al*., 2005). Furthermore, there is little conservation among linker sequences, even for the same receptor from closely related organisms, in contrast

to substantial sequence conservation over much of the receptor cytoplasmic domain (Fig. 3-1(B)).

The importance of the carboxyl-terminal linker for chemoreceptor function and effective chemotaxis, coupled with the several lines of evidence for its role as a flexible arm, prompted us to investigate its structural features. Since a flexible arm would in essence be an unstructured, disordered segment, we chose an experimental approach that would provide specific measurements for any residue of interest, whether in a structured or unstructured region and that could be applied to intact chemoreceptors in their native or reconstituted membrane environment. Thus we chose site-directed spin labeling and electron paramagnetic resonance (EPR) spectroscopy, a combination that has already provided useful information about disordered protein regions (Langen *et al*., 1999; Zhou *et al*., 2005; Morin *et al*., 2006; Belle *et al*., 2008; Kavalenka *et al*., 2010; Pirman *et al*., 2011), and applied this approach to characterize the carboxyl-terminal segment of the extensively studied aspartate receptor Tar from *E. coli*.

RESULTS

Characterization of a putatively unstructured protein segment

Cysteines were introduced by site-directed mutagenesis into the 40-residue sequence at the carboxyl terminus of chemoreceptor Tar, a protein which otherwise lacks this amino acid, to create a collection of receptors with single cysteines at selected positions in that segment and thus provide a reactive side chain for introduction of a

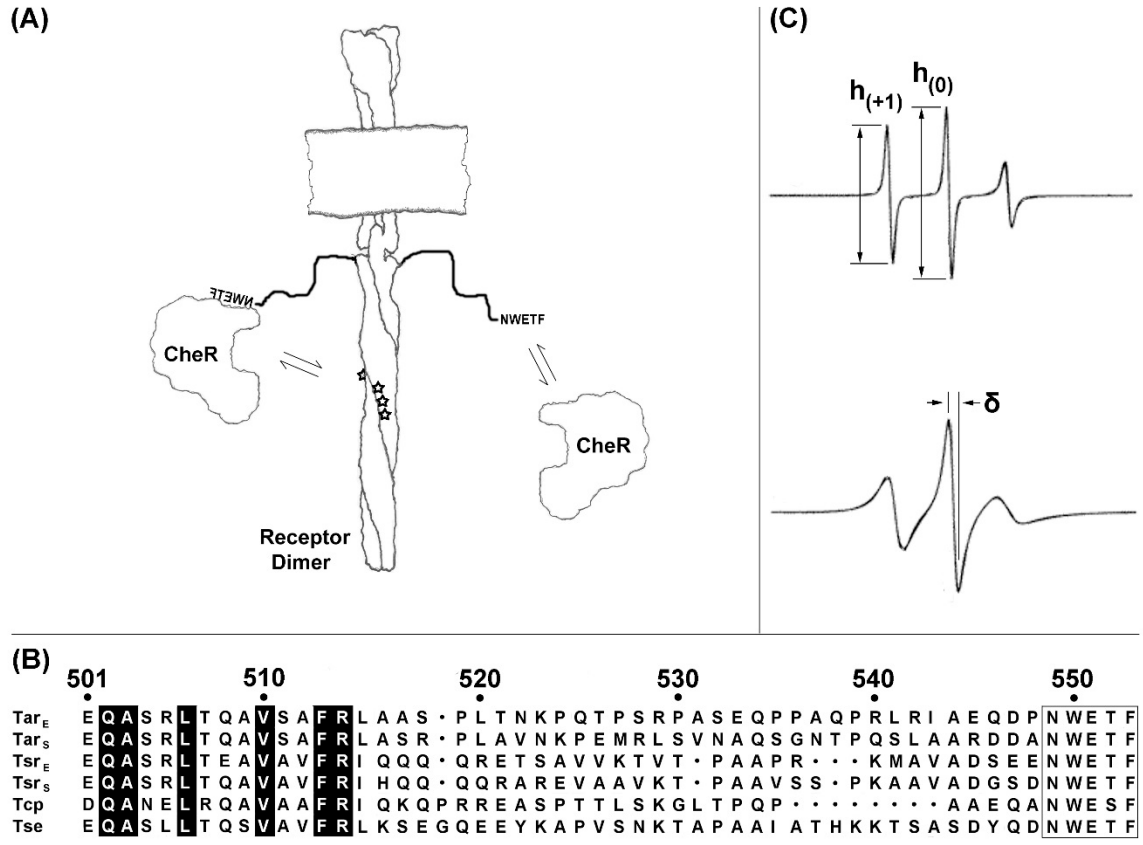

Figure 3-1: Chemoreceptors and EPR spectra

(A) Chemoreceptors and CheR. The cartoon shows a membrane-embedded chemoreceptor dimer with its carboxyl-terminal NWETF pentapeptide unoccupied (right) or bound to methyltransferase CheR (left). Equilibrium arrows indicate interactions of pentapeptide and CheR (right) or tethered CheR with methyl-accepting sites (stars; left). (B) Alignment of carboxyl-terminal sequences of pentapeptide-bearing receptors from *E. coli* and *S. enterica*. Exact matches for the six sequences are highlighted in black and the NWETF/NWESF pentapeptide is boxed. Position numbers are for *E. coli* Tar. (C) Example EPR spectra and illustrations of semiquantitative mobility parameters. The figure shows representative spectra of spin labels in an unstructured protein region (upper spectrum) and at a solvent exposed residue in an alpha helix (lower spectrum; spectra from Columbus and Hubbell, Biochemistry, 2004, 43, 7273–7287, © W.H. Freeman, reproduced by permission). The ratio of the low-field to central peak amplitudes (top spectrum) can be used to derive a semiquantitative mobility parameter $h_{(+1)}/h_{(0)}$. The peak to peak width (δ) of the central line (bottom spectrum) is used to calculate the scaled mobility parameter M_S (see Materials and Methods or Chapter 2).

spin label by reaction with a methanethiosulfonate reagent carrying a nitroxide. Initially, cysteines were placed at five-residue intervals along the segment as well as in place of asparagine in the NWETF pentapeptide and as a one-residue extension following the native carboxyl terminus. Initial spectra indicated a transition from less mobile to more mobile ~ 30 residues from the pentapeptide. To investigate the details of this transition, cysteines were introduced at every position from 514 to 522, except 518 because Tar with a cysteine at that position was produced at too low a level.

Spectra were collected for spin-labeled Tar in two environments: isolated native cytoplasmic membrane vesicles and reconstituted proteoliposomes made with native *E. coli* lipids and pure receptor. Cytoplasmic membrane vesicles were prepared from cells producing high levels of each cysteine-containing Tar. Those membranes were labeled with a nitroxide using a methanethiosulfonate-based reagent. To obtain receptor for reconstitution into proteoliposomes, cysteine-containing forms of Tar were purified from cytoplasmic membrane vesicle preparations utilizing the subunit exchange that occurs between detergent-solubilized forms of the same chemoreceptor (Milligan and Koshland, 1988). Tar heterodimers with one cysteine-containing subunit and one subunit with a carboxyl-terminal six-histidine tag but no cysteine were isolated by mixing detergent-solubilized cytoplasmic membranes containing the two respective receptor forms and purifying these heterodimers (as well as homodimers with two tagged subunits but no cysteine) on a chelated nickel column. Purified receptors were treated with the methanethiosulfonate spin-labeling reagent and reconstituted into proteoliposomes. Formation of heterodimers by subunit exchange allowed purification

of multiple cysteine-substituted forms of Tar using the histidine tag on one subunit in combination with characterization of spin-labeled sites on the subunit with a native carboxyl terminus, thus avoiding the presence of a six-histidine extension that could potentially perturb the linker region (Lai and Hazelbauer, 2005). The alternative, placing the affinity tag at the amino terminus, was not feasible because tags at this location resulted in low levels of protein production (A. Lilly, M. Li and G.L. Hazelbauer, unpublished data). Each preparation of spin-labeled, reconstituted Tar was assessed for structural perturbations by determining extents of deamidation and thus structural recognition by phosphorylated CheB. Approximately half the Tar for each variant (54% ± 3%) was modified, essentially the proportion expected to be accessible to added enzyme if the receptor were randomly oriented in reconstituted proteoliposomes and approximately the accessible proportion of vesicle-inserted Tar lacking a cysteine and a spin label. In any case, the data indicated that receptors with cysteines and thus spin labels at different positions were not differentially perturbed in the course of reconstitution and thus mobilities could be compared directly.

Patterns of EPR spectra for the carboxyl-terminal segment of chemoreceptor Tar

EPR spectra were collected for spin-labeled cysteines at 16 different positions in the final 40 residues of chemoreceptor Tar, including a one-residue carboxyl-terminal cysteine extension. Each spin-labeled receptor was characterized in the native, multi-protein environment of the cytoplasmic membrane (Fig. 3-2) and as the sole protein inserted in reconstituted proteoliposomes (Fig. 3-3). Spectra collected from Tar in

native membrane included a low mobility component from spin labels attached to membrane proteins other than Tar (Fig. 3-2, spectra in dashed-line box). Fortunately this component was sufficiently different from the contributions of spin-labeled Tar that effects of varying the position of the spin label along the linker sequence were clearly evident in the respective spectra and these effects corresponded to those observed for purified Tar inserted in proteoliposomes (Figs. 3-2 and 3-3). In both native membrane and reconstituted proteoliposomes, spectra for positions 514 through 519 had features characteristic of the reduced mobility observed for side chains in structured regions of a protein. In contrast, positions beginning at 520 and extending over 30 residues to the carboxyl terminus had spectra characteristic of the high mobility of side chains in unstructured protein regions (Langen *et al., 1999*; Columbus and Hubbell, 2002*;* Zhou, *et al*., 2005; Morin *et al*., 2006; Belle *et al*., 2008). The pattern of lower mobility for positions through 519 and high mobility thereafter is further illustrated in Fig. 3-4 by two semi-quantitative mobility parameters, M_s, the normalized central line width (Hubbell *et al*., 2000) and $h_{(+1)}/h_{(0)}$, the ratio of the heights of the low-field and central lines (Morin *et al*., 2006) (Fig. 3-1(C)). The slightly lower parameter values for Tar in native membrane versus proteoliposomes likely reflect the influence on the mobility parameters of the lower mobility background spectra in membrane. For positions 520 and beyond, the magnitudes of the M_s values (Fig. 3-4(A)) were comparable to those

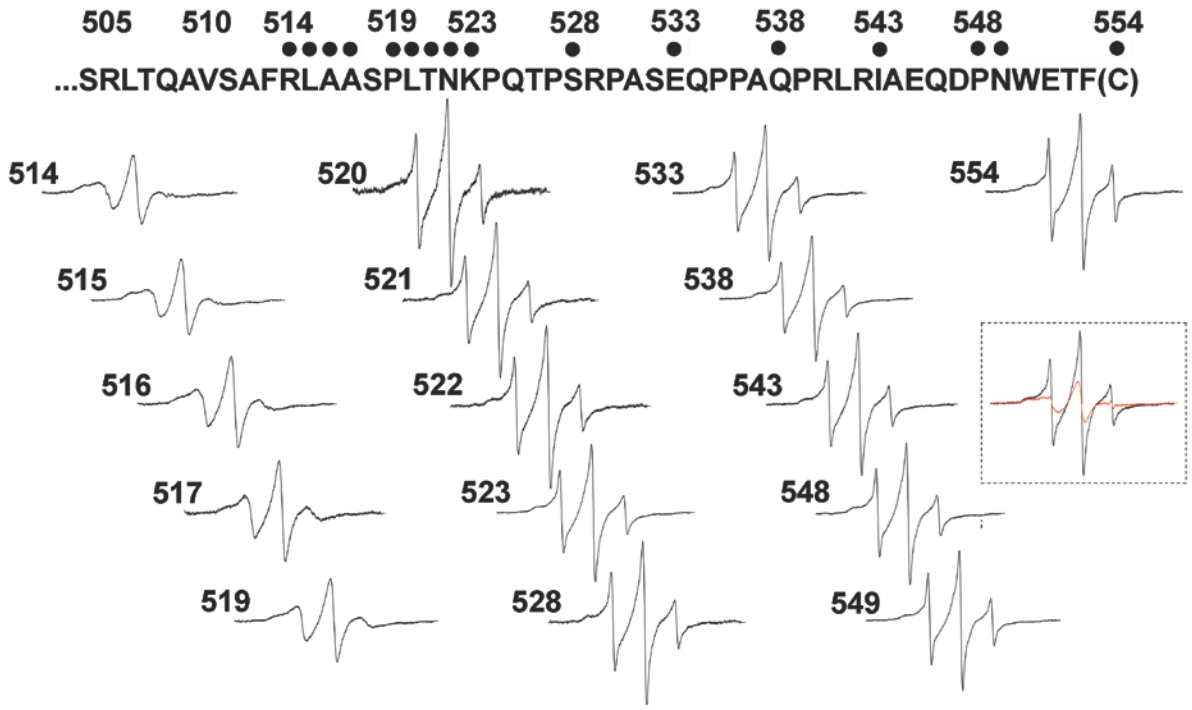

Figure 3-2: Spectra of spin-labeled Tar in native membrane vesicles

Normalized EPR spectra for 16 positions in the Tar carboxyl terminal segment, identified with dots on the sequence above the spectra and position numbers, are shown for receptor embedded in isolated native membrane. The red spectrum in the dashed-line box is derived from membranes, containing Tar with no cysteine, prepared and treated with the spin-labeling reagent in the same way as membranes with cysteine-containing Tar.

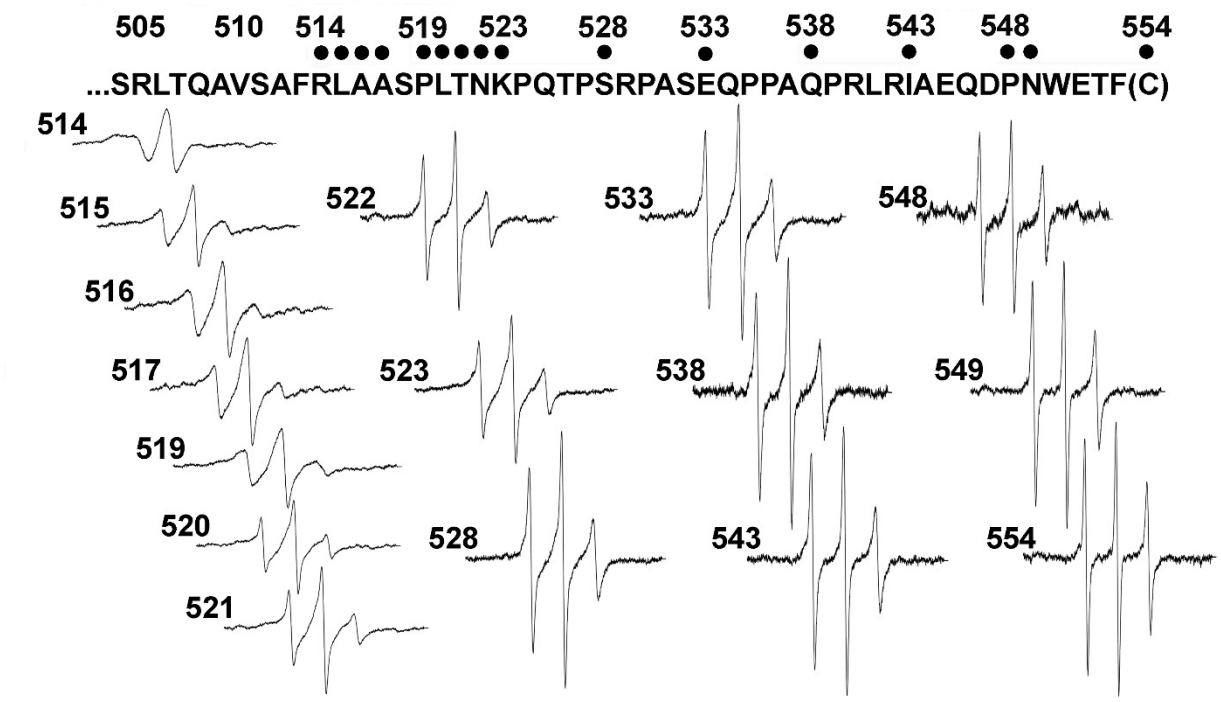

Figure 3-3: EPR spectra of purified, spin-labeled Tar reconstituted into proteoliposomes

Normalized EPR spectra, in Fig. 3.2, are shown for purified Tar reconstituted into proteoliposomes.

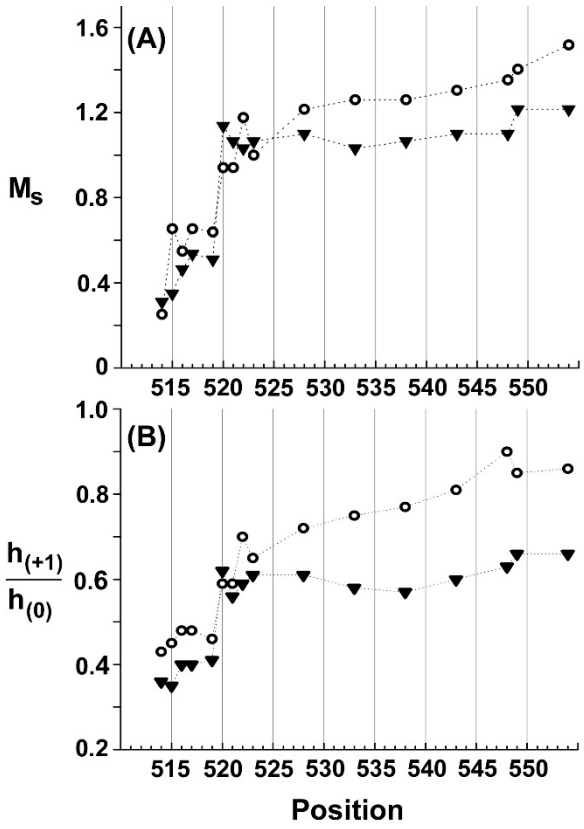

Figure 3-4: Mobility parameters as a function of spin label position for Tar in native vesicles or proteoliposomes

The parameters scaled mobility, M_S (A) and $h_{(+1)}/h_{(0)}$ (B), derived from the spectra in Figs. 3.2 and 3.3, are plotted as a function of spin label position for Tar in native vesicles (closed triangles) or proteoliposomes (open circles). See Materials and Methods or Chapter 2 for descriptions of the parameters. Dotted lines are provided to aid the eye.

observed for highly mobile, unstructured segments in other proteins (Columbus and Hubbell, 2004; Kim *et al*., 2007), as were the magnitudes of $h_{(+1)}/h_{(0)}$ (Fig. 3-4(B)) (Morin *et al*., 2006; Belle *et al*., 2008; Kavalenka *et al*., 2010; Pirman *et al*., 2011). Thus, both qualitative and quantitative assessment of the spectra indicated that the carboxyl terminal sequence of Tar, beginning at approximately position 520 had the features of an unstructured and thus disordered segment.

Test for lack of structure: effects of denaturing urea

To probe the notion that the carboxyl-terminal sequence of Tar beginning at position 520 was essentially unstructured, selected spin-labeled proteins embedded in their native membrane environment were exposed to 5M urea and spectra compared before and after addition of denaturant. For positions 514, 515 and 517, locations at which spectra were characteristic of a structured region, denaturant generated major spectral changes, indicating significant increases in mobility, presumably reflecting loss of regular structure (Fig. 3-5, left-hand spectra). For positions 528, 549 and 554, locations at which the spectra were characteristic of lack of structure, urea generated little change (Fig. 3-5, right-hand spectra), consistent with those positions being in an unstructured, naturally disordered segment and thus not significantly affected.

Effects of CheR on mobility of the carboxyl-terminal segment

Figure 3-5: Effects of denaturant on EPR spectra of spin-labeled Tar

Normalized spectra for Tar in native membranes with spin labels at the indicated positions are shown in the absence (black) and presence (red) of 5M urea. Spectra were corrected for spin labels on other membrane proteins by subtracting the spectrum of native membrane vesicles containing Tar devoid of cysteine and treated with the spin-label reagent in the same way as vesicles containing the respective cysteine-containing form of Tar, scaled to total protein.

The carboxyl-terminal linker is thought to enhance CheR action by serving as a flexible arm that restricts diffusion of pentapeptide-bound enzyme to a volume near the receptor but allows diffusion within that volume and thus increases the probability of enzyme interaction with substrate sites on the receptor body (Wu *et al.*, 1996; Windisch *et al.*, 2006; Muppirala *et al.*, 2009). The effect of CheR binding on mobility of the carboxyl-terminal segment of Tar was probed by collecting EPR spectra of spin-labeled receptors in the presence of a high concentration of CheR. Pentapeptide interacts with CheR by becoming the fourth strand of a beta-sheet in an enzyme subdomain (Djordjevic and Stock, 1998) and thus should become significantly less mobile upon binding. This was the case. CheR binding significantly broadened spectra of spin labels within (549) or at the carboxyl terminus (554) of the pentapeptide (Fig. 3-6) and reduced the mobility parameters M_s and $h_{(+1)}/h_{(0)}$ (Fig. 3-7). About 50% of the population of spin-labeled Tar was expected to be occupied by CheR since this proportion was accessible in proteoliposomes (see above). Fortunately, the magnitudes of the changes in mobility upon CheR binding were sufficiently large to be easily detected even with ~50% occupancy, although the strong influence of the most mobile component on the central line width meant that the proportional change was less for M_s than for $h_{(+1)}/h_{(0)}$. Enzyme binding also reduced mobility of the linker, in a gradient of decreasing effects over 10 to 15 residues from the site of enzyme binding (Fig. 3-7), as might be expected for attaching the end of a flexible arm to a relatively large mass.

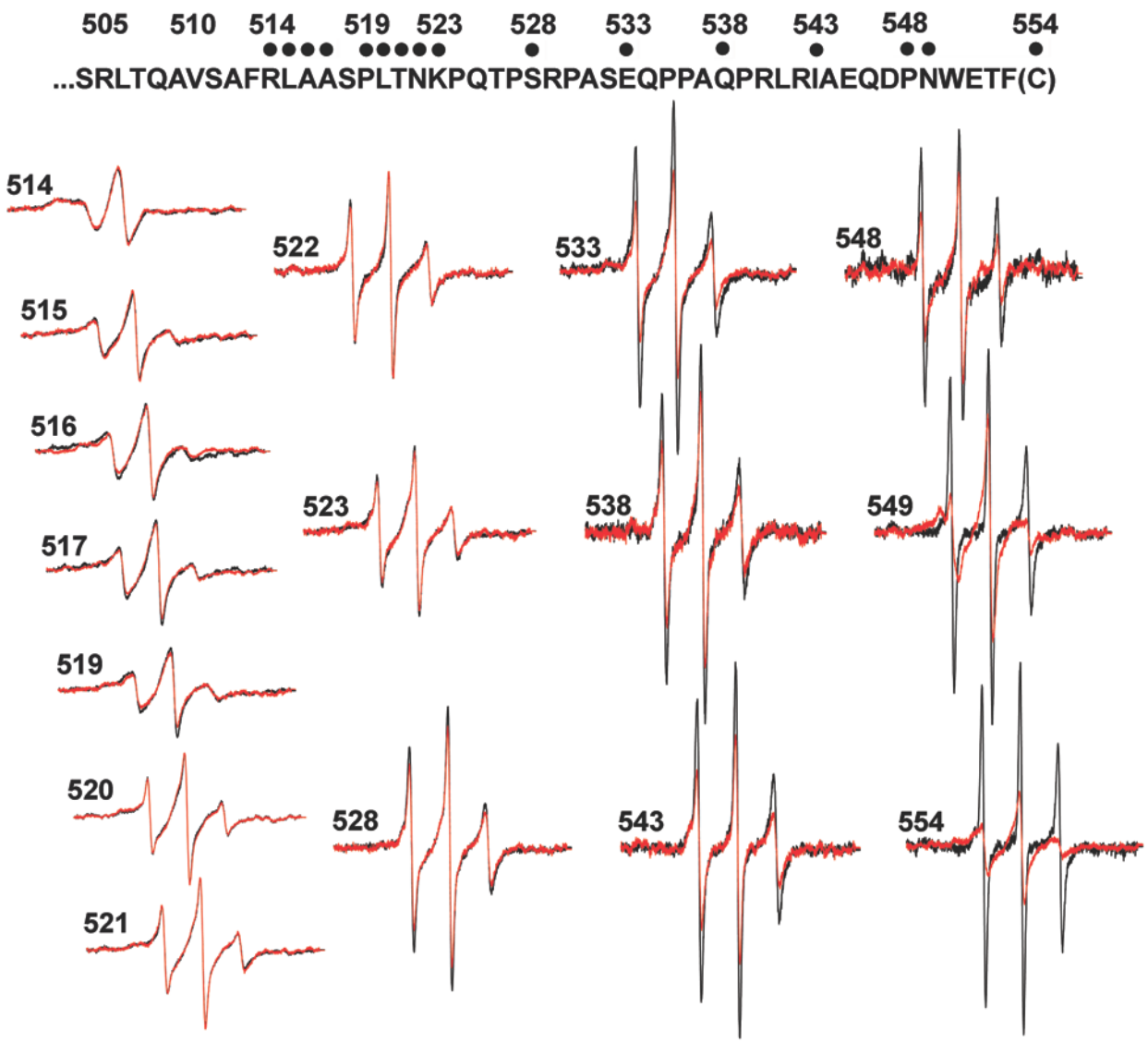

Figure 3-6: Effects of CheR on EPR spectra of spin-labeled Tar

Normalized spectra for purified Tar in reconstituted proteoliposomes with spin labels at the indicated positions are show in the absence (black) and presence (red) of CheR at a concentration sufficient to occupy ~ 97% of accessible Tar-borne pentapeptide.

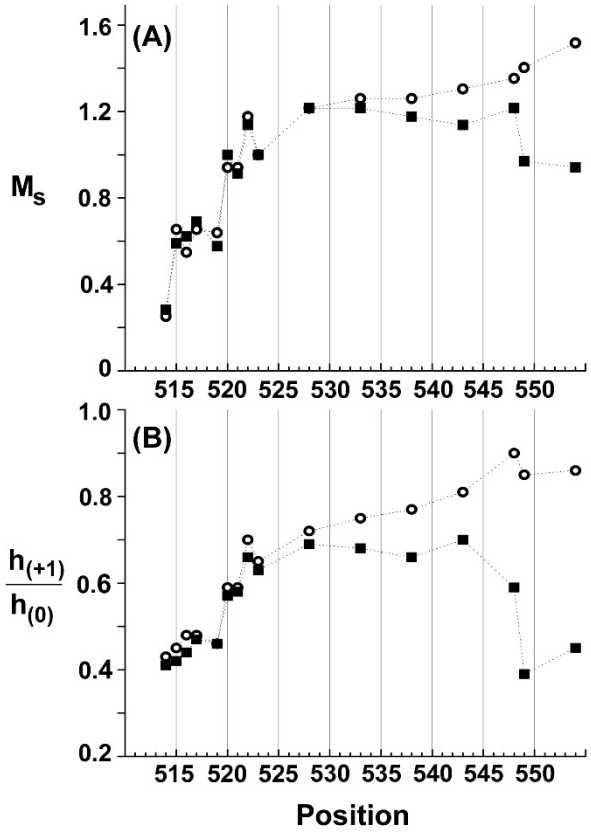

Figure 3-7: Effects of CheR on mobility parameters of spin-labeled Tar

Mobility parameters M_S (A) and $h_{(+1)}/h_{(0)}$ (B) derived from the spectra in Fig. 3.6 are plotted as a function of spin label position for Tar in proteoliposomes in the absence (open circles) or presence (filled squares) of excess CheR.

To determine whether the effects observed upon addition of CheR reflected specific binding to the carboxyl-terminal pentapeptide, a competition experiment was performed using excess free peptide. This synthetic peptide, EENWETF, had the sequence of the final seven residues of *E. coli* chemoreceptor Tsr (Lai *et al*., 2006) and was soluble at the required high concentrations, presumably due to the two amino-terminal glutamyl residues. Addition of a ~10- fold excess of this free heptapeptide relative to receptor-borne pentapeptide essentially eliminated the otherwise drastic effects of CheR on spectra for positions 549 and 554 (Fig. 3.8), providing strong evidence that CheR was indeed binding at its physiologically relevant site. Excess competing peptide also eliminated the more subtle effect of CheR on a linker position, 543, which is outside the enzyme-binding site, indicating that effects on linker mobility were also the result of physiologically relevant binding.

DISCUSSION

An unstructured, flexible linker

Site-directed spin labeling and electron paramagnetic resonance measurements were used to investigate the carboxyl-terminal 40 residues of chemoreceptor Tar, a segment for which there was no direct structural information for any chemoreceptor. EPR spectra collected for 16 positions (Figs. 3-2 and 3-3) and semi-quantitative parameters characterizing those spectra (Fig. 3-4) indicated that much of the segment was notably mobile, beginning at approximately position 520 and extending to the

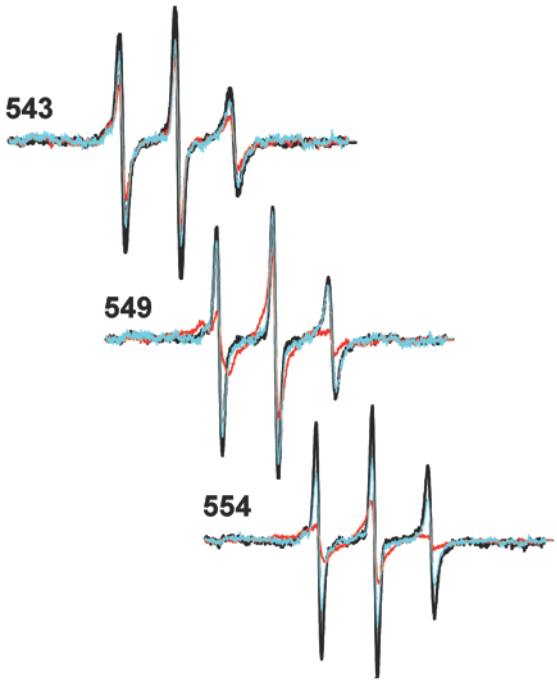

Figure 3-8: Effects of a competitor peptide on CheR-induced changes in spectra of spin-labeled Tar

Normalized spectra for purified Tar, with spin labels at the indicated positions, in reconstituted proteoliposomes are shown without additions (black), with CheR at a concentration calculated to occupy ~ 97% of accessible Tar-borne pentapeptide NWETF (red) and with CheR at the same concentration plus peptide EENWETF at a ten-fold excess relative to Tar-borne pentapeptide (cyan).

carboxyl terminus. The possibility cannot be excluded that introduction of spin-labeled cysteines at positions 520 and beyond disrupted weak structure or weak interactions, but the possibility seems unlikely, since a large body of data has revealed that site-directed spin labeling seldom disrupts protein structure (Altenbach *et al*., 1994; Hubbell *et al*., 1996; Hubbell *et al*., 1998; Columbus and Hubbell, 2002). Thus the conclusion is that the final ~34 carboxyl-terminal residues of Tar constitute an essentially unstructured, disordered region. This lack of stable structure means that the Tar carboxyl-terminal linker has the features of a flexible arm and enzyme tether between the coiled-coil receptor body and the NWETF recognition sequence at the carboxyl terminus (Fig. 3-9).

The semi-quantitative mobility parameters, M_s and $h_{(+1)}/h_{(0)}$ highlighted an abrupt transition from structured to unstructured, occurring primarily between positions 519 and 520 (Fig. 3-4). For purified, spin-labeled Tar inserted in proteoliposomes and thus separated from the interfering background of spin labels on other membrane proteins, the parameters indicated that after the abrupt transition from lower to higher values, mobility continued to increase gradually, as would be expected for an unstructured polypeptide tethered at one end (Columbus and Hubbell, 2004). In native Tar, the transition from structured to unstructured might well begin one residue prior to position 520 because position 519 in the natural sequence is a proline, often a helix breaker. In any case, a boundary between structured and unstructured segments at residues 519-520 is consistent with effects of a family of nested deletions within the Tar carboxyl-terminal linker which all began at the amino terminus of the pentapeptide and

extended toward the receptor body (Li and Hazelbauer, 2006). Kinase activation was significantly reduced only for deletions extending past position 519, implying that only after this position did deletions disrupt the receptor and thus its ability to activate kinase (Li and Hazelbauer, 2006). An additional correlation is provided by the crystal structure of a fragment of the cytoplasmic domain of *E. coli* chemoreceptor Tsr, in which the transition from resolved to unresolved residues occurred in the carboxyl-terminal segment at the position corresponding to Tar residue 518 (Kim *et al*., 1999).

Tethered CheR

The carboxyl-terminal, enzyme-binding pentapeptide in combination with the linker sequence between the pentapeptide and the coiled-coil receptor body are thought to act in concert to enhance action of methyltransferase CheR by binding enzyme and providing a flexible tether that restricts diffusion of bound CheR to a volume near methyl-accepting sites (Windisch *et al*., 2006; Muppirala *et al.*, 2009). CheR binding to pentapeptide at the Tar carboxyl terminus had the expected effect of substantially reducing mobility of a residue within and following the NWETF recognition sequence but reduced only modestly mobility of the linker, in a gradient of decreasing effects for approximately half its length (Figs 3-6 and 3-7). This pattern supports the notion that NWETF-bound CheR is connected to the receptor body by a flexible tether that allows relatively unimpeded diffusion within specific limits and thus increases effective enzyme concentration near substrate sites and thus enzyme action (Wu *et al.*, 1996; Windisch *et al*., 2006; Muppirala *et al.*, 2009).

Experimental strategies

The spin-labeled chemoreceptor Tar was assayed in two membrane environments: 1) native cytoplasmic membrane and 2) reconstituted proteoliposomes. The complementary features of these preparations provided internal checks on validity of our data and deductions. Characterization of Tar embedded in isolated cytoplasmic membrane had the advantage that receptor was in its native membrane environment but the disadvantage that EPR spectra included contributions from other spin-labeled proteins. Characterization of purified Tar reconstituted into proteoliposomes greatly reduced contributions by spin labels on other proteins but introduced the possibility that receptor was perturbed by purification and reconstitution. However, spectra for respective Tar positions shared many essential features, independent of environment and patterns as a function of spin label position were very similar for the two environments. This provided confidence that common spectral features were providing information about the structure of native chemoreceptor.

Subunit exchange among detergent-solubilized forms of the same chemoreceptor, first documented over 20 years ago (Milligan and Koshland, 1988), was effective in creating heterodimers with a targeted feature segregated to one of two respective subunits. For our purposes, these were an affinity tag and a single cysteine for spin labeling on a subunit that had an otherwise unchanged carboxyl terminus. Many other features would be possible, depending on the particular experimental design. Thus this strategy could be useful for future studies.

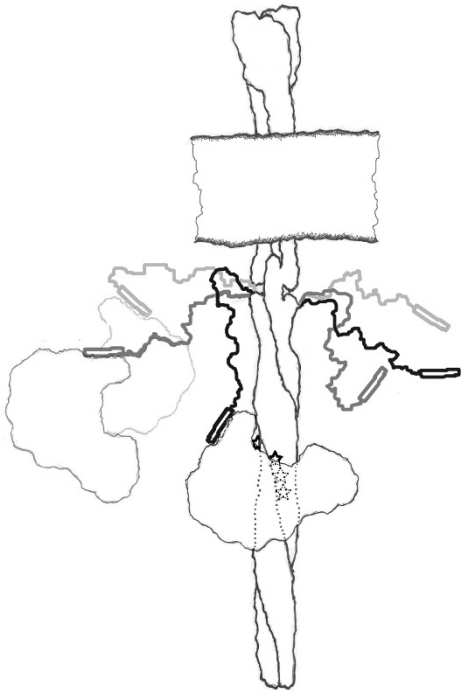

Figure 3-9: A flexible arm and enzyme tether

Cartoon of a membrane-imbedded chemoreceptor illustrating the principle conclusions of this study, that the carboxyl terminal ~ 35 residues of chemoreceptor Tar is a disordered, flexible arm (right-hand carboxyl terminal segment, shown in three snapshots) that can act as a flexible tether for CheR bound to the carboxyl-terminal NWETF pentapeptide (open rectangle) (left-hand carboxyl terminal segment, shown in three snapshots bound to CheR).

MATERIALS AND METHODS

Strains, plasmids and proteins

E. coli K-12 strains RP3808 (Slocum and Parkinson, 1983) and RP3098 (Parkinson and Houts, 1982) carry, respectively, a deletion from *cheA* to *cheZ* that eliminates all *che* genes or a deletion from *flhA* to *flhD* that eliminates the presence or expression of all chemoreceptor and *che* genes. Plasmid pNT201 carries *tar* under control of a modified *lac* promoter and $lacI^q$ (Borkovich *et al*., 1989). A derivative, pAL533, codes for Tar with six histidines added to its carboxyl terminus and glutamines (Q in the single letter code) at all four sites of modification (Tar4Q-6H). Other derivatives, that code for Tar with the wild-type pattern of QEQE at the modification sites and a single introduced cysteine at the indicated position are pAL671 (R514C), pAL672 (L515C), pAL673 (A516C), pAL674 (A517C), pAL675 (P519C), pAL689 (L520C), pAL690 (T521C), pAL691 (N522C), pAL655 (K523C), pAL657 (S528C), pAL656 (E533C), pAL658 (Q538C), pAL659 (I543C), pAL660 (P548C) and pAL661 (Tar 554C). Table 3-1 details all cysteine substitutions generated for the work described in this chapter.

CheR was purified from RP3808 containing pME43 (Simms *et al*., 1987). Luria broth was inoculated at ~ 5 x 10^7 cells per mL and incubated for ~5.5 hours at 35° C with vigorous aeration. The culture was chilled in an ice-water bath and centrifuged 8,000 rpm, 12 min, 4° C in a SLC 6000 rotor. Sedimented cells were suspended in 50 mM Tris-HCl (pH 7.5), 0.5 mM EDTA, 2 mM DTT and 10 % glycerol (TEDG), centrifuged as before, suspended in TEDG with additions of EDTA, PMSF and lysozyme to 5 mM, 1 mM and 0.15 mg/mL, respectively, incubated 40 min on ice and centrifuged 60,000 rpm, 2 hr, 4°

C in a Ti 60 rotor. The supernatant was concentrated in a Centriprep Ultracel YM-10, 10 kDa MWCO (Millipore, Billerica, MA) at 3,000 rpm and 4° C, dialysed against TEDG overnight at 10° C and flash frozen in liquid nitrogen. Concentrated lysate was thawed, diluted ten-fold in 20 mM sodium phosphate (pH 7.0), 1 mM EDTA, 1 mM DTT, 0.5 mM PMSF (column buffer) at 4° C and applied at 2.5 mL/min and 7° C to two 5 mL Hi Trap SP HP columns (GE Healthcare, Little Chalfont, UK) in tandem, equilibrated with 5 bed volumes of column buffer at 5 mL/min and coupled to a P-1 peristaltic pump (Pharmacia) and a UV monitor. The column was washed with column buffer at 5 mL/min until A_{280} returned to a baseline value and eluted with a step gradient of 40 mM, 80 mM, 120 mM, 160 mM, 200 mM and 2M NaCl in column buffer with each higher salt concentration applied once A_{280} returned to a baseline value. Fractions containing CheR, as assessed using SDS polyacrylamide gel electrophoresis, were pooled, concentrated with an Ultra15, 10 kDa MWCO concentrator (Millipore, Billerica, MA) by centrifugation in an SS-34 rotor at 5000 x g, 9° C setting, brought to 10% w/v glycerol, dialyzed overnight against 50 mM Tris-HCl (pH 7.5), 0.5 mM EDTA, 2 mM DTT, 10% w/v glycerol at 7° C and stored at -80° C. The resulting preparation was ~98 % CheR as estimated by relative intensities of enzyme and contaminants on SDS polyacrylamide gels.

Isolation and spin labeling of receptor-containing cytoplasmic membranes

Cytoplasmic membrane vesicles enriched for each form of Tar were isolated from RP3098 harboring the appropriate plasmid, using cell culture conditions, osmotic lysis

and a sucrose gradient as described (Boldog *et al*., 2007). Vesicles were suspended in 50 mM Tris-HCl (pH 7.5), 0.5 mM EDTA, 2 mM DTT and 10% glycerol, flash frozen in liquid nitrogen and stored at -70° C**.** Tar content and total protein content were determined by quantitative immunoblotting (Li and Hazelbauer, 2005) and BCA assays, respectively. Depending upon the particular form of Tar and preparation, receptor was 20-40% of total membrane protein. Membranes containing 600 µg of Tar were diluted to 1 mL in 50 mM Tris-HCl (pH 7.5), 0.5 mM EDTA, 100 mM NaCl, 10% glycerol and centrifuged 15 min, 100,000 RPM in a TL100.2 rotor at 4° C. The pellet was suspended in 1 mL of the same buffer and the process repeated twice more to yield a calculated DTT concentration < 1 µM. Methanethiosulfonate spin label reagent (Toronto Research Chemicals, North York, Canada) was added to 100 µM, a 10-fold molar excess over Tar, and the mixture incubated 1 hr on ice in the dark. Unreacted spin label was removed by centrifugation and suspension as for the removal of DTT, and the labeled vesicles suspended to ~50 µL of the same buffer.

Spectra for each respective spin-labeled forms of Tar were similar in native membrane and reconstituted proteoliposomes, and the same pattern of spectral features was evident in both conditions as a function of spin label position. This indicated that the spectra of spin-labeled native membrane provided information about the receptor, even though Tar was only 20-40 % of total protein. In fact, comparison of spectra for the respective forms of Tar revealed that those from native membrane included a lower mobility component, likely from spin labels on non-Tar membrane proteins. This was confirmed by spectra of membranes, containing Tar with no cysteine,

prepared and treated with the spin-labeling reagent in the same way as membranes with cysteine-containing Tar (Fig. 2, spectra in dashed-line box). We could not be confident of the precise extent of background contribution for any particular membrane preparation and thus subtraction of spectral features contributed by proteins other than Tar would have been arbitrary and might have distorted the data. Fortunately, because spin labels on the Tar linker were notably mobile, background subtraction was not necessary to observe distinct effects of varying the spin label position. Thus, in Fig. 2 we show spectra that have not been processed to remove contributions from spin labels on non-receptor proteins.

Protomer exchange, purification and spin labeling

Two preparations of cytoplasmic membranes, one containing Tar4Q-6H and the other a cysteine-substituted Tar were mixed to provide a 1:1 receptor ratio and 4 mg at 1.5 mg/mL of each receptor in 50 mM Tris-HCl (pH 7.5), 10% glycerol, 2 µM pepstatin, 2 µM leupeptin, 5 µM TLCK and 100 µM PMSF. Beta-D-octyl-glucoside was added to 5.5%, the mixture incubated 1 hr on ice and centrifuged 15 min, 100,000 RPM, 4° C in a TL100.2 rotor. The supernatant was transferred to a new tube, aspartate added to 1 mM to block subunit exchange (Milligan and Koshland, 1988) and the solution applied to a 4 mL bed volume Ni-NTA column equilibrated with 4 bed volumes 50 mM Tris-HCl pH 7.5, 10% glycerol, 100 mM NaCl, 25 mM cholate, 30 mM imidazole, 1 mM aspartate (Buffer A). Four bed volumes of Buffer A and eight volumes of Buffer B (Buffer A with 300 mM imidazole) were passed through the column and 4 mL fractions collected. The

first three fractions following application of Buffer B, which contained the majority of Tar, were combined, spin-label reagent in acetonitrile added at a 5-fold molar excess over the maximum possible amount of cysteine-substituted Tar, the mixture incubated 1 hr on ice in the dark, concentrated to < 1 mL and buffer exchanged using a Nap10 column (GE Healthcare, Little Chalfont, UK) to 50 mM Tris-HCl (pH 7.5), 0.5 mM EDTA, 100 mM NaCl, 25 mM cholate, 10% glycerol, the solution concentrated to ~ 200 µL and stored at -80° C. The resulting Tar dimers were approximately two-thirds heterodimers, consisting of one cysteine-containing, spin-labeled protomer with a natural carboxyl terminus and one histidine-tagged protomer lacking a cysteine, and approximately one-third homodimer, consisting of two histidine-tagged subunits devoid of cysteines and thus no spin label. The proportion of the two Tar forms was determined by SDS polyacrylamide gel electrophoresis, exploiting their differential mobility. Purified Tar was quantified by comparison of intensities of Coomassie Brilliant Blue staining of bands on an SDS polyacrylamide gel to a Tar standard quantified by amino acid analysis.

Reconstitution into proteoliposomes

Detergent-solubilized, spin-labeled Tar was reconstituted into lipid bilayers by combining 1 mg of receptor with *E. coli* lipids (Avanti Polar Lipids, Alabaster, AL), solubilized in 150 mM cholate, in 1 mL of 50 mM Tris-HCl (pH 7.5), 0.5 mM EDTA, 100 mM NaCl, 10% glycerol, 80 mM cholate, 1 µM pepstatin, 1 µM leupeptin, 17 mM *E. coli* lipids and 17 µM spin-labeled Tar. Detergent was removed (Rigaud *et al*., 1998) by adding 1 mL of SM-2 Biobeads (Bio-Rad, Hercules, CA) and incubating with rotation for

1.5 hr, 10° C. Biobeads were removed as described (Boldog *et al*., 2007), 1 mL new Biobeads added and the mixture incubated and processed as before. Resulting proteoliposomes were sedimented by centrifugation 15 min, 100,000 RPM, 10° C in a TL100.2 rotor, suspended in 50 mM Tris-HCl (pH 7.5), 0.5 mM EDTA, 100 mM NaCl, 10 % glycerol and frozen at -80° C. The ability of this procedure to incorporate Tar into proteoliposomes was verified by floatation in a metrizamide gradient. Each preparation of proteoliposome-inserted Tar was assayed for recognition and thus modification by phosphorylated CheB in conditions designed to modify all sites on all accessible and native Tar as described (Li and Hazelbauer, 2006), except that receptor was 30 nM, CheB in the absence of DTT was 1.5 μM and phosphoramidate 50 mM.

EPR spectroscopy

X-band spectra were collected at 20 mW incident microwave power using a Brüker EMX spectrometer (Billerica, MA) equipped with a high-sensitivity resonator. Data for Tar imbedded in membrane vesicles or proteoliposomes were collected with a 100-kHz field modulation of 1 G or 1.2, 1.8 or 2.4 G, respectively. For spectra collected from spin-labeled Tar in proteoliposomes, a low background of non-specific labeling was subtracted (Do Cao *et al*., 2009) using spectra of proteoliposomes made with Tar lacking cysteine acquired for the same Tar concentration, conditions and field modulation as the respective experimental samples. Data processing was performed with Labview software (Christian Altenbach, University of California, Los Angeles). For final data processing and comparisons, spectra were normalized to the same total spins.

For spectra in the presence of CheR, DTT in the CheR storage buffer was reduced to a calculated concentration of < 50 nM by repeated concentration and dilution with the buffer in which proteoliposomes were stored using a 10 kDa-cutoff Nanosep concentrator (Pall Life Sciences, Port Washington, NY). CheR was added to spin-labeled Tar in proteoliposomes at a concentration calculated to occupy ~ 97% of accessible, receptor-borne pentapeptides and thus ~50% of total receptor, since ~ 50% of spin-labeled Tar incorporated into proteoliposomes was accessible (see RESULTS).

Semi-quantitative measures of mobility

M_s is a measure of mobility of a nitroxide spin label at a position of interest normalized to a relatively mobile and a relatively immobile protein-coupled nitroxide. Specifically, $M_s = (\delta_{exp}^{-1} - \delta_i^{-1}) / (\delta_m^{-1} - \delta_i^{-1})$, where δ_i and δ_m are the central line-widths of a relatively immobile and a relatively mobile nitroxide spectra, respectively, and δ_{exp} is the central linewidth of the position under investigation (Columbus and Hubbell, 2002; Hubbell *et al*., 2000). For the analysis of our data we utilized values of the constants previously used in characterization of an unstructured protein segment (Columbus and Hubbell, 2004): $\delta_m = 2.1$ and $\delta_i = 8.4$, corresponding, respectively, to values for a spin label near the end of the disordered carboxyl-terminal sequence of rhodopsin (Langen *et al*., 1999) and the average value of an immobilized, buried residue in a protein undergoing slow rotational diffusion. The mobility parameter $h_{(+1)}/h_{(0)}$, the ratio of amplitudes of the low-field and central spectral lines (Fig. 1C), has been used in

characterization of unstructured protein segments (Morin *et al*., 2006; Belle *et al*., 2008; Pirman *et al*., 2011).

Position	Modification	HB number	Plasmid	Strain
514	QEQE	HB4118	pAL671	RP3098
514	QEQE	HB4123	pAL671	CP362
515	QEQE	HB4119	pAL672	RP3098
515	QEQE	HB4124	pAL672	CP362
516	QEQE	HB4120	PAL673	RP3098
516	QEQE	HB4125	PAL673	CP362
517	QEQE	HB4121	pAL674	RP3098
517	QEQE	HB4126	pAL674	CP362
519	QEQE	HB4122	pAL675	RP3098
519	QEQE	HB4127	pAL675	CP362
520	QEQE	HB4149	pAL689	RP3098
521	QEQE	HB4150	pAL690	RP3098
522	QEQE	HB4151	pAL691	RP3098
523	QEQE	HB4085	pAL655	RP3098
523	QEQE	HB4095	pAL655	CP362
528	QEQE	HB4087	pAL657	RP3098
528	QEQE	HB4097	pAL657	CP362
533	QEQE	HB4086	pAL656	RP3098
533	QEQE	HB4096	pAL656	CP362
538	QEQE	HB4088	pAL658	RP3098
538	QEQE	HB4098	pAL658	CP362
543	QEQE	HB4089	pAL659	RP3098
543	QEQE	HB4099	pAL659	CP362
548	QEQE	HB4090	pAL660	RP3098
548	QEQE	HB4100	pAL660	CP362
549	QEQE	HB4152	pAL692	RP3098
554	QEQE	HB4091	pAL661	RP3098
554	QEQE	HB4101	pAL661	CP362

Table 3-1: Tar cysteine substitutions generated to probe carboxyl-terminal structure

Note that no Tar construct on this list has a histidine tag.

CHAPTER FOUR

Conformational signaling in the Tar cytoplasmic domain

INTRODUCTION

Signal transduction in bacterial chemoreceptors involves the communication of ligand occupancy information from the periplasmic ligand-binding site to an associated cytoplasmic kinase CheA approximately 300 Å away. In active signaling complexes ligand-recognition biases the receptor conformation to a state that inhibits the otherwise active CheA kinase and thus phosphorylation of the response regulator CheY. Covalent modifications at specific sites in the receptor cytoplasmic domain also modulate activity of the associated kinase. This phenomenon influences the efficiency of coupling ligand occupancy to kinase control and the intrinsic degree of kinase activating potential, thus these modifications serve to tune the responsiveness of chemoreceptors (Bornhorst and Falke, 2001). This is how motile cells adapt to sensory signals and is a crucial feature of chemotaxis, as adapted receptors are then tuned to respond to further changes in ligand occupancy.

In the simplest model chemoreceptor signaling can be described by a two-state system where one receptor conformation is kinase-activating and the other kinase-inactivating. The features of ligand occupancy and adaptational modification influence the distribution of receptors in these states. This section will review what is currently known about chemoreceptor signaling with an emphasis on what is known regarding receptor structural features. The reader is directed to figure 4-1 as a guide to receptor functional regions and their location in the receptor structure.

Conformational signaling in the periplasmic ligand-binding domain

The isolated periplasmic ligand-binding domain provided the first determined structures of a chemoreceptor element (Milburn *et al*., 1991; Yeh *et al*., 1993). Ligand recognition occurs at the interface of two receptor subunits each of which presents a ligand-binding motif. The dimer demonstrates half-of-sites saturation due to negative cooperativity (Biemann and Koshland, 1994; Lin *et al*., 1994). Recognition of ligand results in the piston-like shift of a helix that starts at the ligand recognition site and continues through a transmembrane helix towards the cytoplasmic domain; the magnitude of this change is small, only a couple of Angströms (Hughson and Hazelbauer, 1996; Chervitz and Falke, 1996; Otteman *et al*., 1999; Falke and Hazelbauer, 2001). Modification in the cytoplasmic domain, specifically the methylation of certain glutamate residues (or genetically encoded as glutamine residues), reverses the bias of the signaling helix (Lai *et al*., 2006). Strategically placed cysteines can be oxidized to generate disulfides locking the signaling helix in a position biased in the 'up' or 'down' position and these receptors generate the anticipated effect on kinase activity (Lee *et al*., 1995*;* Chervitz and Falke, 1995). In total, the ligand-induced piston-like shift of the transmembrane signaling helix is presently the most certain feature of conformational signaling in bacterial chemoreceptors.

Signal transduction in the cytoplasmic domain

Much less is certain about the specifics of conformational signaling in the chemoreceptor cytoplasmic domain. The piston-like shift of the transmembrane signaling helix first impinges on the HAMP region, a signaling module about which there

is little consensus. So-called because their occurrence in *h*istidine kinases, *a*denylyl cyclases, *m*ethyl-accepting chemotaxis proteins, and *p*hosphotases, HAMP modules are widespread amongst prokaryotic signaling receptors and are generally believed to convert one type of conformational input into a conformational output of distinct nature. The work presented in this dissertation does little to shed light on HAMP conformational signaling and thus the topic will be treated only briefly here.

A few models for signaling in HAMP modules are currently being explored. The first proposal is that the structural consequences of signal transduction involve the coordinated axial rotation of helices that are the result of switching between packing motifs in the HAMP four-helix bundle (Hulko *et al*., 2006; Ferris *et al*., 2011; Ferris *et al*., 2014; Hartmann *et al*., 2014). A second model proposes that signal transduction involves influencing a conformational distribution where one state is more stable than the other (Zhou *et al*., 2009; Parkinson, 2010; Doebber *et al*., 2008). A third model of HAMP signaling, derived from crystallographic analysis, involves helical displacements of a splaying nature that are otherwise rigid helical motions (Airola *et al*., 2013; Airola *et al*., 2010). No model for HAMP domain conformational signaling is presently dominant.

The HAMP AS-2 helix connects to the helix that serves as the primary substrate for the enzymes of adaptational modification. This region is called the modification region and is comprised of the helix connecting the HAMP region to the distal cytoplasmic tip as well as the helix emerging from the tip hairpin turn leading to the disordered carboxyl-terminal region (Bartelli and Hazelbauer, 2011); in the dimer this region is a

four-helix bundle (Fig. 4-1). There are four sites of modification on each subunit. Genetically the sites are encoded as QEQE in the single-letter code as they occur in the sequence. The glutamines (Q) are deamidated by the enzyme CheB to generate glutamates (E) at those sites 9 (Kehry, *et al*., 1983). Glutamate residues are methylated by the methyltransferase CheR to generate methyl-glutamates at those sites (Kort *et al*., 1975). This work attempts to describe the conformational features of the two extremes of modification, either having all glutamates at those sites (termed 4E) or all glutamines at those sites (termed 4Q); the 4Q construct has been shown to be a functionally relevant proxy for a fully methylated receptor (Dunten and Koshland, 1991; Borkovich *et al*., 1992). Modification is an important feature of conformational signaling as the fully modified receptor (4Q) has relatively high intrinsic kinase activating potential and low operational ligand affinity; the fully unmodified receptor (4E) has very low kinase activating potential and relatively high operational ligand affinity (Bornhorst and Falke, 2001). Furthermore, as there are four sites to modify, there is a possibility of 16 combinations of Q's or E's at those sites; if both subunits are considered the number of permutations becomes 16^2 for a total of 256 distinct possibilities (Bornhorst and Falke, 2001). Thus modification permits a large range of receptor responsiveness *in vivo*.

Prior to this work no structural specifics related to conformational signaling in the modification region have been resolved. Biochemical analysis by Falke and co-workers suggested that conformational signaling in this region was the consequence of variable inter-helical packing stability with destabilization being associated with a kinase-off

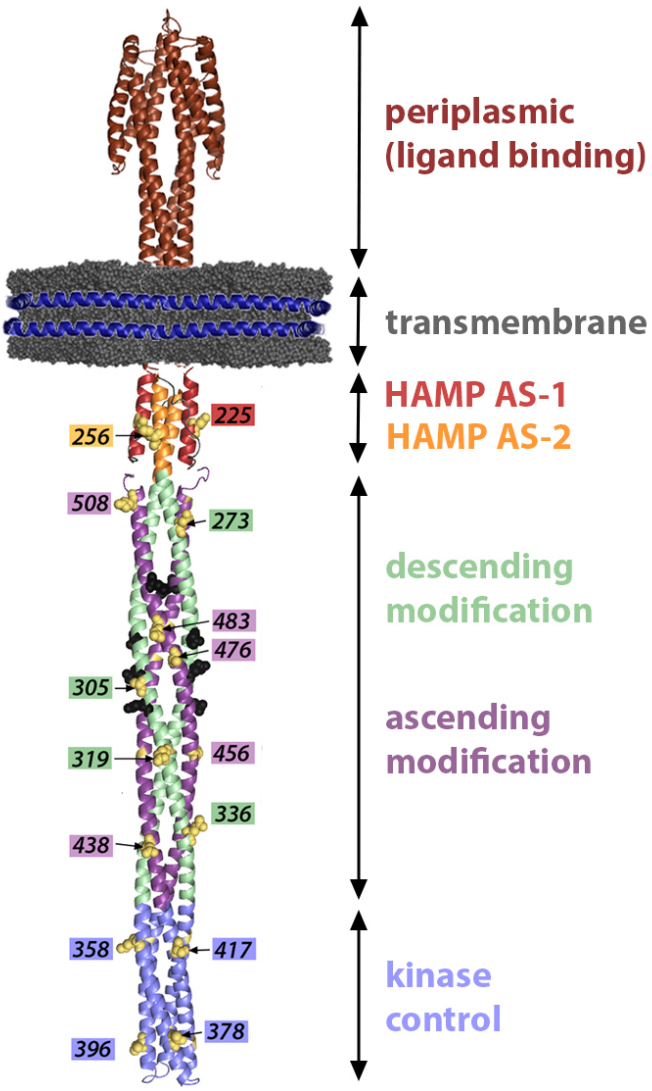

Figure 4-1: **Strategy of probing the Tar cytoplasmic domain by EPR spectroscopy**

A ribbon diagram structural model of a single homodimeric chemoreceptor reconstituted into a Nanodisc. 15 sites were spin labeled and the numbers indicate the position in the amino acid sequence. Spin labeled positions have been rendered in gold with one of the positions per dimer highlighted in CPK. Functional regions have been indicated by color with brown indicating the ligand binding periplasmic domain, red indicated HAMP AS-1, orange indicating HAMP AS-2, green indicating the descending modification helix, violet indicating the ascending modification helix, and the kinase control region has been indicated with blue. Sites of adaptational modification are indicated by black CPK residues. This work probes the effect of ligand binding (L-aspartate) and the effects of having 4 glutamines (4Q) or 4 glutamates (4E) at the sites of adaptational modification.

(ligand bound) signaling state (Starrett and Falke, 2005; Swain *et al*., 2009). Ligand recognition in the periplasmic domain influences the ability of the modification sites to serve as substrates for the enzymes of modification CheR (a methyltransferase) and CheB (a deamidase and methylesterase) (Kleene *et al*., 1979). In both cases, but in opposite directions, ligand recognition results in about a two-fold change in the rate of enzyme-mediated modification (Kleene *et al*., 1979). Thus it is clear that the consequences of ligand recognition are reflected in modification region conformation. Even the extent of modification itself influences the rate of enzyme-mediated modification (Amin and Hazelbauer, 2010).

In signaling complexes, a CheA dimer and two CheW interact with the kinase control region of chemoreceptors (two trimers-of-dimers) to form the ternary signaling complex that is the minimum unit of kinase control (Li and Hazelbauer, 2011). Formation of this complex influences conformation in the modification region, thus the state of the kinase control region is coupled to conformation in the rest of the receptor (Amin and Hazelbauer, 2010). Otherwise little is known for certain about conformational signaling in the kinase control region, particularly for isolated receptor dimers.

The sites of interaction between the receptor kinase control region and the associated signaling proteins have been resolved (Piasta *et al*., 2013; Wang *et al*., 2012; Vu *et al*., 2012; Li *et al*., 2013). It is likely the case that conformational changes at this packing interface are allosterically modulating CheA kinase activity. One model

proposes that, as inter-helical packing is destabilized in the modification region, inter-helical packing is stabilized in the kinase control region and somehow this feature is coupled to CheA activity (Swain *et al*., 2009). In another experiment, the extent of inter-molecular disulfide cross-linking between strategically placed cysteine residues on the receptor and CheA kinase were modulated by ligand addition (Piasta *et al*., 2013). The proposal is that rotations of either the receptor or kinase are influencing the proximity of reactive sulfhydryls, thus implicating a kinase control region twisting-type rearrangement between the kinase activating and inactivating states (Piasta *et al*., 2013). In an alternative approach, molecular modeling of chemoreceptors having a 4Q or 4E modification background implicated subtle biases in kinase control region inter-helical packing distances that were influenced by a novel inter-subunit phenylalanine flipping mechanism (Ortega *et al*., 2013).

Presently there is no consensus on the mechanism of conformational signaling in bacterial chemoreceptors. The following work described in this dissertation attempts to resolve the issue employing biophysical techniques; specifically with an aim of describing conformational signaling in isolated receptor dimers.

A strategy for probing conformational signaling in the Escherichia coli aspartate receptor (Tar) cytoplasmic domain

The work discussed in this dissertation describes the use of a biophysical technique to probe a long-standing question regarding the nature of bacterial chemoreceptors—what is the nature of conformational signaling in the *Escherichia coli* aspartate receptor

(Tar) cytoplasmic domain? EPR spectroscopy is a biophysical technique that, as used in this work, probes peptide backbone dynamics at solvent-exposed alpha-helical sites. The EPR technique requires the site-directed introduction of cysteine residues at positions of interest for the attachment of probes via sulfhydryl chemistry. The following sections will describe the strategy of site selection and the features of conformational signaling that are being investigated.

In total this work describes the exploration of 15 sites in the Tar cytoplasmic domain that were strategically chosen to provide information about various parts of the receptor that have been identified as regions with particular functions or features (Fig. 4-1). In the HAMP region only two sites have been explored, position 225 (residue number) on the AS-1 helix and 256 on the AS-2 helix. This coverage proved insufficient to discern much about HAMP signaling, thus little discussion will be made of those results in this dissertation.

The next region, the modification region, has the greatest degree of coverage and provided the most interesting results. The modification region consists of the two helices contributed by each receptor subunit that in the dimer collectively form a four-helix bundle (Fig. 4-1). The descending modification helix connects HAMP AS-2 to the kinase control region while the ascending helix connects the kinase control region to the disordered carboxyl-terminal region. The terms describe the spatial relationship to the membrane with the descending helix leading away from the membrane and the ascending helix returning. In this work four sites (273, 305, 319, 336) on the receptor

descending modification helix and five sites (438, 456, 476, 483, 508) on the ascending modification helix were explored via EPR spectroscopy.

The kinase control region, as its name implies, interacts with the coupling protein CheW and the kinase CheA in the signaling complex. The assumption is that receptor conformation in this region is coupled to kinase activity. Two inputs modulate kinase activity, adaptational modification and ligand binding. In this work, four sites in the kinase control region were probed via EPR spectroscopy (358, 378, 396, 417).

In total this work reports on the effects of adaptational modification, by comparing the extremes of modification (4Q vs. 4E), and the effect of saturating ligand (L-aspartate). At the time of writing these experiments are ongoing but reported here are important findings regarding both modulators of conformational signaling. Incidentally, this work also revealed information regarding structural details of Tar in two environments, solubilized in the detergent cholate and reconstituted into lipid bilayers.

Although a complete signaling mechanism remains elusive, in total this work resolves that receptors are significantly unstructured when solubilized in cholate, that portions remain structurally dynamic after reconstitution, and that adaptational modification modulates peptide backbone stability for specific regions of the Tar cytoplasmic domain. Furthermore, this work determines that, despite having a similar effect on receptor output, the specific structural consequences of ligand recognition are distinct from those of adaptational modification. Collectively these observations

significantly enhance the understanding of structure and conformational signaling in bacterial chemoreceptors.

RESULTS

Detergent solubilization perturbs the Tar cytoplasmic region

As described in the methods section of this work, Tar is liberated from integral membrane association via solubilization in detergent. Preventing the aggregation of exposed hydrophobic transmembrane portions of membrane proteins requires consistent maintenance in a solubilizing detergent. For most receptor manipulations described in this work, the detergent employed for this purpose is the bile salt sodium cholate. As part of the process of isolation and spin-labeling, EPR spectra were acquired of Tar when solubilized in cholate. The structural consequences of receptor solubilization are notable; much of the cytoplasmic region is significantly destabilized relative to the membrane-associated receptor.

In figures 4-2 and 4-3 the EPR spectra for 15 spin-labeled cytoplasmic domain sites are shown with the receptor having a 4Q or 4E modification state respectively. Solution conditions for these experiments are 50 mM Tris-HCl pH 7.5, 0.5 mM EDTA, 100 mM NaCl, 25 mM sodium cholate, and all spectra were acquired at ambient temperature. In both cases the EPR lineshapes of positions in HAMP helix AS1 (225) and in the kinase control region (358, 378, 396) are typical of those derived from spin-labels at relatively stable solvent-exposed alpha-helical sites (Columbus and Hubbell, 2004). However for sites in the HAMP AS2 helix (256) and receptor modification region (273, 305, 319, 336, 438, 456, 476, 483, and 508) the EPR lineshapes are typical of labels at sites with

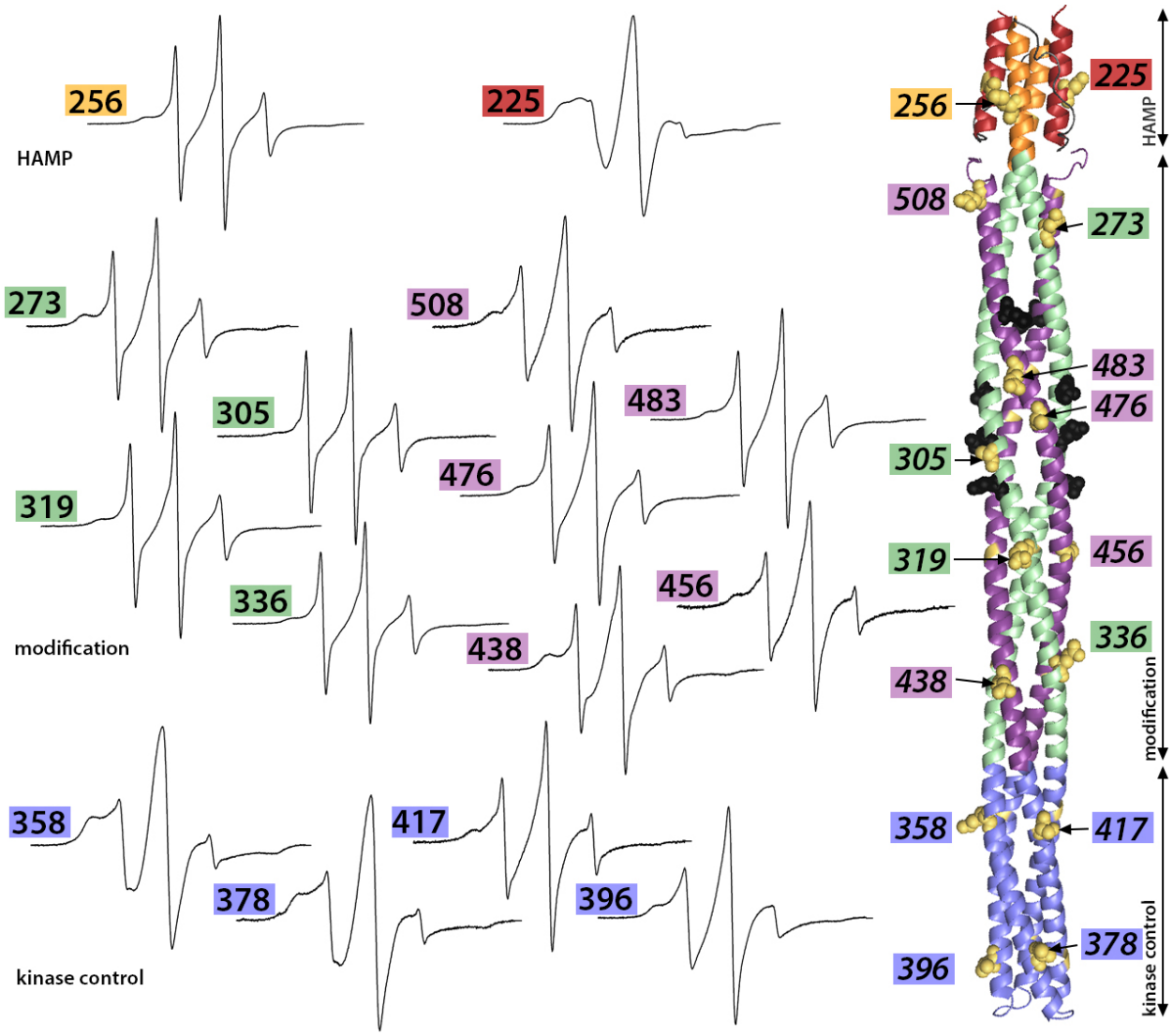

Figure 4-2: **EPR spectra for spin labeled Tar (4Q modification state) in cholate**

Shown are the spectra acquired for 15 spin labeled positions in the Tar cytoplasmic domain. The numbers indicate the Tar amino acid number bearing the spin label. At right is a ribbon diagram structure of a homodimeric chemoreceptor cytoplasmic domain (pdb 3ZX6), the transmembrane region and periplasmic domain are not shown. Spin labeled positions have been rendered in gold; only one of the positions per dimer has been highlighted in CPK. Helices of functional regions have been indicated by color with red indicated HAMP AS-1, orange indicating HAMP AS-2, green indicating the descending modification helix, violet indicating the ascending modification helix, and the kinase control region has been indicated with blue. Sites of adaptational modification are indicated by black CPK residues. Note that position 225 and 438 modification state is QEQE (as they occur in the sequence), not 4Q.

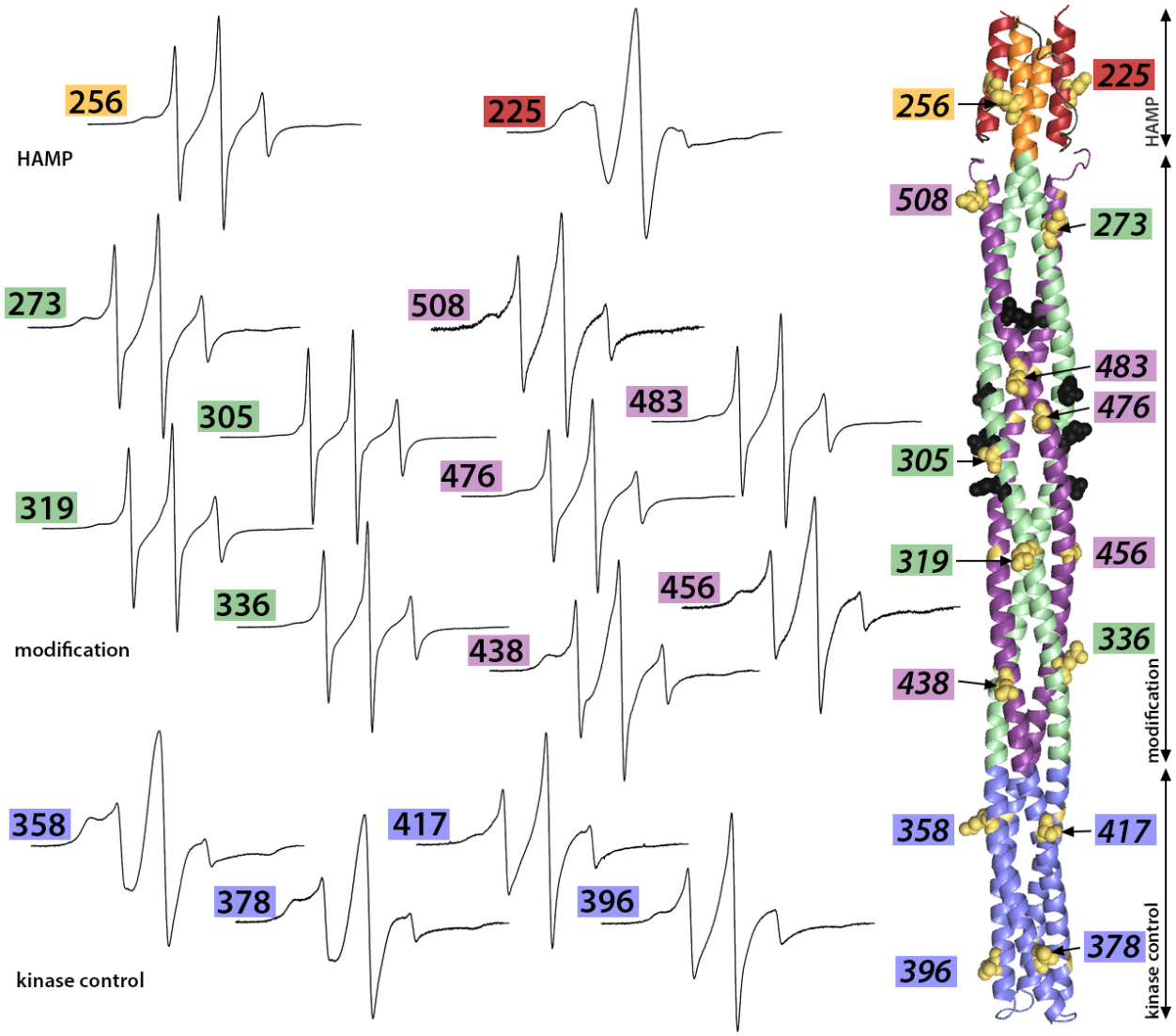

Figure 4-3: EPR spectra for spin labeled Tar (4E modification state) in cholate

Shown are the spectra acquired for 15 spin labeled positions in the Tar cytoplasmic domain. The numbers indicate the Tar amino acid number bearing the spin label. At right is a ribbon diagram structure of a homodimeric chemoreceptor cytoplasmic domain (pdb 3ZX6), the transmembrane region and periplasmic domain are not shown. Spin labeled positions have been rendered in gold; only one of the positions per dimer has been highlighted in CPK. Helices of functional regions have been indicated by color with red indicated HAMP AS-1, orange indicating HAMP AS-2, green indicating the descending modification helix, violet indicating the ascending modification helix, and the kinase control region has been indicated with blue. Sites of adaptational modification are indicated by black CPK residues.

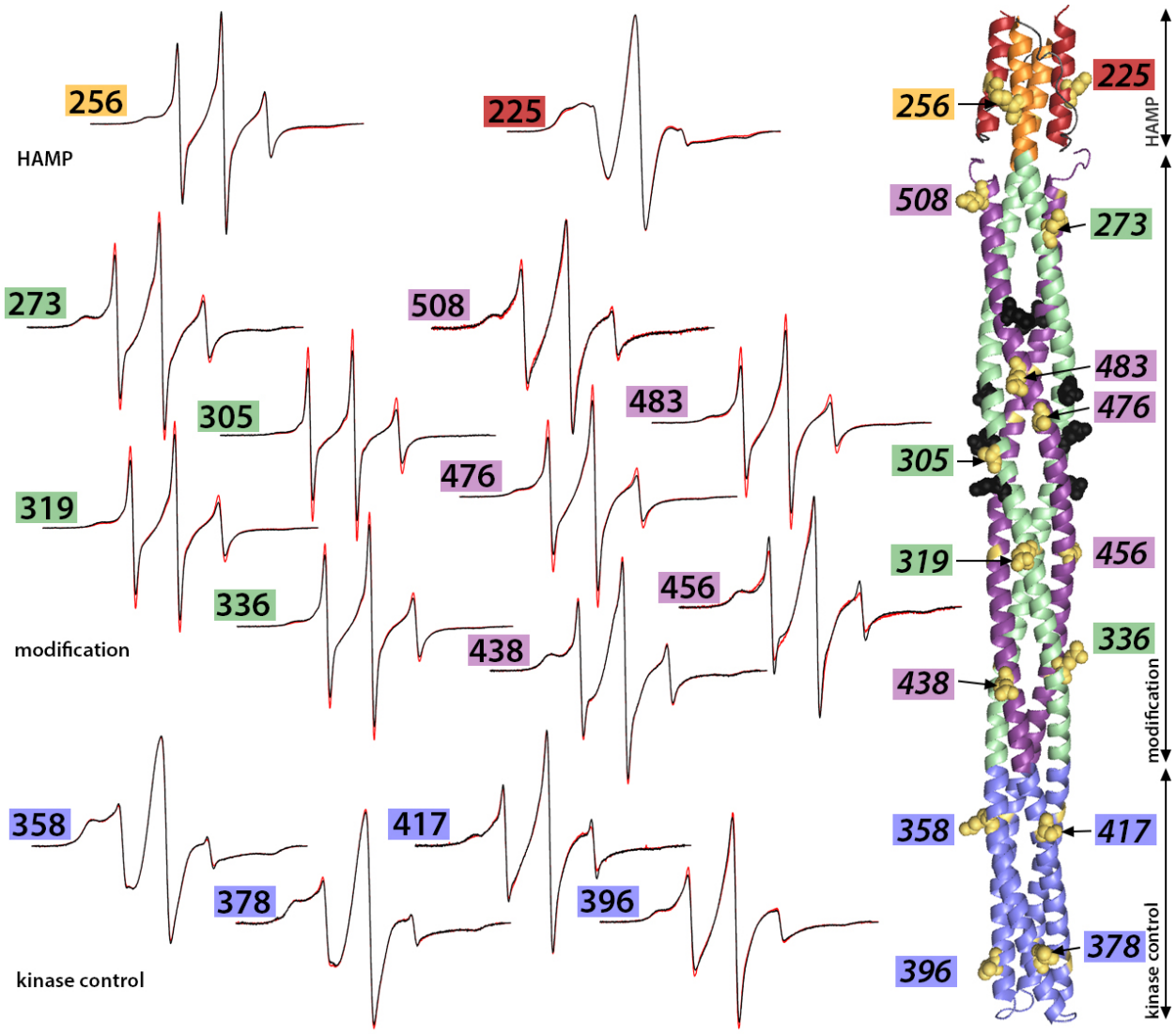

Figure 4-4: **Normalized EPR spectra for spin labeled Tar in cholate comparing 4Q (black lines) and 4E (red lines) modification states**

Shown are the spectra acquired for 15 spin labeled positions in the Tar cytoplasmic domain. The numbers indicate the Tar amino acid number bearing the spin label. At right is a ribbon diagram structure of a homodimeric chemoreceptor cytoplasmic domain (pdb 3ZX6). Spin labeled positions have been rendered in gold; only one of the positions per dimer has been highlighted in CPK. Helices of functional regions have been indicated by color with red indicated HAMP AS-1, orange HAMP AS-2, green the descending modification helix, violet the ascending modification helix, and the kinase control region has been indicated with blue. Sites of adaptational modification are indicated by black CPK residues. Note that position 225 and 438 modification state is QEQE (as they occur in the sequence), not 4Q.

significant peptide backbone fluctuations (Columbus and Hubbell, 2004). Position 417 is an outlier to the observed trend in regional stability; although it is considered to be in the otherwise stable kinase control region, the EPR spectrum suggests that detergent is also perturbing helical stability at this site. Overall these results were unexpected considering that the destabilized sites are distant from what is assumed to be the primary site of receptor-detergent interaction, the helices that associate with the lipid bilayer.

In figure 4-4 the spectra acquired at each site and modification state (4Q or 4E) are normalized and compared directly. For sites in the receptor modification region (273, 305, 319, 336, 476, 483 and 508), the nature of the lineshapes suggest that those respective helices are slightly more disordered in the 4E modification background. Reconstitution of Tar into the lipid bilayer in a Nanodisc restored stability to the receptor modification region, as can be seen when comparing normalized spectra from receptor in Nanodiscs to spectra from receptor solubilized in cholate in the figures 4-5 and 4-6. The degree of reconstitution-mediated stabilization is most prominent for positions on the ascending helix of the modification region (438, 456, 476 and 483) in the 4Q modification background where the spectra assume a lineshape typical of stable solvent-exposed helices (Columbus and Hubbell, 2004). For ease of comparison, a simple metric of spin-label mobility, the quotient of the amplitude of the low-field spectral feature divided by the amplitude of the central feature ($h_{(+1)}/h_{(0)}$), is compared for all conditions discussed here in figure 4-7 (see chapter two for a discussion of this metric).

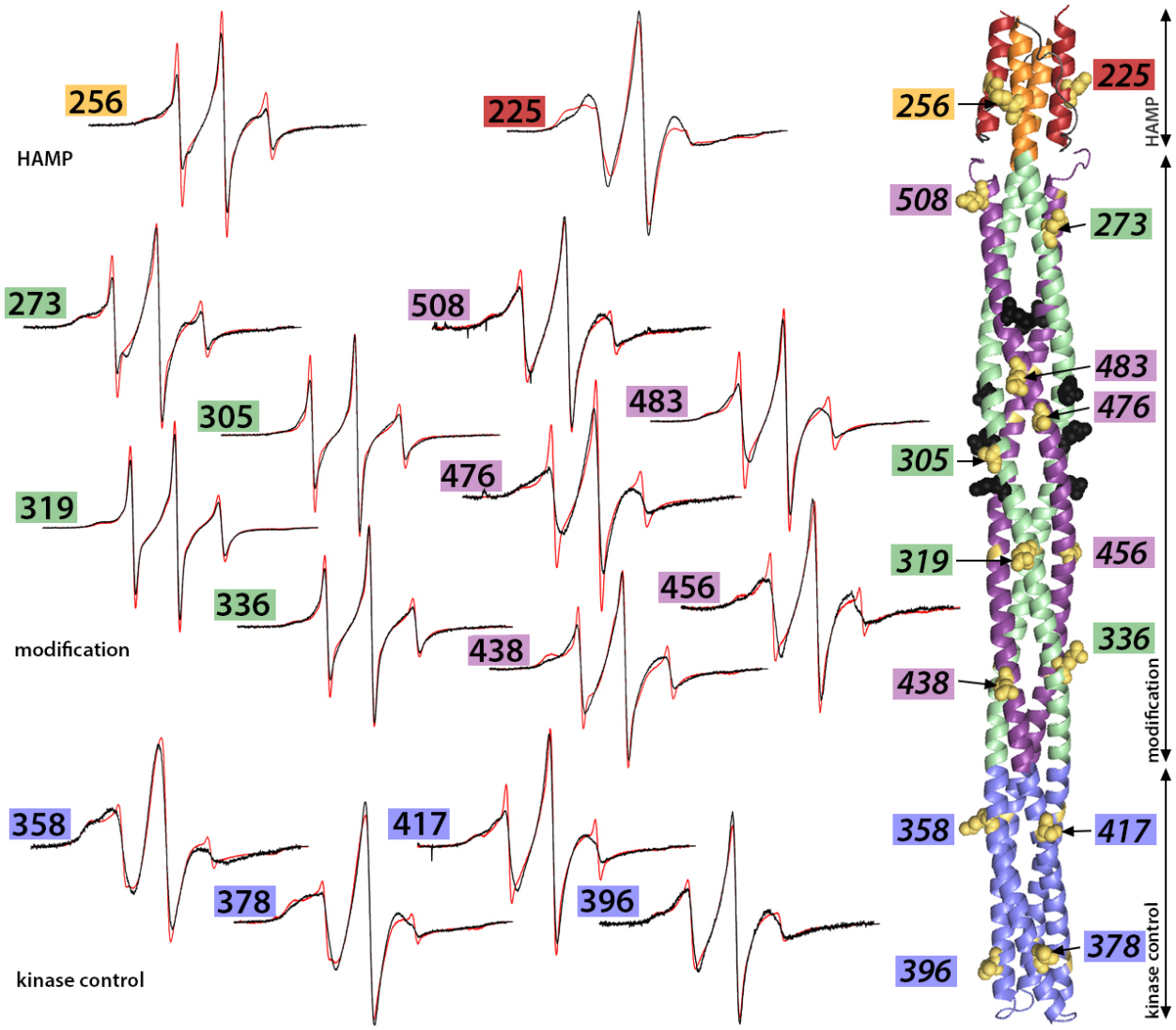

Figure 4-5: **EPR spectra for spin labeled Tar (4Q modification state) in Nanodiscs (black lines) or cholate (red lines)**

Shown are the spectra acquired for 15 spin labeled positions in the Tar cytoplasmic domain. The numbers indicate the Tar amino acid number bearing the spin label. At right is a ribbon diagram structure of a homodimeric chemoreceptor cytoplasmic domain (pdb 3ZX6). Spin-labeled positions have been rendered in gold; one position per dimer has been highlighted in CPK. Helices of particular functional regions have been indicated by color with red indicated HAMP AS-1, orange indicating HAMP AS-2, green indicating the descending modification helix, violet indicating the ascending modification helix, and the kinase control region has been indicated with blue. Sites of adaptational modification are indicated by black CPK residues. Note that positions 225 and 438 are QEQE (as they occur in the sequence), not 4Q.

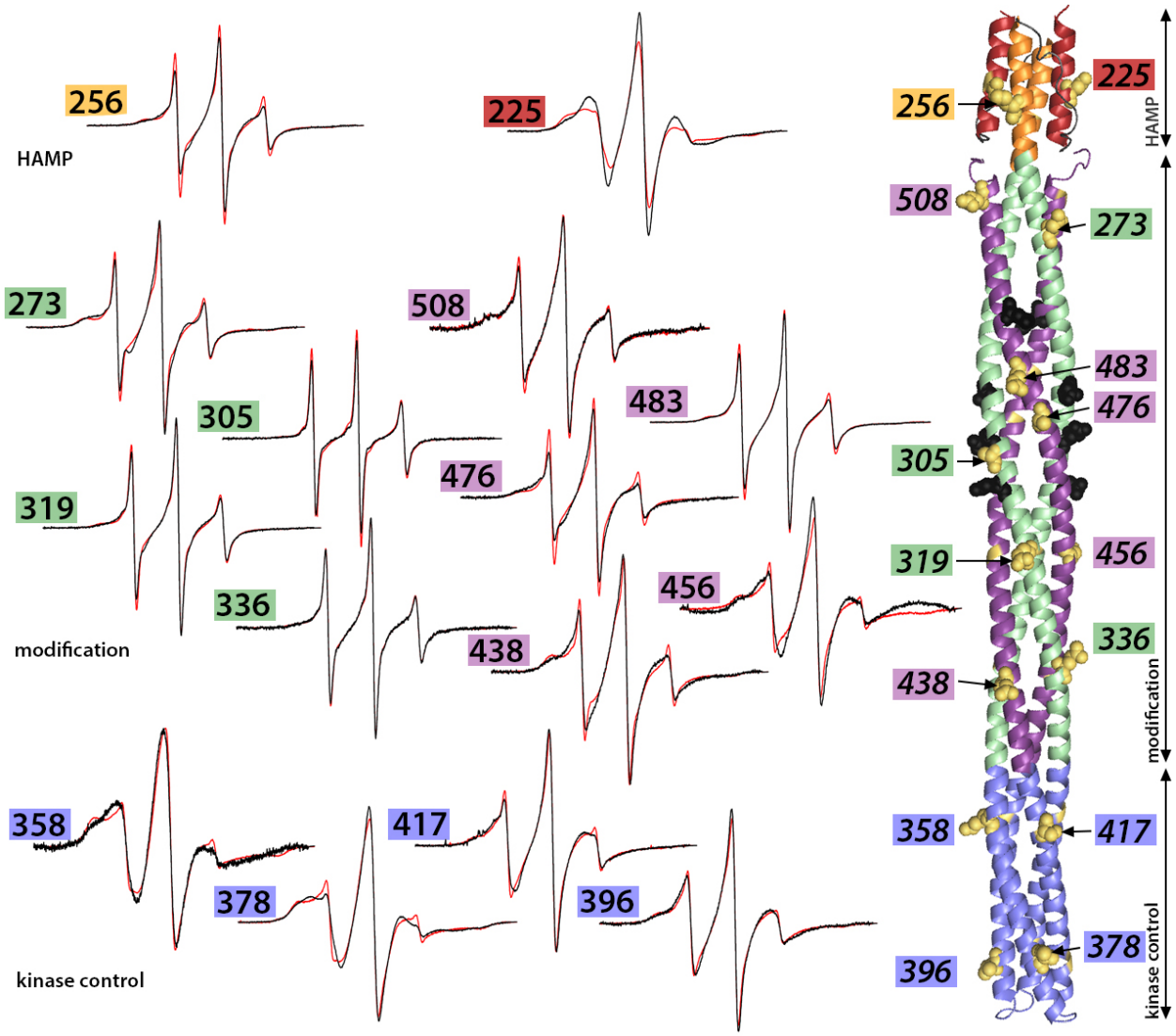

Figure 4-6: **EPR spectra for spin labeled Tar (4E modification state) in Nanodiscs (black lines) or cholate (red lines)**

Shown are the spectra acquired for 15 spin labeled positions in the Tar cytoplasmic domain. The numbers indicate the Tar amino acid number bearing the spin label. At right is a ribbon diagram structure of a homodimeric chemoreceptor cytoplasmic domain (pdb 3ZX6). Spin-labeled positions have been rendered in gold; only one of the positions per dimer has been highlighted in CPK. Helices of particular functional regions have been indicated by color with red indicated HAMP AS-1, orange indicating HAMP AS-2, green indicating the descending modification helix, violet indicating the ascending modification helix, and the kinase control region has been indicated with blue. Sites of adaptational modification are indicated by black CPK residues.

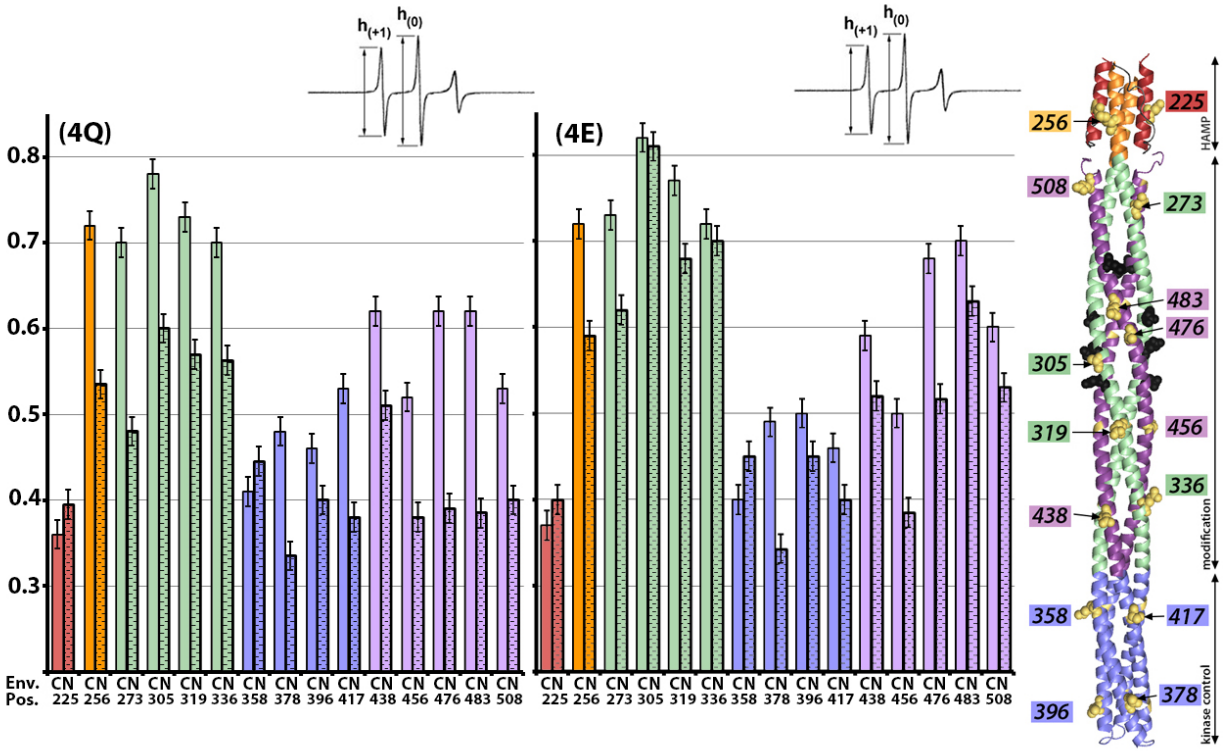

Figure 4-7: **Quantitative comparison ($h_{(+1)}/h_{(0)}$) of spin-labeled Tar in cholate (no fill) or Nanodisc (dash fill)**

The receptor environment is also noted beneath the bars with C standing for cholate and N standing for Nanodisc. The histograms present values for receptor with 4Q at the sites of modification (left) or 4E (right). Values of 0.35-0.4 are typical of stable helices and values of 0.75 and greater are typical of disordered sites. At far right is a ribbon diagram structure of a homodimeric chemoreceptor cytoplasmic domain (pdb 3ZX6). Spin-labeled positions have been rendered in gold; only one of the positions per dimer has been highlighted in CPK. The bars are colored according to functional region and correspond to those in the structure where red indicates HAMP AS-1, orange HAMP AS-2, green the descending modification helix, violet the ascending modification helix, and the kinase control region has been indicated with blue. Sites of adaptational modification are indicated by black CPK residues. Note that positions 225 and 438 are QEQE (as they occur in the amino acid sequence), not 4Q.

Structural consequences of adaptational modification in the Tar cytoplasmic domain

EPR spectra were acquired for 15 sites in the Tar cytoplasmic domain; these receptors encoded either 4Q or 4E at the sites of modification. These spectra were acquired with Nanodisc-reconstituted receptor at room temperature in 50 mM Tris-HCl pH 7.5, 100 mM NaCl, 50 mM KCl and 5 mM $MgCl_2$. The spectra are shown in figures 4-8 (4Q) and 4-9 (4E). A couple of important features are readily observed. The first is that the spectra derived from the HAMP AS2 helix position (256) and from the connected descending modification helix (273, 305, 319, 336) are typical of helical sites with intrinsically high peptide backbone dynamics (Columbus and Hubbell, 2004). The trend is more easily assessed by the quantitative metric of spin label mobility ($h_{(+1)}/h_{(0)}$), represented in figure 4-10, where these sites produce values greater than expected for a stable solvent-exposed helix regardless of modification state. The most important observation is that receptors encoding 4E at the sites of modification demonstrate increased peptide backbone dynamics in both the descending and ascending modification helices when compared to the 4Q receptors. This pattern is apparent in figure 4-11 where the normalized spectra from each modification background are compared. The most pronounced destabilizations occur at the ascending modification helix sites (476, 483) physically nearest the sites of modification themselves.

The structural consequence of modification is to modulate peptide backbone stability in the modification helices of Tar; this feature is not conserved in the kinase control region of the receptor. Figure 4-12 shows that only modest spin label mobilizations are seen at two sites (396, 417); in neither case are the differences as

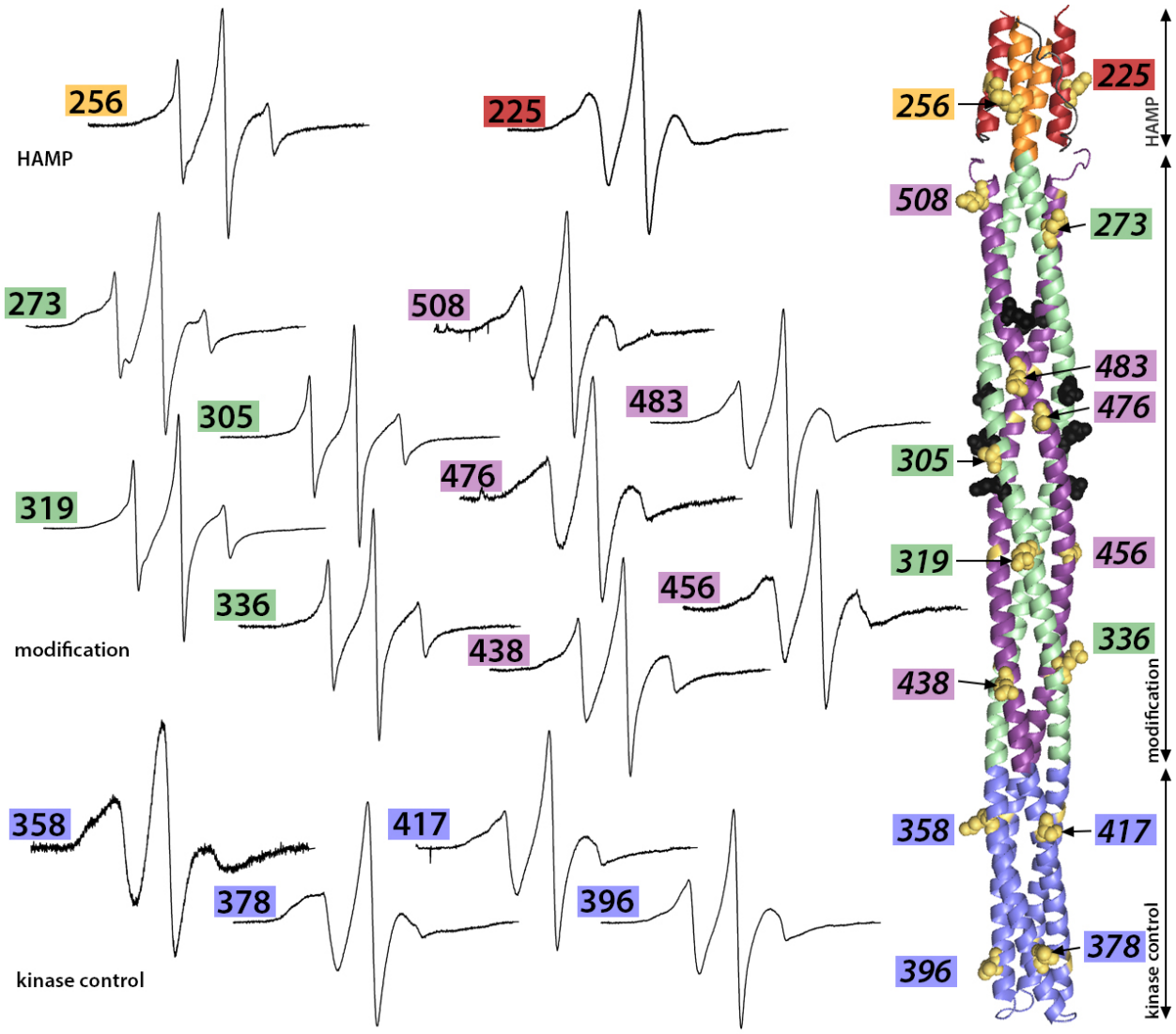

Figure 4-8: **EPR spectra for spin labeled Tar (4Q modification state) in Nanodiscs**

Shown are the spectra acquired for 15 spin labeled positions in the Tar cytoplasmic domain. The numbers indicate the Tar amino acid number bearing the spin label. At right is a ribbon diagram structure of a homodimeric chemoreceptor cytoplasmic domain (pdb 3ZX6). Spin-labeled positions have been rendered in gold; only one of the positions per dimer has been highlighted in CPK. Helices of particular functional regions have been indicated by color with red indicated HAMP AS-1, orange indicating HAMP AS-2, green indicating the descending modification helix, violet indicating the ascending modification helix, and the kinase control region has been indicated with blue. Sites of adaptational modification are indicated by black CPK residues. Note that position 225 and 438 modification state is QEQE (as they occur in the amino acid sequence), not 4Q.

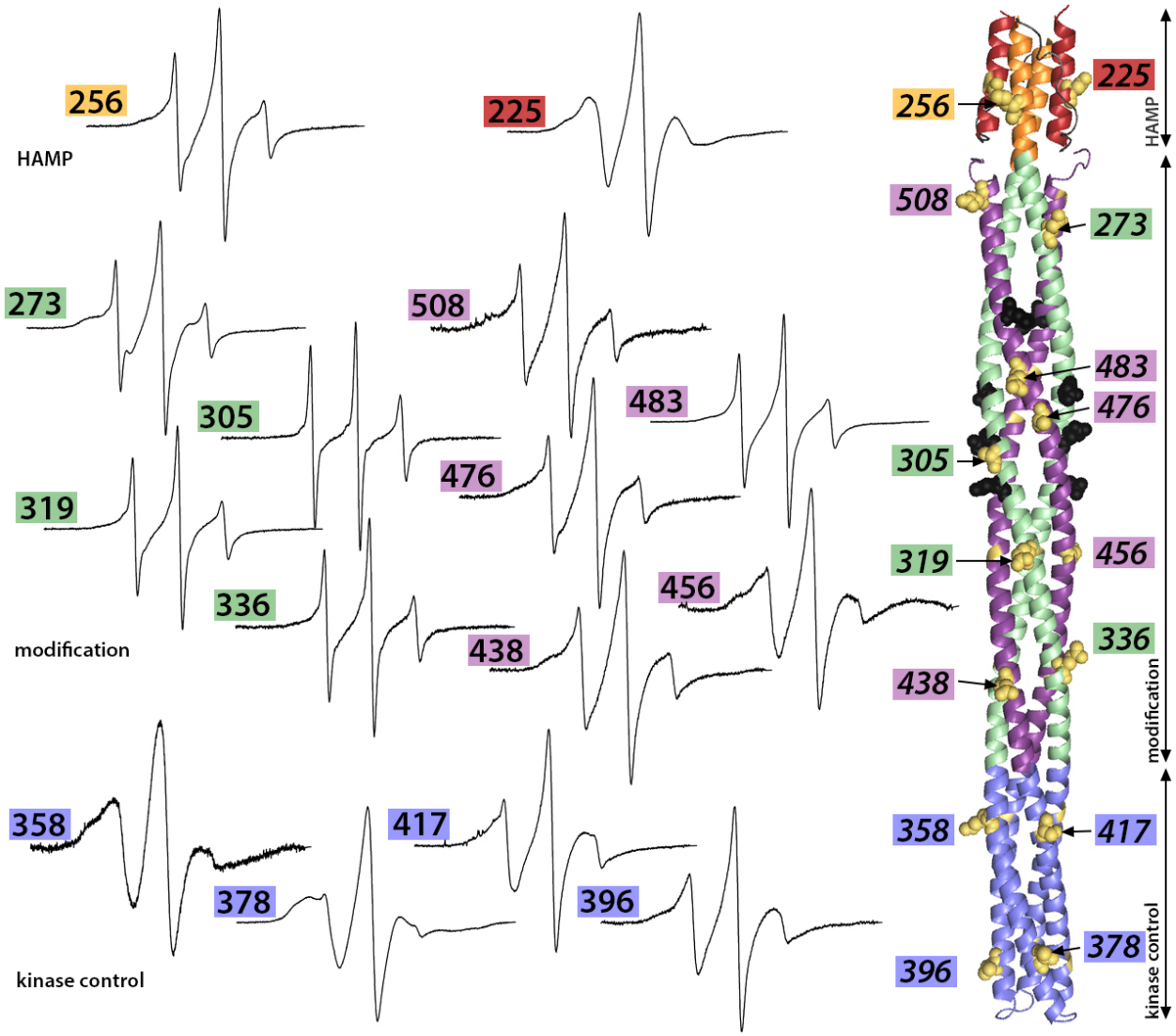

Figure 4-9: **EPR spectra for spin labeled Tar (4E modification state) in Nanodiscs**

Shown are the spectra acquired for 15 spin labeled positions in the Tar cytoplasmic domain. The numbers indicate the Tar amino acid number bearing the spin label. At right is a ribbon diagram structure of a homodimeric chemoreceptor cytoplasmic domain (pdb 3ZX6), the transmembrane region and periplasmic domain are not shown. Spin-labeled positions have been rendered in gold; only one of the positions per dimer has been highlighted in CPK to allow for easier recognition. Helices of particular functional regions have been indicated by color with red indicated HAMP AS-1, orange indicating HAMP AS-2, green indicating the descending modification helix, violet indicating the ascending modification helix, and the kinase control region is indicated with blue. Sites of adaptational modification are indicated by black CPK residues.

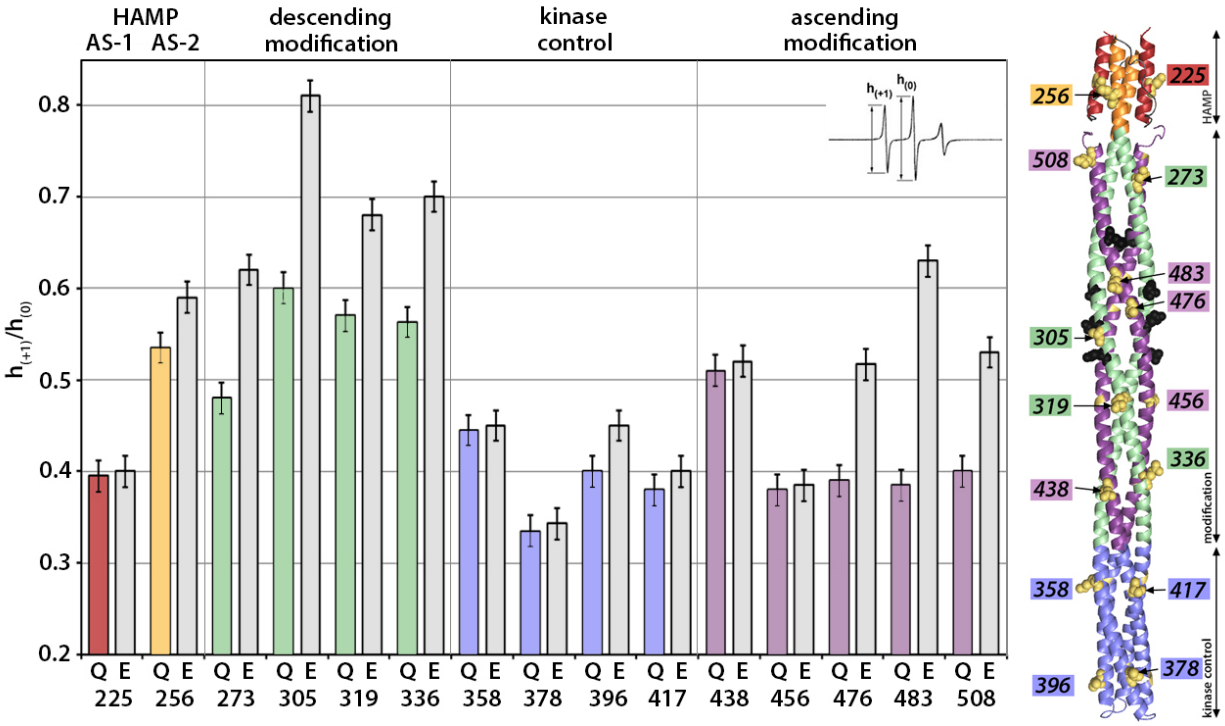

Figure 4-10: **Quantitative comparison ($h_{(+1)}/h_{(0)}$) of 4Q (colored bars) versus 4E (grey bars) modification states for Tar in Nanodiscs**

At right is a ribbon diagram structure of a homodimeric chemoreceptor cytoplasmic domain (pdb 3ZX6), the transmembrane region and periplasmic domain are not shown. Spin-labeled positions have been rendered in gold; only one of the positions per dimer has been highlighted in CPK to allow for easier recognition. Helices of particular functional regions have been indicated by color with red indicated HAMP AS-1, orange indicating HAMP AS-2, green indicating the descending modification helix, violet indicating the ascending modification helix, and the kinase control region has been indicated with blue. Sites of adaptational modification are indicated by black CPK residues. Note that positions 225 and 438 are QEQE (as they occur in the sequence), not 4Q.

large as those seen in the modification helices (Fig. 4-11). However, modification is likely modulating some feature of kinase control region conformation but the nature of the change is not the same phenomenon as occurs in the modification region. A possible clue is derived from analyzing the lineshapes acquired for labels at position 378. The lineshape features of position 378, in particular the broadening of the low-field spectral component, suggest that the label may be making contact with the adjacent helix. Although a simple interpretation of the lineshape change at this site is presently elusive, it is possible that the degree of tertiary contact is being modulated by the modification state.

Structural consequences of ligand recognition in the Tar cytoplasmic domain

An important goal of this work was to address the nature of conformational change elicited in the Tar cytoplasmic domain when ligand is recognized in the periplasmic domain. Thus, continuous wave EPR spectra were also acquired of spin-labeled, Nanodisc-reconstituted, Tar in the presence of saturating L-aspartate. Nanodiscs of the type used in this study are known to communicate ligand occupancy in the periplasmic domain, through the membrane, and to the sites of adaptational modification in the cytoplasmic domain (Boldog *et al*., 2006; Amin and Hazelbauer, 2010). In the work described here, the ligand addition experiments were conducted with 1 to 8 mM L-aspartate in a solution of 50 mM Tris-HCl pH 7.5, 100 mM NaCl, 50 mM KCl and 5 mM $MgCl_2$. Tar has a K_D for aspartate of 2-10 μM (Clarke and Koshland, 1979; Amin and Hazelbauer, 2010). As shown in figure 4-13 the spectra acquired in the presence of saturating aspartate overlay with those acquired in the same solution conditions, but

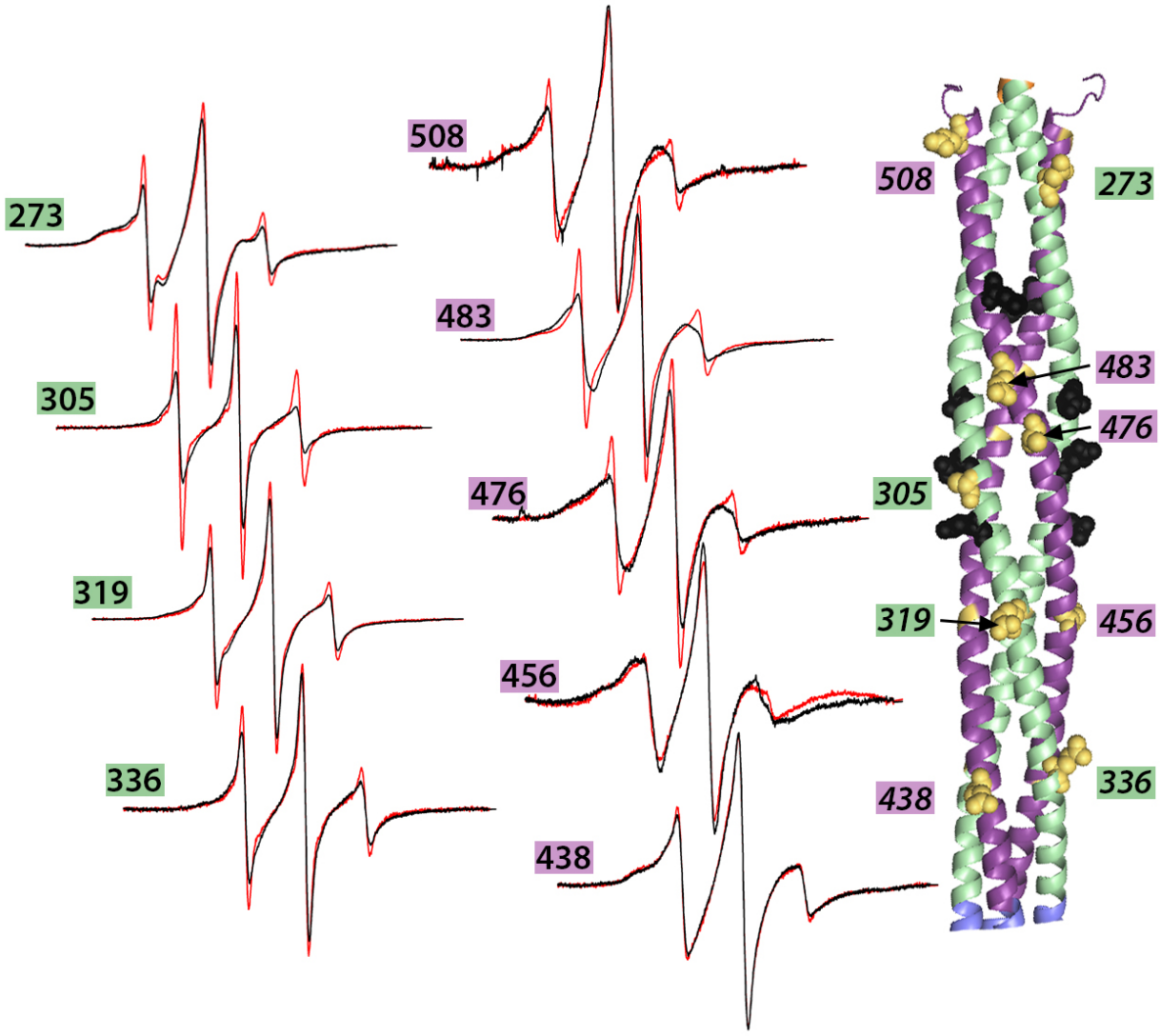

Figure 4-11: **EPR spectra from the Tar modification region comparing the 4Q (black lines) versus 4E (red lines) modification states**

Shown are the spectra acquired for 9 spin labeled positions in the Tar cytoplasmic modification region. All spectra were derived from Nanodisc-reconstituted Tar. The numbers indicate the Tar amino acid number bearing the spin label. At right is a ribbon diagram structure of a homodimeric chemoreceptor cytoplasmic domain (pdb 3ZX6). Spin-labeled positions have been rendered in gold; only one of the positions per dimer has been highlighted in CPK to allow for easier recognition. Helices of particular functional regions have been indicated by color with red indicated HAMP AS-1, orange indicating HAMP AS-2, green indicating the descending modification helix, violet indicating the ascending modification helix, and the kinase control region has been indicated with blue. Sites of adaptational modification are indicated by black CPK residues. Note that position 438 is QEQE (as they occur in the sequence), not 4Q.

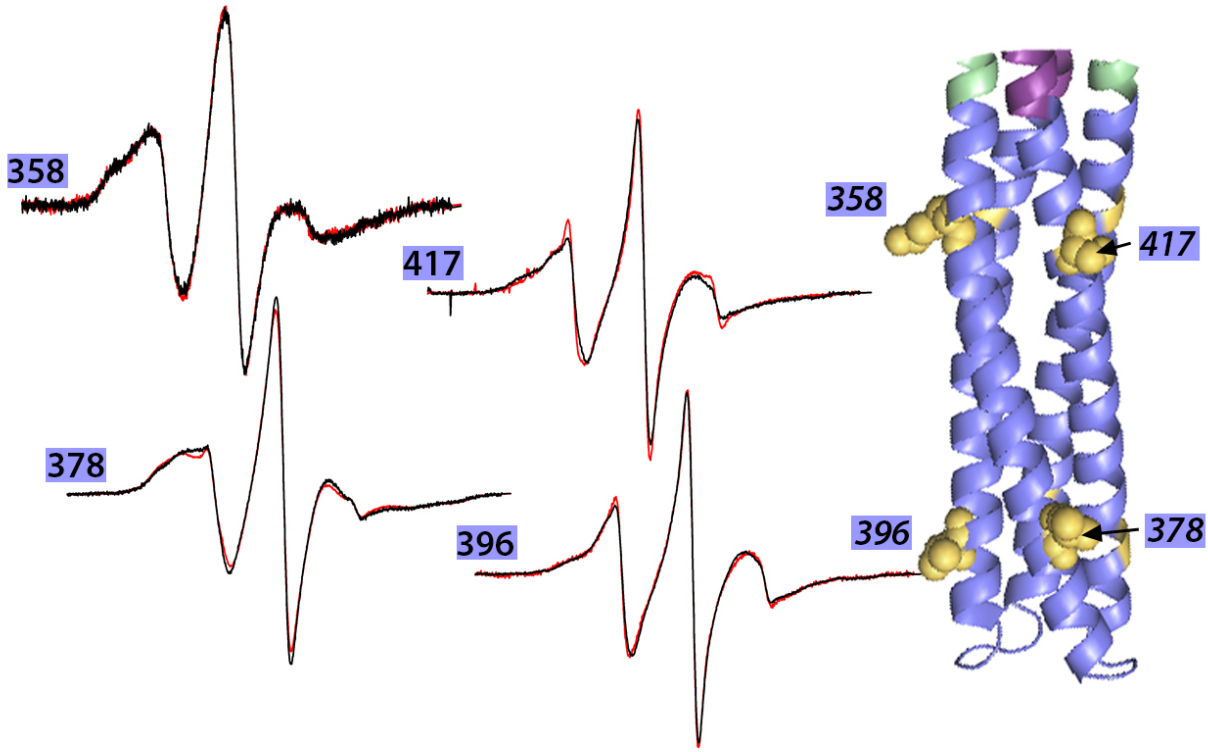

Figure 4-12: **EPR spectra from the Tar kinase control region comparing the 4Q (black lines) versus 4E (red lines) modification states**

Shown are the spectra acquired for 4 spin labeled positions in the Tar cytoplasmic kinase control region. The numbers indicate the Tar amino acid number bearing the spin label. At right is a ribbon diagram structure of a homodimeric chemoreceptor cytoplasmic domain (pdb 3ZX6). Spin-labeled positions have been rendered in gold; only one of the positions per dimer has been highlighted in CPK to allow for easier recognition. Helices of particular functional regions have been indicated by color with red indicated HAMP AS-1, orange indicating HAMP AS-2, green indicating the descending modification helix, violet indicating the ascending modification helix, and the kinase control region has been indicated with blue. Sites of adaptational modification are indicated by black CPK residues.

without aspartate. This implies that the recognition of aspartate in the periplasmic binding domain is not detectably modulating peptide backbone stability in the Tar cytoplasmic domain. Similar results were acquired with spin-labeled Tar reconstituted into proteoliposomes. Again, as seen in figure 4-13 the lineshapes overlay regardless of condition. It should be noted that the solution conditions were slightly different than for experiments done in Nanodiscs; in the case of proteoliposomes the solution was 50 mM Tris-HCl pH 7.5, 0.5 mM EDTA, 100 mM NaCl, 10% glycerol, plus or minus saturating L-aspartate.

For both reconstitution environments, in most cases these spin-labeled receptors are native and respond to aspartate. As shown in figure 4-14, most spin-labeled Tar constructs were efficiently modified suggesting that they were sufficiently native to be recognized by the enzymes of adaptational modification. Furthermore, as shown in figure 4-15, ligand addition altered the rate of modification for most constructs indicating functional transmembrane signaling. Similarly, spin-labeled receptors in proteoliposomes assembled with and exhibited ligand-dependent control of the kinase CheA (Fig. 4-16).

DISCUSSION

Detergent mediated destabilization of the Tar cytoplasmic region

The significant instability of much of the Tar cytoplasmic domain was not anticipated, particularly considering that cholate-solubilized Tar is much less prone to proteolytic degradation as compared to when solubilized in n-Dodecyl-beta-D-maltoside

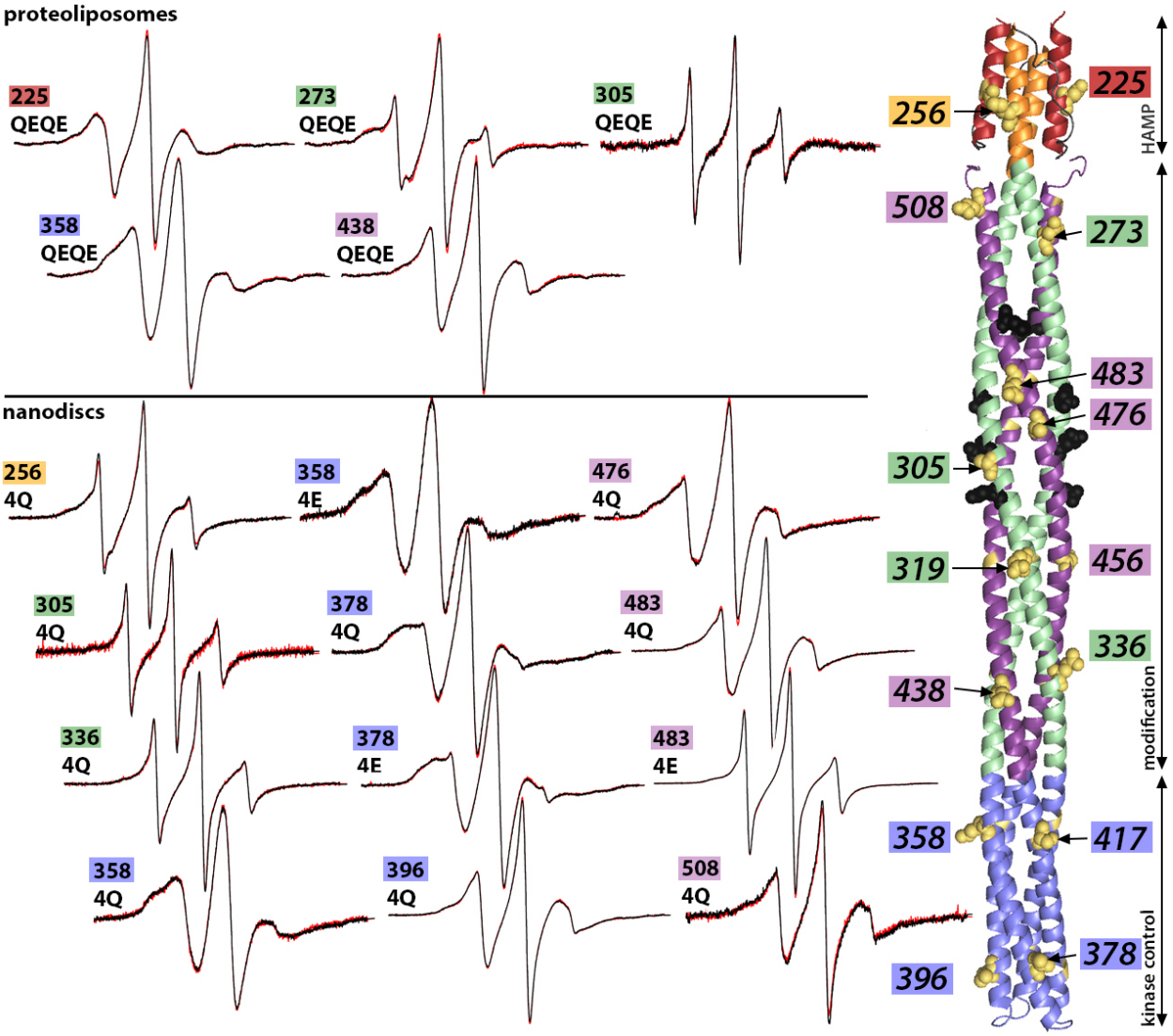

Figure 4-13: **EPR spectra for spin labeled Tar in proteoliposomes (top portion) or Nanodiscs (bottom portion) in the presence (red lines) or absence (black lines) of saturating aspartate**

The numbers indicate the Tar amino acid number bearing the spin label. The modification state varies and is indicated by the spectra. At right is a ribbon diagram structure of a homodimeric chemoreceptor cytoplasmic domain (pdb 3ZX6). Spin-labeled positions have been rendered in gold; only one of the positions per dimer has been highlighted in CPK to allow for easier recognition. Helices of particular functional regions have been indicated by color with red indicated HAMP AS-1, orange indicating HAMP AS-2, green indicating the descending modification helix, violet indicating the ascending modification helix, and the kinase control region has been indicated with blue.

(unpublished observation). It is not known whether there are detergent specific features of chemoreceptor structural perturbation and this may be an interesting question addressed by future research.

The detergent-induced disruption of Tar is likely the reason that chemoreceptors and receptor complexes fail to activate kinase or serve as substrates for modification enzymes when solubilized (Boldog *et al*., 2006). The observations made in this work are especially notable as even sites distal from the transmembrane region are structurally perturbed when detergent has replaced the native bilayer. The receptor transmembrane helices present the longest stretches of surface hydrophobic residues and are likely the dominant site of receptor-detergent interaction. It has already been demonstrated that modulating the transmembrane environment via lipid composition effects Tar conformation at the sites of adaptational modification and the effect of detergent observed here may be a similar phenomenon (Amin and Hazelbauer, 2012). In other words, conformational features of the receptor cytoplasmic domain are crucially sensitive to the transmembrane environment.

Modification modulates helical backbone stability in the modification region

This work presents the first direct structural resolution of the effects of modification at the sites of adaptation, a phenomenon first observed nearly 40 years ago (Kort *et al*., 1975). The results presented here show that the receptor modification region is destabilized in the 4E receptor versus the 4Q receptor. This observation is consistent with conclusions extrapolated from biochemical methods employed by Falke

and co-workers (Starrett and Falke, 2005; Swain *et al*., 2009). However that work did not reveal the specific nature of stability differences (backbone perturbation), nor the differences between the descending and ascending modification helices that are observations unique to the work presented here. Overall the modification region is characterized by high peptide backbone dynamics particularly the descending helix. Some previous nuclear magnetic resonance spectroscopy has suggested the potential that the cytoplasmic domain is intrinsically dynamic (Murphy *et al*., 2001; Seeley *et al*., 1996), however those works were done with a soluble cytoplasmic receptor known to be destabilized versus the intact receptor. The junction between the HAMP AS-2 helix and the descending modification helix is the most frequent target of proteolytic cleavage, this phenomenon is likely facilitated by the unstable backbone (Mowbray *et al*., 1985).

The kinase control region is intrinsically stable

EPR spectroscopy indicates that the kinase control region is stable both when reconstituted and when the receptor is solubilized in detergent. The independent stability in this receptor region may be why native-like receptor arrays and kinase-activating potential can be achieved with receptor cytoplasmic fragments lacking a transmembrane region (Ames and Parkinson, 1994; Koshy *et al*., 2013). Receptor cytoplasmic domain conformation is modulated by interactions at the transmembrane region as evidenced by this work (detergent results) and previous work from this laboratory (Amin and Hazelbauer, 2012), this feature suggests that strategies to study

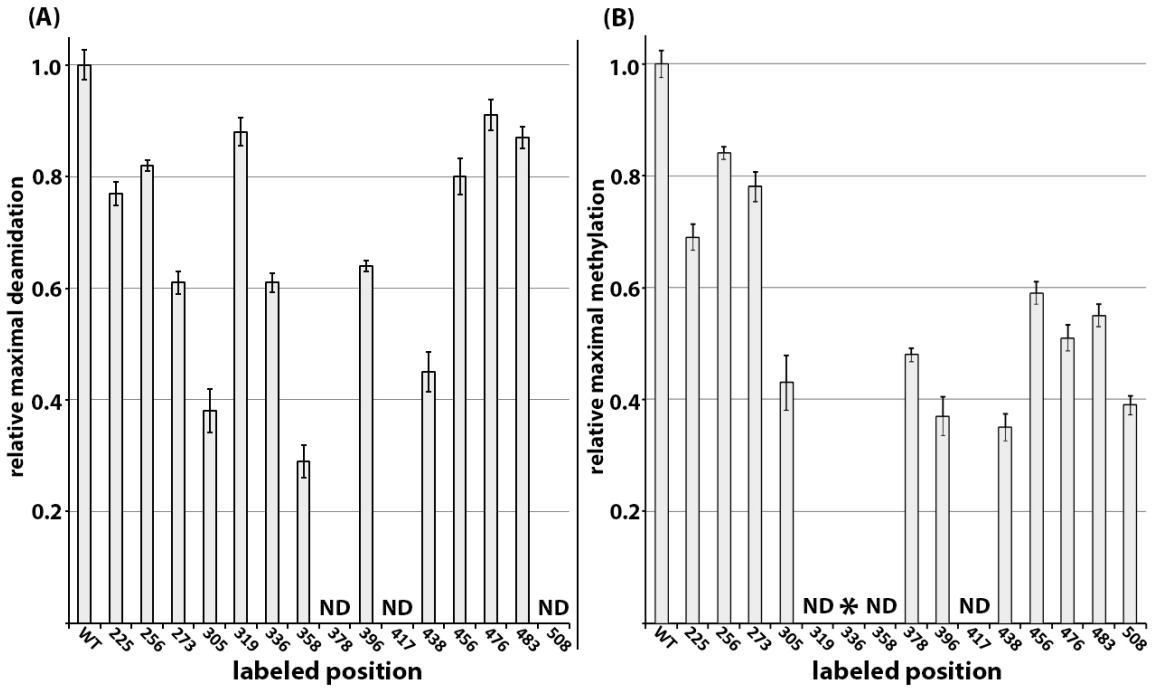

Figure 4-14: Relative extents of maximal deamidation and demethylation

(A) Relative maximal extent of phospho-CheB-mediated deamidation of spin-labeled Tar bearing 4Q at the sites of modification. Note that positions 225 and 438 are QEQE (as they occur in the sequence), not 4Q. (B) Relative maximal extent of CheR-mediated methylation of spin-labeled Tar bearing 4E at the sites of modification. All labeled receptors are reconstituted in Nanodiscs. The asterisk (*) indicates that this position was modified at too low of a percent to reliably quantify. Extent of modification is normalized to a cysteineless Tar (WT 4Q or 4E) submitted to the same labeling and reconstitution reactions as the labeled receptors. ND indicates that the experiment has not been done, but is in progress.

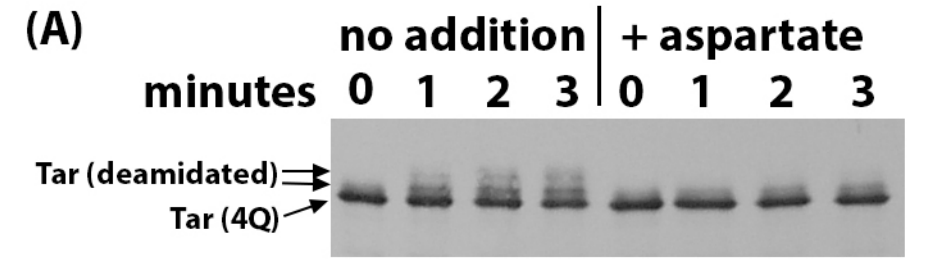

(B)

aspartate responsive ?

Position	4Q deamidation	4E methylation
WT	Yes	Yes
225	ND	ND
256	No	ND
273	Yes	ND
508	ND	ND
483	Yes	ND
476	Yes	ND
305	No*	ND
319	Yes	ND
456	Yes	ND
336	No	ND
438	ND	ND
358	ND	ND
417	ND	ND
378	ND	ND
396	Yes	ND

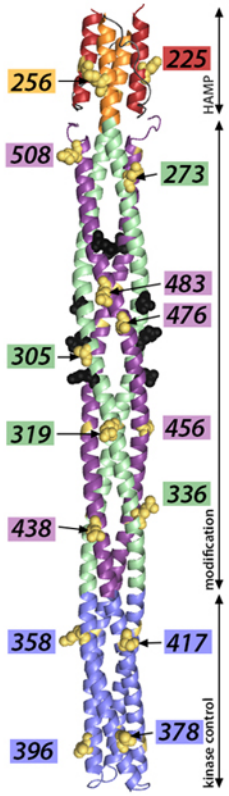

Figure 4-15: Rate of enzymatic modification as a function of the ligand aspartate

(A) An example of the electrophoretic shift induced upon deamidation of a 4Q receptor. Methylation of 4E receptors induces the opposite change in shift. For deamidation, the presence of aspartate reduces the rate of modification. For methylation, the presence of aspartate increases the rate of modification. (B) A table indicating whether spin-labeled, Nanodisc-reconstituted Tar was responsive to L-aspartate in the two assays of adaptational modification (deamidation of 4Q Tar or demethylation of 4E Tar). ND indicates that the experiment has not been done but is in progress. It is difficult to be confident that the null result for position 305 is due to functional perturbation or steric hindrance via the label, thus the asterisk. A ribbon diagram structure of the receptor cytoplasmic domain is pictured at right. Functional regions are indicated by label and color.

conformational signaling by models lacking a transmembrane segment are less likely to be productive than those employing full-length receptor reconstituted into a native-like lipid bilayer.

Ligand binding and adaptational modification are conformationally distinct phenomenon

The results of ligand addition were expected to mirror those acquired from receptors with a 4E modification background as both conditions turn off kinase activity. Even single dimers show evidence that a 4E state has a similar conformation to an aspartate bound receptor as assessed by rates of enzymatic modification (Amin and Hazelbauer, 2010). Thus, the lack of detectable effect upon ligand addition was unexpected. The results reported here lead to a hypothesis that the consequences of ligand recognition are distinct from the consequences of adaptational modification. This is a novel and important proposal.

It is known that ligand occupancy results in a shift of a transmembrane helix towards the cytoplasmic domain, and methyl-glutamates or glutamines at the sites of modification shift the signaling helix in the opposite direction (Hughson and Hazelbauer, 1996; Chervitz and Falke, 1996; Otteman, 1999; Falke and Hazelbauer, 2001; Lai *et al*., 2006). Also, it is well established that the recognition of ligand results in a receptor state that inactivates the associated kinase and that methylation or glutamines at the sites of modification maximizes activity of the kinase (Bornhorst and Falke, 2001). By these assays modification and ligand recognition seem to be acting on the same receptor functions.

The most conservative prediction would be that, even if there were unique conformational features of ligand recognition and adaptational modification, the effects at the output, the receptor kinase control region, would be identical as both inputs modulate kinase control. This does not seem to be the case as aspartate addition does not alter the spectra at positions 378 or 396, whereas modification does. Both of those sites and nearby residues are implicated in interacting with the signaling complex, the kinase CheA or the coupling protein CheW, thus are likely important for kinase regulation (Piasta *et al*., 2013; Wang *et al*., 2012; Vu *et al*., 2012; Li *et al*., 2013).

The site most likely to have revealed the similar nature of ligand recognition and modification is position 483 where the EPR spectral differences are the most extreme between the 4Q and 4E states. Ligand binding and the 4E modification state have similar effects on the kinase CheA, both conditions result in low activity. For position 483, the peptide backbone is substantially destabilized in the 4E versus the 4Q state. Thus, the prediction would be that aspartate recognition promotes the destabilized state seen in the 4E receptor. As seen in figure 4-13 this is clearly not the case and the binding of L-aspartate is not detectably modulating peptide backbone stability.

Does lack of signaling complex decouple ligand recognition from cytoplasmic domain conformational signaling?

Interpretation of the null ligand-binding results as a ligand-specific and distinct phenomenon to adaptational modification has raised a particular counterargument;

what if the lack of signaling complex (CheA/W) has decoupled ligand recognition from conformational signaling in the cytoplasmic domain?

The existing evidence suggests that this is unlikely. It is well demonstrated that isolated receptor dimers in Nanodiscs communicate ligand recognition information to the sites of adaptational modification in the cytoplasmic region as assessed by a 2-fold change in modification rate when aspartate is present (Amin and Hazelbauer, 2010). This implies that isolated dimers are capable of transmembrane signaling in the absence of the ternary signaling complex.

There is a means to probe whether Tar requires an associated signaling complex to reveal ligand-induced changes in EPR spectra on an order similar to the effect of modification. Spin-labeled receptor can be reconstituted into proteoliposomes, followed by the addition of CheA/W to form the ternary complex. EPR spectra could be acquired of this system in the absence and presence of saturating ligand. There are numerous pitfalls to account for in this proposed experiment, however it should reveal if there is a dependence of signaling complex formation to detect ligand-induced conformational changes of a similar nature to those induced by adaptational modification.

A model for conformational signaling in the Escherichia coli aspartate receptor Tar cytoplasmic domain

Tar is an allosteric signaling protein that recognizes the ligand L-aspartate and communicates that occupancy information from the periplasmic ligand-binding site,

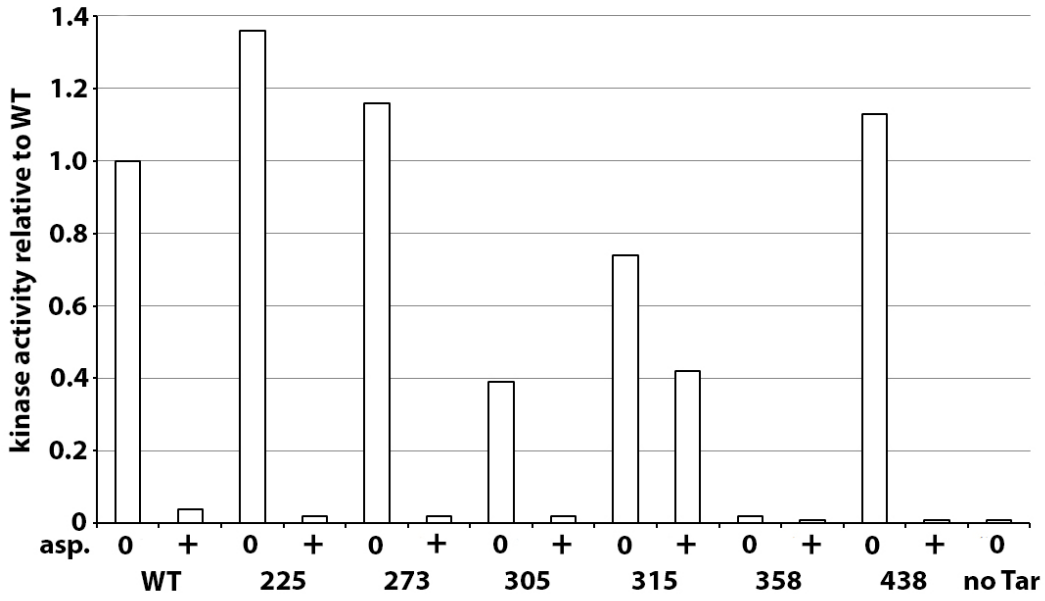

Figure 4-16: Kinase activation and control by spin-labeled Tar in proteoliposomes

A select number of positions (QEQE modification state) were spin-labeled and reconstituted into proteoliposomes. After the addition of CheA, CheW and CheY kinase activity was assessed when L-aspartate was present (+) or absent (0); all experiments were done under non-reducing conditions. A reduction in activity indicates that transmembrane signaling is occurring. No error bars are indicated as the experiment was performed one time. Note that position 315 is not featured elsewhere in this dissertation.

through the membrane, and to the associated cytoplasmic kinase CheA approximately 300 (Å) away. Thus, Tar itself is an allosteric modulator of CheA. This considerable action at a distance is accomplished via ligand-dependent conformational changes in the receptor cytoplasmic domain. Ligand recognition is not the only way to modulate receptor conformation as covalent modification at sites in the receptor dimer cytoplasmic domain result in 256 potential combinations of modified/unmodified residues, a subset of which have been probed and demonstrated to have a strong effect on CheA kinase activity (Bornhorst and Falke, 2001). In this dissertation it is shown that adaptational modification modulates nanosecond peptide backbone stability in the receptor modification region as assessed by continuous-wave EPR spectroscopy. The same technique revealed that the consequences of ligand recognition are conformationally distinct from adaptational modification.

There have been previous clues in the literature that the effects of adaptational modification may be distinct from the effects of ligand recognition. When kinase control and ligand affinity data were compared for various Tar expressing 16 iterations of modification, the authors found that the data did not fit well to a model where the two phenomenon were the same. Instead they proposed that modification was modulating subtle features of a two-state system resulting in regional heterogeneity in an otherwise binary conformational equilibrium (Bornhorst and Falke, 2001). Further supporting this notion, those same authors have reported increased cysteine cross-linking in the modification region for receptors with a 4E versus 4Q modification

background (Starrett and Falke, 2005) yet cannot replicate that effect via ligand addition (personal communication).

From the observations in this dissertation a revised model for conformational signaling in bacterial chemoreceptors is considered. The effect of adaptational modification is likely acting as a modulator of receptor conformation with the results effecting conformational bias in the periplasmic domain (Dunten and Koshland, 1991), the transmembrane region (Lai *et al*., 2006), the modification region (Amin and Hazelbauer, 2010) and the kinase control region of the cytoplasmic domain (Bornhorst and Falke, 2001). As a consequence, the efficiency of coupling ligand recognition to kinase activity is also affected (Bornhorst and Falke, 2001). This type of regulation may be an important global feature of proteins that are modified post-translationally, and certainly for bacterial chemoreceptors for which adaptation is a common phenomenon (Alexander and Zhulin, 2007). Ligand binding has a distinct conformational consequence from adaptational modification, one that does not involve changes in peptide backbone stability. The results of the work presented here do not resolve that change but do not eliminate models involving changes in helical packing motifs like those proposed by others (Ferris *et al*., 2014; Piasta *et al*., 2013; Ortega *et al*., 2013), or any other model that does not involve altered backbone dynamics. Indeed, such changes would specifically *not* be expected to be detected by continuous wave EPR spectroscopy except at sites of interhelical contact, and those types of sites were specifically avoided for this study.

MATERIALS AND METHODS

Strains, plasmids, and proteins

The *E. coli* K-12 strain RP3098 (Parkinson and Houts, 1982) carries a deletion from *flhA* to *flhD* that eliminates the presence or expression of all chemoreceptor and *che* genes. All Tar proteins discussed in this work were expressed in this strain. Plasmid pNT201 carries *tar* under control of a modified *lac* promoter and *lacI*^{q} (Borkovich *et al*., 1989). A derivative, pAL533, codes for Tar with six histidines (Tar-6H) added to its carboxyl terminus and glutamines (Q in the single letter code) at all four sites of modification (Tar-6H 4Q). Alternatively pAL529 encodes glutamates (E in the single letter code) at all four sites of modification (Tar-6H 4E). Cysteine substitutions were generated in these backgrounds; a full list of cysteine substituted Tar-6H constructs generated for this study is provided in table 4-1. Some substitutions, those with the notation pNB##, were generated by contract with Mutagenex, Inc (Piscataway, NJ). All other substitutions were generated by Angela Lilly (Membrane Group, University of Missouri).

Purification and spin labeling of cysteine substituted Tar

In a 1 mL preparation, 1-2 mg of cysteine-substituted Tar-6H in isolated native vesicles were solubilized in 50 mM Tris-HCl, 10% w/v glycerol, 5.5% Octyl β-D-glucopyranoside, 2 μM pepstatin, 2 μM leupeptin, 5 μM TLCK, 100 μM PMSF. This solution was incubated 0.5 hour on ice. Insoluble material was pelleted by a 5-minute centrifugation in an Eppendorf 5415 D table-top centrifuge at 13,200 RPM, 10˚ C. The supernatant from this step was then applied to a pre-equilibrated gravity flow Ni-NTA

(Qiagen) column of 1.5 mL bed volume. Unbound material was removed by a wash with equilibration/wash solution (50 mM Tris-HCl pH 7.5, 30 mM imidazole, 100 mM NaCl, 25 mM sodium cholate). Pure cysteine substituted Tar-6H was then eluted with 4.5 mL elution solution (same as above except with 300 mM imidazole). To this solution was added methanethiosulfonate spin label reagent (Toronto Research Chemicals, North York, Canada) to 25 μM final concentration, approximately a 5-fold molar excess over anticipated yield. The spin labeling reaction was allowed to proceed for 2 hours, on ice, in the dark. The completed reaction was then concentrated to less than 1 mL via an Amicon Ultra-4 centrifugal filter device (Millipore, Billerica, MA) and solution exchanged using a Nap10 column (GE Healthcare, Little Chalfont, UK) to 50 mM Tris-HCl pH 7.5, 0.5 mM EDTA, 100 mM NaCl, 25 mM sodium cholate. The Nap10 eluate was concentrated again via an Amicon Ultra-4 centrifugal filter device to approximately 200 μL. This procedure typically yielded 100-250 μL of 50-150 μM spin-labeled Tar-6H.

Reconstitution of spin labeled Tar-6H into single dimer per disc Nanodiscs

In a 500 μL volume, 15-25 μM spin labeled Tar-6H was combined with 7.5 mM *E. coli* polar lipids (Avanti Polar Lipids, Alabaster, AL), 125 μM MSP1D1(-) (the minus indicates that the MSP histidine tag has been cleaved by TEV protease) (Boldog *et al*., 2007), 2 μM leupeptin, 2 μM pepstatin, and 100 μM PMSF, all buffered by 50 mM Tris-HCl pH 7.5. This mixture was incubated for 0.5 hour at room temperature. Detergent removal (about 40 mM cholate) was mediated by the addition of 750 μL SM-2 Biobeads (Bio-Rad, Hercules, CA) followed by 1 hour incubation on a rotator at ambient

temperature. The Nanodiscs were separated from the Biobeads by using a syringe needle to generate small perforations in the tube and then centrifuging the solution into a larger tube such that the solution is eluted and the beads retained. The Nanodiscs were then applied to a pre-equilibrated Ni-NTA (Qiagen) column of 1 mL bed volume. Empty Nanodiscs were eluted by washing the column with 5 mL of equilibration/wash solution (50 mM Tris-HCl pH 7.5, 30 mM imidazole, 100 mM NaCl). Tar-6H containing Nanodiscs were eluted by the addition of 4 mL elution solution (same as above except with 300 mM imidazole). The eluted Nanodiscs were concentrated to about 250 µL via an Amicon Ultra-4 centrifugal filter device (Millipore, Billerica, MA). The concentrated material was diluted via the addition of 3 mL TNKM 7.5 (50 mM Tris-HCl pH 7.5, 100 mM NaCl, 50 mM KCl, 5 mM $MgCl_2$); this step resulted in an exchange of solution conditions. The Nanodiscs were then concentrated again in the same filter device to about 250 µL. Finally the Nanodiscs were concentrated in a Nanosep 30K Omega centrifugal concentrator (Pall Life Sciences, Port Washington, NY) to 30-45 µL, yielding spin-labeled Tar-6H at 30-100 µM concentration.

Enzymatic modification of Tar-6H in Nanodiscs

The propensity of spin-labeled Tar-6H in Nanodiscs to assume native structure was assessed via CheB-mediated maximum deamidation for receptors encoding 4Q at the sites of modification and via CheR-mediated maximum methylation for receptors encoding 4E at the sites of modification. The ability of those same receptors to recognize and respond to aspartate was assessed via probing the approximately 2-fold

change in enzymatic modification rate in the absence or presence of saturating aspartate.

Maximal deamidation was assessed by combining 5 μM Nanodisc-reconstituted Tar with 5 μM CheB and 50 mM Phosphoramidate in TNKM 7.5 (50 mM Tris-HCl pH 7.5, 100 mM NaCl, 50 mM KCl, 5 mM $MgCl_2$). This mixture was incubated for 2 hours at room temperature and run on a 7% gel, stained with Coomassie Brilliant Blue, and quantified by densitometry. Observed changes in rates of deamidation were assessed via the same solution conditions as maximal deamidation except the reaction was performed with the presence or absence of 8 mM L-aspartate and taking time-points at 60 s, 120 s and 180 s. Instead of in-gel staining the receptors were electrophoretically transferred to nitrocellulose and probed via Western blotting with an antibody to Tar. Whether aspartate had effected the rate was assessed by quantitating and comparing the shifted Tar bands. Maximal extents of methylation of spin-labeled Tar (4E) was assessed under the same solution conditions as maximal deamidation (TNKM 7.5) but instead supplemented with 5 μM CheR and 80 mM S-adenosylmethionine. Whether aspartate had effected the rate was assessed via the same strategy as the CheB-mediated demethylation assays.

Reconstitution of spin labeled Tar-6H into proteoliposomes

Purified and spin labeled Tar-6H was combined, at a final concentration of 8.3 μM, with 16.5 mM sodium cholate solubilized *E. coli* polar lipid extract (Avanti Polar Lipids, Alabaster, AL), 1 μM pepstatin, 1 μM leupeptin in a total volume of 500 μL and with

additional solution conditions of 50 mM Tris-HCl pH 7.5, 0.5 mM EDTA, 100 mM NaCl, 10% glycerol and 75 mM sodium cholate. This mixture was then incubated on ice for 30 minutes. Detergent removal was initiated by addition of 1 mL SM-2 Biobeads (Bio-Rad, Hercules, CA). The proteoliposome/Biobead reaction was allowed to proceed for 1.5 hours on a rotator at 10° C with constant turning before the Biobeads were removed. Then an additional 1 mL Biobeads were added and the incubation repeated. After Biobead removal the proteoliposomes were pelleted by centrifuging for 17 minutes in a Beckman TL100.2 rotor at 100,000 RPM and 10° C. Finally the proteoliposomes were suspended in 40 μL TENG (50 mM Tris-HCl pH 7.5, 0.5 mM EDTA, 100 mM NaCl, 10% glycerol).

Kinase activity assays of proteoliposome reconstituted and spin labeled Tar-6H

400 μM radiolabeled ATP (^{32}P at the γ-phosphate) was combined at .025 μCi/μL with 5 μM spin labeled Tar-6H, 250 nM CheA, 8 μM CheW and 20 μM CheY in a 20 μL solution of 50 mM Tris-HCl pH 7.5, 10% glycerol, 50 mM KCl, 100 mM NaCl, 5 $MgCl_2$. When assayed, L-aspartate was included at 1 mM final concentration. The reaction was initiated by the addition of ATP, but prior to this, receptor, CheA, CheW and CheY were allowed to incubate for 1 hour at ambient temperature to form signaling complexes. Each reaction was stopped after 15 seconds by the addition of reducing SDS-PAGE sample buffer containing 20 mM EDTA. The reactions were run on a 14% SDS-PAGE gel. The gel was then stained with Coomassie Brilliant Blue, dried and exposed to a phosphoimager plate overnight. The plate was imaged with a Fujifilm FLA-3000 imager

and the quantity of radiolabeled CheY was quantified by densitometry and comparison to a ^{32}P-ATP standard.

Electron Paramagnetic Resonance (EPR) Spectroscopy

X-band spectra were collected at 20 mW incident microwave power using a Brüker EMX spectrometer (Billerica, MA) equipped with a high-sensitivity resonator. In all cases, spectra were collected at room temperature. Data was collected via 8 to 64 x-scans, depending on the signal strength, at a 100-kHz field modulation of variable Gauss, but never exceeding ΔHpp minus 0.5 Gauss. The scan width was a 100 G window centered at the central lineshape feature. Typically the samples were 5 µL in volume and measurements were made in glass capillaries. EPR data processing was performed with Labview software developed by Christian Altenbach (University of California, Los Angeles). For final data processing and comparisons, spectra were normalized to the same total spins. The number of times a particular EPR experiment was performed varied from 1 to 4 times. As a means of comparing spin label mobility quantitatively we employ a metric ($h_{(+1)}/h_{(0)}$) that is the quotient of the amplitude of the low-field spectral feature divided by the amplitude of the central feature (see chapter 2 for more information) (Morin *et al*., 2006; Belle *et al*., 2008; Pirman *et al*., 2011). Error bars for this metric were derived from the ($h_{(+1)}/h_{(0)}$) standard deviation that resulted from 32 instances where multiple experiments were performed; this deviation was then applied to all values.

Position	Modification	HB number	Plasmid	Strain
A221	4Q	HB4236	pAL775	RP3098
A221	4E	HB4332	pAL823	RP3098
A225	4Q	HB4218	pAL753	RP3098
A225	QEQE	HB4158	pAL568	RP3098
A225	4E	HB4230	pAL765	RP3098
Q252	4Q	HB4314	pNB7	RP3098
Q252	4E	HB4322	pNB9	RP3098
H256	4Q	HB4314	pAL754	RP3098
H256	QEQE	HB4159	pAL699	RP3098
H256	4E	HB4231	pAL766	RP3098
D263	4Q	HB4315	pNB2	RP3098
D263	4E	HB4323	pNB10	RP3098
D273	4Q	HB4192	pAL726	RP3098
D273	QEQE	HB4167	pAL706	RP3098
D273	4E	HB4193	pAL727	RP3098
A284	4Q	HB4316	pNB3	RP3098
A284	4E	HB4324	pNB11	RP3098
S298	4Q	HB4227	pAL762	RP3098
A305	4Q	HB4194	pAL728	RP3098
A305	QEQE	HB4160	pAL700	RP3098
A305	4E	HB4239	pAL780	RP3098
K315	QEQE	HB4170	pAL708	RP3098
D319	4Q	HB4222	pAL757	RP3098
D319	QEQE	HB4171	pAL709	RP3098
D319	4E	HB4233	pAL769	RP3098
Q336	4Q	HB4224	pAL759	RP3098
Q336	4E	HB4310	pAL826	RP3098
K358	4Q	HB4216	pAL751	RP3098
K358	QEQE	HB4168	pAL711	RP3098
K358	4E	HB4228	pAL763	RP3098
L378	4Q	HB4317	pNB4	RP3098
L378	4E	HB4325	pNB12	RP3098
A381	4Q	HB4318	pNB5	RP3098
A381	4E	HB4326	pNB13	RP3098
V396	4Q	HB4226	pAL760	RP3098
V396	4E	HB4326	pAL827	RP3098
V397	4Q	HB4331	pNB18	RP3098
V397	4E	HB4330	pNB17	RP3098
A417	4Q	HB4319	pNB6	RP3098
A417	4E	HB4327	pNB14	RP3098
E438	4Q	HB4241	pAL752	RP3098
E438	QEQE	HB4162	pAL702	RP3098
E438	4E	HB4229	pAL764	RP3098
E456	4Q	HB4246	pAL777	RP3098
E456	4E	HB4312	pAL828	RP3098
S476	4Q	HB4221	pAL756	RP3098
S476	QEQE	HB4191	pAL733	RP3098
S476	4E	HB4232	pAL768	RP3098
Q483	4Q	HB4223	pAL758	RP3098
Q483	QEQE	HB4195	pAL732	RP3098
Q483	4E	HB4234	pAL770	RP3098
A497	QEQE	HB4187	pAL712	RP3098
Q502	4Q	HB4320	pNB7	RP3098
Q502	4E	HB4328	pNB15	RP3098
Q508	4Q	HB4321	pNB8	RP3098
Q508	4E	HB4329	pNB16	RP3098

Note: all plasmids titled pNB## were made via contract with Mutagenex, Inc.
Note: Tar V397C 4Q and 4E do not have a 6-histidine (6H) tag

Table 4-1: Tar (his-tagged) cysteine substitutions generated to probe conformational signaling

Literature Cited

Airola, M.V., Watts, K.J., Bilwes, A.M., Crane, B.R. 2010. Structure of concatenated HAMP domains provides a mechanism for signal transduction. Structure. 18(4):436-48.

Airola, M.V., Sukomon, N., Samanta, D., Borbat, P.P., Freed, J.H., Watts, K.J., Crane, B.R. 2013. HAMP domain conformers that propagate opposite signals in bacterial chemoreceptors. PLoS Biol. 11(2):e1001479.

Alexander, R.P., Zhulin, I.B. 2007. Evolutionary genomics reveals conserved structural determinants of signaling and adaptation in microbial chemoreceptors. Proc. Natl. Acad. Sci. U S A. 104(8):2885-90.

Altenbach, C., Greenhalgh, D.A., Khorana, H.G., Hubbell, W.L. 1994. A collision gradient method to determine the immersion depth of nitroxides in lipid bilayers: application to spin-labeled mutants of bacteriorhodopsin. Proc. Natl. Acad. Sci. U S A. 91(5):1667-71.

Ames, P., Parkinson, J.S. 1994. Constitutively signaling fragments of Tsr, the Escherichia coli serine chemoreceptor. J. Bacteriol. 176(20):6340-8.

Amin, D.N., Hazelbauer, G.L. 2010. Chemoreceptors in signaling complexes: shifted conformation and asymmetric coupling. Mol. Microbiol. 78(5):1313-23.

Amin, D.N., Hazelbauer, G.L.. 2010. The chemoreceptor dimer is the unit of conformational coupling and transmembrane signaling. J. Bacteriol. 192(5):1193-200.

Amin, D.N., Hazelbauer, G.L. 2012. Influence of membrane lipid composition on a transmembrane bacterial chemoreceptor. J. Biol. Chem. 287(50):41697-705.

Baker, M.D., Wolanin, P.M., Stock, J.B. 2006. Signal transduction in bacterial chemotaxis. Bioessays. 28(1):9-22.

Barnakov, A.N., Barnakova, L.A., Hazelbauer, G.L. 1998. Comparison in vitro of a high- and a low-abundance chemoreceptor of Escherichia coli: similar kinase activation but different methyl-accepting activities. J. Bacteriol. 180(24):6713-8.

Barnakov, A.N., Barnakova, L.A., Hazelbauer, G.L. 1999. Efficient adaptational demethylation of chemoreceptors requires the same enzyme-docking site as efficient methylation. Proc. Natl. Acad. Sci. U S A. 96(19):10667-72.

Barnakov, A.N., Barnakova, L.A., Hazelbauer, G.L. 2001. Location of the receptor-interaction site on CheB, the methylesterase response regulator of bacterial chemotaxis. J. Biol. Chem. 276(35):32984-9.

Barnakov, A.N., Barnakova, L.A., Hazelbauer, G.L. 2002. Allosteric enhancement of adaptational demethylation by a carboxyl-terminal sequence of chemoreceptors. J. Biol.

Chem. 277(44):42151-6.

Bartelli, N.L., Hazelbauer, G.L. 2011. Direct evidence that the carboxyl-terminal sequence of a bacterial chemoreceptor is an unstructured linker and enzyme tether. Protein Sci. 20(11):1856-66.

Belle, V., Rouger, S., Costanzo, S., Liquière, E., Strancar, J., Guigliarelli, B., Fournel, A., Longhi, S. 2008. Mapping alpha-helical induced folding within the intrinsically disordered C-terminal domain of the measles virus nucleoprotein by site-directed spin-labeling EPR spectroscopy. Proteins. 73(4):973-88.

Biemann, H.P., Koshland, D.E. Jr. 1994. Aspartate receptors of Escherichia coli and Salmonella typhimurium bind ligand with negative and half-of-the-sites cooperativity. Biochemistry. 33(3):629-34.

Bilwes, A.M., Alex, L.A., Crane, B.R., Simon, M.I. 1999. Structure of CheA, a signal-transducing histidine kinase. Cell. 96(1):131-41.

Boldog, T., Grimme, S., Li. M., Sligar, S. G., Hazelbauer, G. L. 2006. Nanodiscs separate chemoreceptor oligomeric states and reveal their signaling properties. Proc. Natl. Acad. Sci. USA. 103: 11509-11514.

Boldog, T. Li, M., Hazelbauer, G. L. 2007. Using Nanodiscs to create water-soluble transmembrane chemoreceptors inserted in lipid bilayers. Meth. In Enzym. 423: 317-335.

Borkovich, K.A., Kaplan, N., Hess, J.F., Simon, M.I. (1989) Transmembrane signal transduction in bacterial chemotaxis involves ligand-dependent activation of phosphate group transfer. Proc. Natl. Acad. Sci. USA. 86: 1208–1212.

Borkovich, K.A., Simon, M.I. 1990. The dynamics of protein phosphorylation in bacterial chemotaxis. Cell. 63(6):1339-48.

Borkovich, K.A., Alex, L.A., Simon, M.I. 1992. Attenuation of sensory receptor signaling by covalent modification. Proc. Natl. Acad. Sci. U S A. 89(15):6756-60.

Bornhorst, J.A., Falke, J.J. 2001. Evidence that both ligand binding and covalent adaptation drive a two-state equilibrium in the aspartate receptor signaling complex. J. Gen. Physiol. 118(6):693-710.

Bren, A., Eisenbach, M. 1998. The N terminus of the flagellar switch protein, FliM, is the binding domain for the chemotactic response regulator, CheY. J. Mol. Biol. 278(3):507-14.

Briegel, A., Ortega, D.R., Tocheva, E.I., Wuichet, K., Li, Z., Chen, S., Müller, A., Iancu, C.V., Murphy, G.E., Dobro, M.J., Zhulin, I.B., Jensen, G.J. 2009. Universal architecture of bacterial chemoreceptor arrays. Proc. Natl. Acad. Sci. U S A. 106(40):17181-6.

Briegel, A., Li, X., Bilwes, A.M., Hughes, K.T., Jensen, G.J., Crane, B.R. 2012. Bacterial chemoreceptor arrays are hexagonally packed trimers of receptor dimers networked by rings of kinase and coupling proteins. Proc. Natl. Acad. Sci. U S A. 109(10):3766-71.

Briegel, A., Wong, M.L., Hodges, H.L., Oikonomou, C.M., Piasta, K.N., Harris, M.J., Fowler, D.J., Thompson, L.K., Falke, J.J., Kiessling, L.L., Jensen, G.J. 2014. New insights into bacterial chemoreceptor array structure and assembly from electron cryotomography. Biochemistry. 53(10):1575-85.

Brown, M.T., Delalez, N.J., Armitage, J.P. 2011. Protein dynamics and mechanisms controlling the rotational behavior of the bacterial flagellar motor. Curr. Opin. Microbiol. 14(6):734-40.

Cantwell, B.J., Draheim, R.R., Weart, R.B., Nguyen, C., Stewart, R.C. 2003. CheZ phosphatase localizes to chemoreceptor patches via CheA-short. J. Bacteriol. 185:2354–2361.

Chang, C., Stewart, R.C. 1998. The two-component system. Regulation of diverse signaling pathways in prokaryotes and eukaryotes. Plant Physiol. 117(3):723-31.

Chervitz, S.A., Falke, J.J. 1995. Lock on/off disulfides identify the transmembrane signaling helix of the aspartate receptor. J. Biol. Chem. 270(41):24043-53.

Chervitz, S.A., Falke, J.J. 1996. Molecular mechanism of transmembrane signaling by the aspartate receptor: a model. Proc. Natl. Acad. Sci. U S A. 93(6):2545-50.

Clarke, S., Koshland, D.E. Jr. 1979. Membrane receptors for aspartate and serine in bacterial chemotaxis. J. Biol. Chem. 254(19):9695-702.

Columbus, L., Hubbell, W.L. 2002. A new spin on protein dynamics. Trends Biochem. Sci. 27:288-295.

Columbus, L., Hubbell, W. L. 2004. Mapping backbone dynamics in solution with site-directed spin labeling: GCN4-58 bZip free and bound to DNA. Biochemistry. 43: 7273-7287.

Cooper, D.B., Smith, V.F., Crane, J.M., Roth, H.C., Lilly, A.A., Randall, L.L. 2008. SecA, the motor of the secretion machine, binds diverse partners on one interactive surface. J Mol. Biol. 382(1):74-87.

Djordjevic, S., Stock, A.M. 1997. Crystal structure of the chemotaxis receptor

methyltransferase CheR suggests a conserved structural motif for binding S-adenosylmethionine. Structure. 5(4):545-58.

Djordjevic, S., Stock, A.M. 1998. Chemotaxis receptor recognition by protein methyltransferase CheR. Nat. Struct. Biol. 5(6):446-50.

Do Cao, M.A., Crouzy, S., Kim, M., Becchi, M., Cafiso, D.S., Di Pietro, A., Jault, J.M. 2009. Probing the conformation of the resting state of a bacterial multidrug ABC transporter, BmrA, by a site-directed spin labeling approach. Protein Sci. 18(7):1507-20.

Doebber, M., Bordignon, E., Klare, J. P., Holterhues, J., Martell, S., Mennes, N., Li, L., Engelhard, M., Steinhoff, H-. J. 2008. Salt-driven equilibrium between two conformations in the HAMP domain from Natronomonas pharaonis: the language of signal transfer? J. Biol. Chem. 283: 28691-28701.

Dunker, A.K., Silman, I., Uversky, V.N., Sussman, J.L. 2008. Function and structure of inherently disordered proteins. Curr. Opin. Struc. Biol. 18:756-764.

Dunten, P., Koshland, D.E. Jr. 1991. Tuning the responsiveness of a sensory receptor via covalent modification. J. Biol. Chem. 266(3):1491-6.

Dyer, C.M., Dahlquist, F.W. 2006 Switched or not?: the structure of unphosphorylated CheY bound to the N terminus of FliM. J. Bacteriol. 188(21):7354-63.

Engström, P., Hazelbauer, G.L. 1980. Multiple methylation of methyl-accepting chemotaxis proteins during adaptation of E. coli to chemical stimuli. Cell. 20(1):165-71.

Falke, J. J., Hazelbauer, G. L. 2001. Transmembrane signaling in bacterial chemoreceptors. Trends Biochem. Sci. 26:257-265.

Fanucci, G.E., Cafiso, D.S. 2006. Recent advances and applications of site-directed spin labeling. Curr. Opin. Struct. Biol. 16(5):644-53.

Feng, X., Baumgartner, J.W., Hazelbauer, G.L. 1997. High- and low-abundance chemoreceptors in Escherichia coli: differential activities associated with closely related cytoplasmic domains. J. Bacteriol. 179(21):6714-20.

Feng, X., Lilly, A.A., Hazelbauer, G.L. 1999. Enhanced function conferred on a low-abundance chemoreceptor Trg by methyltransferase-docking site. J. Bacteriol. 181(10):3164-71.

Ferris, H.U., Dunin-Horkawicz, S., Mondéjar, L.G., Hulko, M., Hantke, K., Martin, J., Schultz, J.E., Zeth, K., Lupas, A.N., Coles, M. 2011. The mechanisms of HAMP-mediated signaling in transmembrane receptors. Structure. 19(3):378-85.

Ferris, H.U., Zeth, K., Hulko, M., Dunin-Horkawicz, S., Lupas, A.N. 2014. Axial helix rotation as a mechanism for signal regulation inferred from the crystallographic analysis of the E. coli serine chemoreceptor. J. Struct. Biol. 186(3):349-56.

Fleissner, M.R., Cascio, D., Hubbell, W.L. 2009. Structural origin of weakly ordered nitroxide motion in spin-labeled proteins. Protein Sci. 18(5):893-908.

Flores Jiménez, R.H., Do Cao, M.A., Kim, M., Cafiso, D.S. 2010. Osmolytes modulate conformational exchange in solvent-exposed regions of membrane proteins. Protein Sci. 19(2):269-78.

Hartmann, M.D., Dunin-Horkawicz, S., Hulko, M., Martin, J., Coles, M., Lupas, A.N. 2014. A soluble mutant of the transmembrane receptor Af1503 features strong changes in coiled-coil periodicity. J. Struct. Biol. 186(3):357-66.

Hazelbauer**,** G.L., Park, C., Nowlin, D.M. 1989. Adaptational "crosstalk" and the crucial role of methylation in chemotactic migration by Escherichia coli. Proc. Natl. Acad. Sci. U S A. 86(5):1448-52.

Hazelbauer, G.L., Falke, J.J., Parkinson, J.S. 2008. Bacterial chemoreceptors: high-performance signaling in networked arrays. Trends Biochem. Sci. 33(1):9-19.

Hazelbauer G.L., Lai, W.-C. 2010. Bacterial chemoreceptors: providing enhanced features to two-component signaling. Curr. Opin. Microbiol. 13(2):124-32.

Hubbell, W.L., Mchaourab, H.S., Altenbach, C., Lietzow, M.A. 1996. Watching proteins move using site-directed spin labeling. Structure. 4(7):779-83.

Hubbell, W.L., Gross, A., Langen, R., Lietzow, M.A. 1998. Recent advances in site-directed spin labeling of proteins. Curr. Opin. Struct. Biol. 8(5):649-56.

Hubbell, W.L., Cafiso, D.S., Altenbach, C. 2000. Identifying conformational changes with site-directed spin labeling. Nat. Struct. Mol. Biol. 7:735-739.

Hubbell, W.L., López, C.J., Altenbach, C., Yang, Z. 2013. Technological advances in site-directed spin labeling of proteins. Curr. Opin. Struct. Biol. Oct;23(5):725-33.

Hughson, A.G., Hazelbauer, G.L. 1996. Detecting the conformational change of transmembrane signaling in a bacterial chemoreceptor by measuring effects on disulfide cross-linking in vivo. Proc. Natl. Acad. Sci. U S A. 93(21):11546-51.

Hulko, M., Berndt, F., Gruber, M., Linder, J. U., Truffault, V., Schultz, A., Martin, J., Schultz, J. E., Lupas, A. N., Coles, M. 2006. The HAMP domain structure implies helix rotation in transmembrane signaling. Cell. 126: 929-940.

Kavalenka, A., Urbancic, I., Belle, V., Rouger, S., Costanzo, S., Kure, S., Fournel, A., Longhi, S., Guigliarelli, B., Strancar, J. 2010. Conformational analysis of the partially disordered measles virus N(TAIL)-XD complex by SDSL EPR spectroscopy. Biophys J. 98(6):1055-64.

Kehry, M.R., Bond, M.W., Hunkapiller, M.W., Dahlquist, F.W. 1983. Enzymatic deamidation of methyl-accepting chemotaxis proteins in Escherichia coli catalyzed by the cheB gene product. Proc. Natl. Acad. Sci. U S A. 80(12):3599-603.

Kim, K.K., Yokota, H., Kim, S.H. 1999. Four-helical-bundle structure of the cytoplasmic domain of a serine chemotaxis receptor. Nature. 400(6746):787-92.

Kim, M., Fanucci, G.E., Cafiso, D.S. 2007. Substrate-dependent transmembrane signaling in TonB-dependent transporters is not conserved. Proc. Natl. Acad. Sci. U S A. 104(29):11975-80.

Kim, M., Xu, Q., Murray, D., Cafiso, D.S. 2008. Solutes alter the conformation of the ligand binding loops in outer membrane transporters. Biochemistry. 47(2):670-9.

Kleene, S.J., Hobson, A.C., Adler, J. 1979. Attractants and repellents influence methylation and demethylation of methyl-accepting chemotaxis proteins in an extract of Escherichia coli. Proc. Natl. Acad. Sci. U S A. 76(12):6309-13.

Klug, C.S., Feix, J.B. 2008. Methods and applications of site-directed spin labeling EPR spectroscopy. Methods Cell Biol. 84:617-58.

Kort, E.N., Goy, M.F., Larsen, S.H., Adler, J. 1975. Methylation of a membrane protein involved in bacterial chemotaxis. Proc. Natl. Acad. Sci. U S A. 72(10):3939-43.

Koshy, S.S., Eyles, S.J., Weis, R.M., Thompson, L.K. 2013. Hydrogen exchange mass spectrometry of functional membrane-bound chemotaxis receptor complexes. Biochemistry. 52(49):8833-42.

Lai, W.-C., Hazelbauer, G.L. 2005. Carboxyl-terminal extensions beyond the conserved pentapeptide reduce rates of chemoreceptor adaptational modification. J. Bacteriol. 187(15):5115-21.

Lai, W.-C., Barnakova, L.A., Barnakov, A.N., Hazelbauer, G.L. 2006. Similarities and differences in interactions of the activity-enhancing chemoreceptor pentapeptide with the two enzymes of adaptational modification. J. Bacteriol. 188(15):5646-9.

Lai. W.-C., Beel, B. D., Hazelbauer, G. L. 2006. Adaptational modification and ligand occupancy have opposite effects on positioning of the transmembrane signaling helix of a chemoreceptor. Mol. Micro. 61: 1081-1090.

Langen, R., Cai, K., Altenbach, C., Khorana, H.G., Hubbell, W.L. 1999. Structural features of the C-terminal domain of bovine rhodopsin: a site-directed spin-labeling study. Biochemistry. 38(25):7918-24.

Langen, R., Oh, K.J., Cascio, D., Hubbell, W.L. 2000. Crystal structures of spin labeled T4 lysozyme mutants: implications for the interpretation of EPR spectra in terms of structure. Biochemistry. 39(29):8396-405.

Le Moual, H., Quang, T., Koshland, D.E. Jr. 1997. Methylation of the Escherichia coli chemotaxis receptors: intra- and interdimer mechanisms. Biochemistry. 36(43):13441-8.

Lee, G.F., Dutton, D.P., Hazelbauer, G.L. 1995. Identification of functionally important helical faces in transmembrane segments by scanning mutagenesis. Proc. Natl. Acad. Sci. U S A. 92(12):5416-20.

Levit, M.N., Liu, Y., Stock, J.B. 1999. Mechanism of CheA protein kinase activation in receptor signaling complexes. Biochemistry. 38:6651–6658.

Li, J., Li, G., Weis, R.M. 1997. The serine chemoreceptors from Escherichia coli is methylated through an inter-dimer process. Biochemistry. 36(39):11851-7.

Li, M., Hazelbauer, G.L. 2005. Adaptational assistance in clusters of bacterial chemoreceptors. Mol. Microbiol. 56(6):1617-26.

Li, M., Hazelbauer, G.L. 2006. The carboxyl-terminal linker is important for chemoreceptor function. Mol. Microbiol. 60(2):469-79.

Li, M., Hazelbauer, G.L. 2011. Core unit of chemotaxis signaling complexes. Proc. Natl. Acad. Sci. U S A. 108(23):9390-5.

Li, X., Fleetwood, A.D., Bayas, C., Bilwes, A.M., Ortega, D.R., Falke, J.J., Zhulin, I.B., Crane, B.R. 2013. The 3.2 Å resolution structure of a receptor: CheA:CheW signaling complex defines overlapping binding sites and key residue interactions within bacterial chemosensory arrays. Biochemistry. 52(22):3852-65.

Lin, L.N., Li, J., Brandts, J.F., Weis, R.M. 1994. The serine receptor of bacterial chemotaxis exhibits half-site saturation for serine binding. Biochemistry. 33(21):6564-70.

Liu, J., Hu, B., Morado, D.R., Jani, S., Manson, M.D., Margolin, W. 2012. Molecular architecture of chemoreceptor arrays revealed by cryoelectron tomography of Escherichia coli minicells. Proc. Natl. Acad. Sci. U S A. 109(23):E1481-8.

Liu, Y., Levit, M., Lurz, R., Surette, M.G., Stock, J.B. 1997. Receptor-mediated protein kinase activation and the mechanism of transmembrane signaling in bacterial chemotaxis. Embo J. 16:7231–7240.

López. C. J., Fleissner, M. R., Guo, Z., Kusnetzow, A. K. and Hubbell, W. L. 2009. Osmolyte perturbation reveals conformational equilibria in spin-labeled proteins. Prot. Sci. 18: 1637-1652.

López, C.J., Oga, S., Hubbell, W.L. 2012. Mapping molecular flexibility of proteins with site-directed spin labeling: a case study of myoglobin. Biochemistry. 51(33):6568-83.

Mchaourab, H.S., Lietzow, M.A., Hideg, K., Hubbell, W.L. 1996. Motion of spin-labeled side chains in T4 lysozyme. Correlation with protein stucture and dynamics. Biochemistry. 35(24):7692-704.

Milburn, M.V., Privé, G.G., Milligan, D.L., Scott, W.G., Yeh, J., Jancarik, J., Koshland, D.E. Jr, Kim, S.H. 1991. Three-dimensional structures of the ligand-binding domain of the bacterial aspartate receptor with and without a ligand. Science. 254(5036):1342-7.

Milligan, D.L., Koshland, D.E. Jr. 1988. Site-directed cross-linking. Establishing the dimeric structure of the aspartate receptor of bacterial chemotaxis. J. Biol. Chem. 263(13):6268-75.

Morin, B., Bourhis, J.M., Belle, V., Woudstra, M., Carrière, F., Guigliarelli, B., Fournel, A., Longhi, S. 2006. Assessing induced folding of an intrinsically disordered protein by site-directed spin-labeling electron paramagnetic resonance spectroscopy. J. Phys. Chem. B. 110(41):20596-608.

Mowbray, S.L., Foster, D.L., Koshland, D.E. Jr. 1985. Proteolytic fragments identified with domains of the aspartate chemoreceptor. J. Biol. Chem. 260(21):11711-8.

Muppirala, U.K., Desensi, S., Lybrand, T.P., Hazelbauer, G.L., Li, Z. 2009. Molecular modeling of flexible arm-mediated interactions between bacterial chemoreceptors and their modification enzyme. Protein Sci. 18(8):1702-14.

Murphy, O.J. 3rd, Yi, X., Weis, R.M., Thompson, L.K. 2001. Hydrogen exchange reveals a stable and expandable core within the aspartate receptor cytoplasmic domain. J. Biol. Chem. 276(46):43262-9.

Natale, A.M., Duplantis, J.L., Piasta, K.N., Falke, J.J. 2013. Structure, function, and on-off switching of a core unit contact between CheA kinase and CheW adaptor protein in the bacterial chemosensory array: A disulfide mapping and mutagenesis study. Biochemistry. 52(44):7753-65.

Okumura, H., Nishiyama, S., Sasaki, A., Homma, M., Kawagishi, I. 1998. Chemotactic adaptation is altered by changes in carboxyl-terminal sequence conserved among the major methyl-accepting chemoreceptors. J. Bacteriol. 180(7):1862-8.

Oldfield, C.J., Cheng, Y., Cortese, M.S., Brown, C.J., Uversky, V.N., Dunker, A.K. 2005. Comparing and combining predictors of mostly disordered proteins. Biochemistry. 44(6):1989-2000.

Ortega, D.R., Yang, C., Ames, P., Baudry, J., Parkinson, J.S., Zhulin, I.B. 2013. A phenylalanine rotameric switch for signal-state control in bacterial chemoreceptors. Nat. Commun. 4:2881.

Ottemann, K.M., Xiao, W., Shin, Y.K., Koshland, D.E. Jr. 1999. A piston model for transmembrane signaling of the aspartate receptor. Science. 285(5434):1751-4.

Parkinson, J.S., Houts, S.E. 1982. Isolation and behavior of Escherichia coli deletion mutants lacking chemotaxis functions. J. Bacteriol. 151(1):106-13.

Parkinson, J.S. 2010. Signaling mechanisms of HAMP domains in chemoreceptors and sensor kinases. Annu. Rev. Microbiol. 64:101-22.

Perez, E., Stock, A.M. 2007. Characterization of the Thermotoga maritima chemotaxis methylation system that lacks pentapeptide-dependent methyltransferase CheR:MCP tethering. Mol. Microbiol. 63(2):363-78.

Piasta, K.N., Ulliman, C.J., Slivka, P.F., Crane, B.R., Falke, J.J. 2013. Defining a key receptor-CheA kinase contact and elucidating its function in the membrane-bound bacterial chemosensory array: a disulfide mapping and TAM-IDS study. Biochemistry. 52(22):3866-80.

Pirman, N.L., Milshteyn, E., Galiano, L., Hewlett, J.C., Fanucci, G.E. 2011. Characterization of the disordered-to-α-helical transition of IA_3 by SDSL-EPR spectroscopy. Protein Sci. 20(1):150-9.

Rigaud, J.L., Levy, D., Mosser, G., Lambert, O. 1998. Detergent removal by non-polar polystyrene beads. Eur. Biophys. J. 27: 305–319.

Saudek, V., Pasley, H.S., Gibson, T., Gausepohl, H., Frank, R., Pastore, A. 1991. Solution structure of the basic region from the transcriptional activator GCN4. Biochemistry. 30(5):1310-7.

Seeley, S.K., Weis, R.M., Thompson, L.K. 1996. The cytoplasmic fragment of the aspartate receptor displays globally dynamic behavior. Biochemistry. 35(16):5199-206.

Scharf, B.E., Fahrner, K.A., Turner, L., Berg, H.C. 1998. Control of direction of flagellar rotation in bacterial chemotaxis. Proc. Natl. Acad. Sci. USA 95:201–206.

Simms, S.A., Stock, A.M., Stock, J.B. 1987. Purification and characterization of the S-adenosylmethionine:glutamyl methyltransferase that modifies membrane chemoreceptor proteins in bacteria. J. Biol. Chem. 262(18):8537-43.

Slocum, M.K., Parkinson, J.S. 1983. Genetics of methyl-accepting chemotaxis proteins in Escherichia coli: organization of the tar region. J. Bacteriol. 155(2):565-77.

Sourjik, V., Berg, H.C. 2002. Receptor sensitivity in bacterial chemotaxis. Proc. Natl. Acad. Sci. U S A. 99(1):123-7.

Starrett, D. J., Falke, J. J. 2005. Adaption mechanism of the aspartate receptor: electrostatics of the adaptation subdomain play a key role in modulating kinase activity. Biochemistry. 44:1550-1560.

Stewart, R.C. 1997. Kinetic characterization of phosphotransfer between CheA and CheY in the bacterial chemotaxis signal transduction pathway. Biochemistry. 36(8):2030-40.

Stock, A.M., Robinson, V.L., Goudreau, P.N. 2000. Two-component signal transduction. Annu. Rev. Biochem. 69:183-215.

Swain, K. E., Gonzalez, M. A., Falke, J. J. 2009. Engineered socket study of signaling through a four-helix bundle: evidence for a yin-yang mechanism in the kinase control module of the aspartate receptor. Biochemistry. 48: 9266-9277.

Swanson, R.V., Bourret, R.B., Simon, M.I. 1993. Intermolecular complementation of the kinase activity of CheA. Mol. Microbiol. 8(3):435-41.

Uversky, V.N., Dunker, A.K. 2010. Understanding protein non-folding. Biochim. Biophys. Acta. 1804(6):1231-64.

Vu, A., Wang, X., Zhou, H., Dahlquist, F.W. 2012. The receptor-CheW binding interface in bacterial chemotaxis. J. Mol. Biol. 415(4):759-67.

Wang, X., Vu, A., Lee, K., Dahlquist, F.W. 2012. CheA-receptor interaction sites in bacterial chemotaxis. J. Mol. Biol. 422(2):282-90.

Weerasuriya, S., Schneider, B.M., Manson, M.D. 1998. Chimeric chemoreceptors in Escherichia coli: signaling properties of Tar-Tap and Tap-Tar hybrids. J. Bacteriol. 180(4):914-20.

Weil, J.A., Bolton, J.R., Wertz, J.E. 1994. Electron paramagnetic resonance. Wiley-

Interscience.

Weis, R.M., Koshland, D.E. Jr. 1988. Reversible receptor methylation is essential for normal chemotaxis of Escherichia coli in gradients of aspartic acid. Proc. Natl. Acad. Sci. U S A. 85(1):83-7.

Weis, R.M., Chasalow, S., Koshland, D.E. Jr. 1990. The role of methylation in chemotaxis. An explanation of outstanding anomalies. J. Biol. Chem. 265(12):6817-26.

Windisch, B., Bray, D., Duke, T. 2006. Balls and chains—a mesoscopic approach to tethered protein domains. Biophys. J. 91(7):2383-92.

West, A.H., Stock, A.M. 2001. Histidine kinases and response regulator proteins in two-component signaling systems. Trends. Biochem. Sci. 26(6):369-76.

Wu, J., Li, J., Li, G., Long, D.G., Weis, R.M. 1996. The receptor binding site for the methyltransferase of bacterial chemotaxis is distinct from the sites of methylation. Biochemistry. 35(15):4984-93.

Wuichet, K., Alexander, R.P., Zhulin, I.B. 2007. Comparative genomic and protein sequence analyses of a complex system controlling bacterial chemotaxis. Methods Enzymol. 422:1-31.

Wuichet, K., Zhulin, I.B. 2010. Origins and diversification of a complex signal transduction system in prokaryotes. Sci. Signal. 3(128):ra50.

Yamamoto, K., Macnab, R.M., Imae, Y. 1990. Repellent response functions of the Trg and Tap chemoreceptors of Escherichia coli. J. Bacteriol. 172(1):383-8.

Yeh, J.I., Biemann, H.P., Privé, G.G., Pandit, J., Koshland, D.E. Jr, Kim, S.H. 1996. High-resolution structures of the ligand binding domain of the wild-type bacterial aspartate receptor. J. Mol. Biol. 262(2):186-201.

Zhao, X., Norris, S.J., Liu, J. 2014. Molecular architecture of bacterial flagellar motor in cells. Biochemistry. [Epub ahead of print].

Zhou, H., McEvoy, M.M., Lowry, D.F., Swanson, R.V., Simon, M.I., Dahlquist, F.W. 1996. Phosphotransfer and CheY-binding domains of the histidine autokinase CheA are joined by a flexible linker. Biochemistry. 35(2):433-43.

Zhou, Q., Ames, P., Parkinson J. S. 2009. Mutational analysis of HAMP helices suggest a dynamic bundle model of input-output signaling in chemoreceptors. Mol. Micro. 73:801-814.

Zhou, Z., DeSensi, S.C., Stein, R.A., Brandon, S., Dixit, M., McArdle, E.J., Warren, E.M.,

Kroh, H.K., Song, L., Cobb, C.E., Hustedt, E.J., Beth, A.H. 2005. Solution structure of the cytoplasmic domain of erythrocyte membrane band 3 determined by site-directed spin labeling. Biochemistry. 44(46):15115-28.

VITA

Nicholas Lee Bartelli was born January 28th, 1981 in Kansas City, Missouri. In 2006 he was awarded a B.S. in Biology from the University of Missouri – Kansas City. At this time he joined the laboratory of Joe Lutkenhaus at the University of Kansas Medical School as a research assistant. In this laboratory he contributed to research pertaining to the molecular mechanisms of cell division in *Escherichia coli*. In 2008 Nicholas was accepted into the University of Missouri, Department of Biochemistry graduate studies program where he joined the laboratory of Gerald Hazelbauer for his dissertation work. In this position he explored features important to the molecular mechanism of chemotaxis signaling in *Escherichia coli*. Nicholas completed his Ph.D. studies in the summer of 2014.

Outside the laboratory Nicholas is an active painter producing large art works in acrylic and oil media. Typical works include abstract landscape and abstract expressionist themes. He has no formal training in these pursuits.